UNIVERSITÀ DEGLI STUDI FIRENZE

DOTTORATO DI RICERCA IN SCIENZE CHIMICHE

CICLO XXXIII

COORDINATORE Prof. PIERO BAGLIONI

DEVELOPMENT OF BIOMIMETIC NANOSTRUCTURED SENSORS IN FOOD AND ENVIRONMENTAL APPLICATIONS

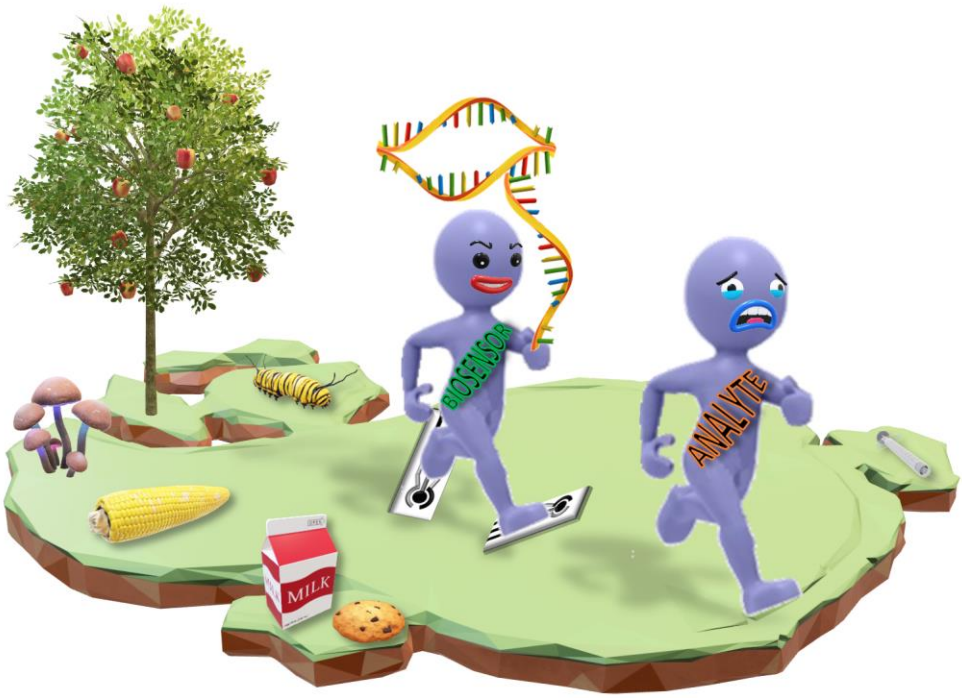

Dottorando
Dott. Giulia Selvolini

Tutore
Prof. Giovanna Marrazza

UNIVERSITÀ
DEGLI STUDI
FIRENZE

DOTTORATO DI RICERCA IN SCIENZE CHIMICHE

CICLO XXXIII

COORDINATORE Prof. PIERO BAGLIONI

DEVELOPMENT OF BIOMIMETIC NANOSTRUCTURED SENSORS IN FOOD AND ENVIRONMENTAL APPLICATIONS

Settore Scientifico Disciplinare CHIM/01

Dottorando
Dott. Giulia Selvolini

Tutore
Prof. Giovanna Marrazza

Coordinatore
Prof. Piero Baglioni

Anni 2017/2020

“If one day, my words are against science, choose science”

Mustafa Kemal Atatürk

Table of Contents

Preface

Abstract

The presence of harmful chemicals and microorganisms in food is often addressed ad food contamination, which can cause consumer illness at different levels of severity. Potential hazardous residues in food include several different substances: natural and environmental contaminants (*e.g.* toxins, heavy metal ions), agrochemicals pollutants like pesticides, drugs, growth promoters, packaging components, etc. The detection of contaminants is then of utterly importance in food safety and environmental analysis; thus, it requires highly sensitive and easy-to-use analytical procedures to be developed.

Conventional analytical methods used for this kind of analysis include separation techniques (*e.g.* high-performance liquid chromatography, tandem mass spectrometry), which often provide sensitive and selective results. Despite the advantages of these techniques, the high costs, the expensive instrumentation, the technical skills needed for users and the complex pretreatment processes are pushing scientists to find out rapid, low cost, highly sensitive and simple alternative analytical methods.

For this purpose, biosensors can act as an option for solving the problems mentioned before or become a helpful tool at least.
Biosensors development can be classified as an interdisciplinary field and one of the most active research areas in analytical chemistry. As well as other analytical methods, biosensors performance is evaluated by considering their detection limit, their sensitivity, selectivity and reproducibility in terms of linear and dynamic range and response to interfering substances. The most used receptors in biosensing applications are probably the antibodies, which are able to bind target molecules with high selectivity and sensitivity, but their use is characterized by some

limitations.

As one of the drawbacks in developing contaminants biosensors is the synthesis of antibodies for these highly toxic targets, the use of biomimetic receptors has recently become an interesting alternative. This kind of probes includes biological "bricks" assembled *in vitro* or synthetic molecules assembled to mimic the recognition capabilities of antibodies.

The advances in nanotechnology have led to the discovery and the employment of a great number of new materials in nanoscale dimensions (comprised between 1 and 100 nm, even if for biological application dimensions can raise up to 500 nm and rarely up to 700 nm). Because the common biological systems (such as proteins, viruses, membranes, etc.) are nanostructured and their interactions take place at nanometric scale, nanomaterials become ideal candidates for the development of advanced biosensing devices. Nanostructures present several advantages in analytical applications and can be mainly used as transducers (due to their unique optical, chemical, electrical, and catalytic properties) or as a component of the recognition element of a biosensing device (due to the high surface-to-volume ratio that increases the number of bioreceptors attached to the sensing surface).

This thesis presents different strategies for the development of electrochemical biosensors based on nanostructured sensing platforms and biomimetic probe molecules for the determination of a pattern of contaminants (*e.g.* pesticides, toxins, allergens) related to food and environmental analysis.

The dissertation is subdivided in ten chapters.

- *Chapter 1*. The definition of biosensors is provided, highlighting the classification and advantages of electrochemical ones. Moreover, a short description of aptamers, Affibodies® and molecularly imprinted polymers as bioreceptors is presented. A particular

attention has been posed in the description of different aptamer assay formats and the aptasensing approaches based on screen-printed electrochemical transducers.

- *Chapter 2*. The role of biosensors in contaminants detection for food analysis is described. A classification of the contaminants analyzed in this work is also given, divided by their chemical classes, underlining their hazardous potential.
- *Chapter 3*. The electrochemical techniques (cyclic voltammetry, differential pulse voltammetry and electrochemical impedance spectroscopy) used in this work are introduced, describing their basic principles. The experimental set-up, including the graphite screen-printed cells used as transducers in this thesis, is described.
- *Chapter 4*. An overview of the conductive nanostructured materials for sensing platforms development is presented. In particular, a short description of the conductive polymers (*i.e.* polyaniline, poly(aniline-*co*-anthranilic acid), poly-L-lysine) and the gold nanoparticles used in this work is given, also providing their electrodeposition protocols and electrochemical characterization.
- *Chapter 5*. The application of a sensing platform based on gold nanoparticles and polyaniline-modified graphite screen-printed electrodes for dopamine detection is reported. Dopamine was chosen as a model analyte due to its easiness of determination by being oxidized at an electrodic surface. The analytical usefulness of the sensor was also demonstrated by analyzing spiked commercial serum samples.
- *Chapter 6*. Profenofos pesticide is detected by means of an aptasensor based on a competitive format, which employs a gold/polyaniline-modified transducer as sensor platform and an enzyme-linked label for a dual amplification of the signal. The nanostructured electrodes

were modified with a mixed monolayer of a thiol-tethered DNA probe and 6-mercapto-1-hexanol. A biotinylated DNA aptamer was incubated with the pesticide and then dropped onto the sensing surface: the aptamer sequences which did not bind the analyte were free to hybridize with the immobilized DNA probe. The binding was traced with the addition of streptavidin-alkaline phosphatase enzyme conjugate: the enzymatic substrate 1-naphthyl phosphate was converted into the electroactive product 1-naphthol, which was finally oxidized and detected by differential pulse voltammetry.
The bindings of the aptamer with the analyte and the DNA probe were also preliminary assessed by melting temperatures study.

- *Chapter 7*. Aflatoxin B_1 mycotoxin is detected by means of an enzyme-linked oligonucleotide array based on a competitive format.
  The developed assay makes use of a sensing platform composed of poly(aniline-*co*-anthranilic acid)-modified electrodes; a conjugate between aflatoxin B_1 and bovine serum albumin was immobilized by amide coupling between the carboxylic groups of the copolymer and the amine groups of the protein. Each phase involved in the assembly of the aptasensor was characterized and evaluated by means of cyclic voltammetry and electrochemical impedance spectroscopy techniques. The competition was achieved between free and immobilized AFB_1 molecules for the binding with a biotinylated DNA aptamer and the affinity reaction was traced by streptavidin-alkaline phosphatase in the same way as previously described.
  Preliminary experiments in maize flour samples spiked with AFB_1 were also conducted.
- *Chapter 8*. Deoxynivalenol mycotoxin is detected by means of an aptasensor based on a competitive format. The sensing strategy is somehow similar to that employed for the pesticide detection, as it shares with the aforementioned assay both the nanostructured

platform and the enzymatic labeling. However, in this case, a thiol-tethered DNA aptamer was immobilized on the electrodic surface, while the competition occurs in solution between deoxynivalenol molecules and a biotinylated complementary DNA sequence.
The enzyme and its substrate were then used for the electrochemical detection by differential pulse voltammetry. Apart from being one of the first electrochemical aptasensors reported for deoxynivalenol detection, the novelty of the work consists in the investigation of the molecular interaction between the aptamer and the mycotoxin by a docking study, which allows to verify if the aptamer region binding with the complementary oligonucleotide sequence chosen for the competitive assay includes the interaction sites between the mycotoxin and the DNA aptamer, while also determining the preferred orientation assumed by DON in the binding event.

- *Chapter 9*. β-Lactoglobulin milk allergen is detected by means of a switch-on assay employing a gold/poly-L-lysine-modified transducer as the sensing platform. The nanostructured electrodes were modified with a mixed monolayer of a thiol-tethered DNA aptamer, bearing the electroactive methylene blue moiety to the free 3'-end, and 6-mercapto-1-hexanol. Upon the binding with the analyte, the aptamer changed its conformation, making the labeled end to be closer to the electrodic surface and to be more easily oxidized. The electrochemical folding-based aptasensor allowed unambiguous identification of the protein, while no significant non-specific signals were detected in case of negative controls.
- *Chapter 10*. Concluding remarks are reported.

Scientific Production

Papers

- H. Subak, G. Selvolini, M. Macchiagodena, D. Ozkan-Ariksoysal, M. Pagliai, P. Procacci, G. Marrazza. Mycotoxins Aptasensing: from Molecular Docking to Electrochemical Detection of Deoxynivalenol. *Bioelectrochemistry*, **2020**, *138*, 107691.
  DOI: 10.1016/j.bioelechem.2020.107691. IF: 4.722
- O. Amor-Gutiérrez, G. Selvolini, M. T. Fernández-Abedul, Alfredo de la Escosura-Muñiz, G. Marrazza. Folding-Based Electrochemical Aptasensor for the Determination of β-Lactoglobulin on Poly-L-Lysine Modified Graphite Electrodes. *Sensors*, **2020**, *20*(8), 2349.
  DOI: 10.3390/s20082349. IF: 3.275
- G. Selvolini, C. Lazzarini, G. Marrazza. Electrochemical Nanocomposite Single-Use Sensor for Dopamine Detection. *Sensors*, **2019**, *19*(14), 3097. **DOI**: 10.3390/s19143097. IF: 3.275
- G. Selvolini, M. Lettieri, L. Tassoni, S. Gastaldello, M. Grillo, C. Maran, G. Marrazza. Electrochemical Enzyme-Linked Oligonucleotide Array for Aflatoxin B_1 Detection. *Talanta*, **2019**, *203*, 49.
  DOI: 10.1016/j.talanta.2019.05.044. IF: 5.339
- G. Selvolini, I. Băjan, O. Hosu, C. Cristea, R. Săndulescu, G. Marrazza. DNA-based Sensors for the Detection of an Organophosphorus Pesticide: Profenofos. *Sensors*, **2018**, *18*(7), 2035.
  DOI: 10.3390/s18072035. IF: 3.275
- O. Hosu, G. Selvolini, G. Marrazza. Recent Advances of Immunosensors for Detecting Food Allergens. *Curr. Op. Elec.*, **2018**, *10*, 149. **DOI**: 10.1016/j.coelec.2018.05.022. IF: 5.579
- G. Selvolini, G. Marrazza. MIP-based Sensors: Promising New Tools for Cancer Biomarker Determination. *Sensors*, **2017**, *17*(4), 718.

DOI: 10.3390/s17040718. IF: 3.275

Proceedings/Book Chapters

- G. Selvolini, A. Adumitrachioaie, M. Lettieri, O. Hosu, C. Cristea, G. Marrazza. Electrochemical Sensors Based on Conducting Polymers: Characterization and Applications. *Sensors and Microsystems — Proceedings of the 20th AISEM 2019 National Conference*. Springer International Publishing, **2020**, 233–237.
- G. Selvolini, O. Hosu, G. Marrazza. Immunosensors for Food Allergens: An Overview. *Immunosensors*. Eds. M. U. Ahmed, M. Zourob, E. Tamiya. RSC Publishing, **2019**, 135–155.
- G. Selvolini, I. Băjan, O. Hosu, C. Cristea, R. Săndulescu, G. Marrazza. Electrochemical DNA-Based Sensor for Organophosphorus Pesticides Detection. *Sensors — Proceedings of the Fourth National Conference on Sensors, February 21–23, 2018, Catania, Italy*. Eds. B. Andò, F. Baldini, C. Di Natale, V. Ferrari, V. Marletta, G. Marrazza, V. Militello, G. Miolo, M. Rossi, L. Scalise, P. Siciliano. Springer International Publishing, **2019**, 111–115.
- G. Marrazza, O. Hosu, G. Selvolini. Conducting Polymer-Based Platform for Electrochemical Sensors. *6th Workshop on Specific Methods for Food Safety and Quality*. Ed. V. Vasić. Vinča Institute of Nuclear Sciences, **2018**, 71–77.

In-Fieri Material

- G. Selvolini, H. Subak, B. Taneri, D. Ozkan-Ariksoysal, G. Marrazza. Electrochemiluminescent and Photoelectrochemical Aptasensors based on Quantum Dots for Mycotoxins and Pesticides Analysis. *Electroanalytical Applications of Quantum Dot Based Biosensors*. Ed. B. Uslu. Elsevier, **2021** (accepted).

- G. Selvolini, A.-M. Drăgan, G. Melinte, C. Cristea, G. Marrazza. A Smart Colorimetric Sensor for the Enzymatic Detection of L-Lactate in Screening Analysis. *Biosensors* (submitted).
- M. Invernici, M. Piccioli, G. Selvolini, G. Marrazza. Aconitase-like Interconversion Between Glutathione Bound [Fe-S] Complexes. *JACS* (submitted).

Not-included Material

- G. Melinte, G. Selvolini, C. Cristea, G. Marrazza. Aptasensors for Lysozyme Detection: Recent Advances. *Talanta*, **2021**, *226*, 122169. **DOI**: 10.1016/j.talanta.2021.122169. IF: 5.339
- O. Hosu, G. Selvolini, C. Cristea, G. Marrazza. Electrochemical Immunosensors for Disease Detection and Diagnosis. *Curr. Med. Chem.*, **2018**, *25*(33), 4119. **DOI**: 10.2174/0929867324666170727104429. IF: 4.184
- M. Raudino, G. Selvolini, C. Montis, M. Baglioni, M. Bonini, D. Berti, P. Baglioni. Polymer Films Removed from Solid Surfaces by Nanostructured Fluids. Microscopic Mechanism and Implications for the Conservation of Cultural Heritage. *ACS Appl. Mater. Interfaces*, **2015**, *7*, 6244. **DOI**: 10.1021/acsami.5b00534. IF: 8.758

List of Abbreviations

1-NPOH	1-naphthol
1-NPP	1-naphthyl phosphate
AA	Anthranilic acid
AC	Alternating (alternate current)
AFB_1	Aflatoxin B_1
AFB_2	Aflatoxin B_2
AFG_1	Aflatoxin G_1
AFG_2	Aflatoxin G_2
AFL	Aflatoxicol
AFM_1	Aflatoxin M_1
AFM_2	Aflatoxin M_2
AFP_1	Aflatoxin P_1
AFQ_1	Aflatoxin Q_1
ALP	Alkaline phosphatase
ANI	Aniline
AuNP	Gold nanoparticle
BSA	Bovine serum albumin
CMA	Cow's milk allergy
CV	Cyclic voltammetry
DA	Dopamine
DAS	Diacetoxyscirpenol
DC	Direct (direct current)
DDT	Dichlorodiphenyltrichloroethane
DEA	Diethanolamine
DON	Deoxynivalenol
DPV	Differential pulse voltammetry
DTT	DL-dithiothreitol
EDC	1-ethyl-3-(3-dimethylaminopropyl)

	carbodiimide
EFSA	European food safety authority
EIS	Electrochemical impedance spectroscopy
ELISA	Enzyme-linked immunosorbent assay
FAO	Food and agriculture organization
FDA	Food and drug administration
GMP	Good manufacturing practice
GSPE	Graphite screen-printed electrode
HACCP	Hazard analysis of critical control points
HPLC	High-performance liquid chromatography
HRP	Horseradish peroxidase
IARC	International agency of research on cancer
IUPAC	International union of pure and applied chemistry
LA	Lactalbumin
LF	Lactoferrin
LFIA	Lateral-flow immunoassay
LG	Lactoglobulin
LOD	Limit of detection
LSPR	Localized surface plasmon resonance
LSV	Linear sweep voltammetry
MB	Methylene blue
MCH	6-mercapto-1-hexanol
MIP	Molecularly imprinted polymer
NHS	N-hydroxysuccinimide
NIAID	National institute of allergy and infectious diseases
NIV	Nivalenol
NP	Nanoparticle
OPP	Organophosphorus pesticide

OTA	Ochratoxin A
PAA	Polyanthranilic acid
PAc	Polyacetylene
PANI	Polyaniline
P(ANI-*co*-AA)	Poly(aniline-*co*-anthranilic acid)
PBS	Phosphate buffer saline
PCR	Polymerase chain reaction
PEDOT	Poly(3,4-ethylenedioxythiophene)
PLL	Poly-L-lysine
POCT	Point-of-care testing
PPy	Polypyrrole
PTh	Polythiophene
QD	Quantum dot
RSD	Relative standard deviation
SAM	Self-assembled monolayer
SELEX	Systematic evolution of ligands by exponential enrichment
SEM	Scanning electron microscopy
SPC	Screen-printed cell
SPE	Screen-printed electrode
SPPS	Solid phase peptide synthesis
SPR	Surface plasmon resonance
ssDNA	Single-stranded DNA
ssRNA	Single-stranded RNA
SWV	Square wave voltammetry
TEG	Triethylene glycol
TRIS	Tris(hydroxymethyl) aminomethane

1. Introducing Biosensors

1.1 Definitions

A biosensor is defined by the International Union of Pure and Applied Chemistry (IUPAC) as "a self-contained integrated device which is capable of providing specific quantitative or semi-quantitative analytical information using a biological recognition element (biochemical receptor or bioreceptor) which is in direct spatial contact with a transducer.
The transducer is used to convert the (bio)chemical signal resulting from the interaction of the analyte with the bioreceptor into an electronic one. The intensity of the signal is proportional to the analyte concentration" [1].

The biorecognition element is able to convert an information about the target analyte, usually its concentration, into a chemical output signal that can be detected by a transducer. The biorecognition element should provide high selectivity towards the chosen target (*specific biorecognition*) or the chosen chemical class (*non-specific biorecognition*). Being connected to a detector, the transducer is in charge to produce a detectable signal. The signal is then processed by a signal processor that collects, amplifies and displays it [2].

The general scheme of a biosensor is shown in **Figure 1.1**.

Figure 1.1. *Schematic representation of a biosensor.*

Biosensors may be classified according to the biological specificity-conferring mechanism, or to the mode of the signal transduction or, alternatively, by a combination of these two. Generally, there are two categories of biosensors: affinity biosensors and catalytic biosensors [3]. Catalytic biosensors are kinetic devices that measure steady-state concentration of a transducer-detectable species formed/lost due to a biocatalytic reaction, with the bioreceptor constituted by mono- or multienzymes, microorganisms, organelles or tissue samples.
Affinity biosensors are devices in which receptor molecules bind the analyte molecules causing a physicochemical change that is detected by a transducer [4].

Biosensors are also categorized according to the basic principles of signal transduction and biorecognition elements. According to the transducing element, biosensors can be classified as:

- *optical*, which exploit the change in the optical property of a biomolecule as a results of its interaction with the target analyte, or the use of different kinds of labels and probes [5];
- *piezoelectric*, in which the analytical signal is produced by the application of a mechanical stress on the surface of a piezoelectric crystal, onto the surface of which the bioreceptor is immobilized [6];
- *thermometric*, based on the measurement of the heat absorbed or evolved during a biochemical reaction [7];
- *magnetic*, which reveal the variation of the magnetic properties of the system for the detection of the analyte [8];
- *electrochemical*, based on the determination of electroactive species that can be produced and consumed at the electrode surface, or bound to the receptor molecules, working as electrochemical mediators, as they let the electric current to flow from the bulk solution to the electrode surface [9].

1.1.1 Electrochemical Biosensors

Electrochemical biosensors are a class of sensors in which an electrode is used as the transduction element and constitute the category on which this thesis will be focused on. The electrochemical transduction system is particularly interesting due to some peculiar features, as low cost, high detection speed, high sensitivity, portability and, above all, high compatibility with miniaturized technology.

In affinity biosensors, the transducer (which oversees the conversion of the chemical information into a measurable signal) incorporates a biological or biomimetic receptor molecule which can reversibly bind the target analyte with high selectivity, *e.g.* antibodies, nucleic acids, peptides. In electrochemical affinity biosensors, the binding is detected by the change in currents and/or voltages at the localized surface. Depending on their operating principle, the transduction techniques employed by electrochemical biosensors can be classified into six main ensembles: potentiometric, amperometric, voltammetric, impedimetric, conductometric and field effect [10].

Potentiometric biosensors measure the changes in the potential, recorded at a working electrode against a proper reference electrode, when no current flows into the electrochemical cell. The signal response is high even for small concentration changes, making this technique useful to measure low concentrations.

Amperometric biosensors are based on continuous measurements of the current resulting from the oxidation or reduction of electroactive species after the application of a fixed potential to the working electrode. The measured current is directly proportional to the electron transfer rate of the reaction and, therefore, also to the concentration of the analyte. Plotting the current against time gives a characteristic graph, called amperogram.

Voltammetric biosensors rely on the measurement of the current generated after the application of a potential sweep, within a selected range, to the working electrode. Depending on the waveform, this technique can be declined in cyclic voltammetry (CV), linear sweep voltammetry (LSV), differential pulse voltammetry (DPV), square wave voltammetry (SWV), etc. By recording the position of different peaks, which are characteristic of different electroactive compounds under analysis, this technique is able to detect multiple analytes in a single potential sweep. Moreover, voltammetry is characterized by a low signal noise, which can endow the biosensor with a higher sensitivity.

Impedimetric biosensors rely on electrochemical impedance spectroscopy (EIS) and can be divided into faradaic impedance methods and non-faradaic capacitance methods. This technique monitors the changes in the impedance values at the solution/electrode interface caused by the biorecognition event between the probe and the analyte. Even if EIS can provide label-free detection, the obtained limit of detection (LOD) values are higher if compared to the traditional electrochemical methods.

Conductometric biosensors detect changes in the conductance (and thus in the ionic concentration) induced by the biorecognition event by applying an alternating potential to two separated electrodes into the electrochemical cell. Despite several technical advantages (*e.g.* no need of the reference electrode, low cost, ease of miniaturization), this technique is strongly buffer-sensitive and owns a lower sensitivity in comparison to the others.

Field effect biosensors are based on field effect transistor semiconductors, which are formed by a source and a drain separated by a gate. When charged molecules, such as biomolecules, bind to the gate (which is usually a dielectric material), a change in the charge distribution of the underlying semiconductor occurs, resulting in a change of conductance in the transistor channel. The analytical signal, called drain

current, is proportional to the analyte concentration.

Apart from the chosen transduction technique, the electrochemical detection of the captured analyte can be achieved by following two main routes.

- *Labeled assay*. Non-electroactive analytes need to be marked with an electroactive detection probe. The electrical signal obtained in presence of the label is proportional to the number of analyte molecules bound to the electrode surface [11];
- *Label-free assay*. The changing of electrode surface properties (*i.e.* capacitance, resistance, conductibility, etc.) can be directly measured after the affinity reaction [12].

1.2 Biomimetic Receptors

Antibodies are probably the most used receptors in biosensing, as they provide high sensitivity and selectivity but are also subjected to some limitations. First of all, both monoclonal and polyclonal antibodies are selected and produced by inducing immune reactions in cavy animals: this production method becomes clearly problematic when the target molecule belongs to a toxic or not-well-tolerated class of compounds.
Furthermore, the exploitation of host animals presents non-neglectable ethical issues [13].

As biorecognition probes, the antibodies are thermosensitive, and their reactivity might vary from batch to batch. Recent progresses in bioanalytical applications led to the synthesis and characterization of new classes of biomimetic receptors. Biomimetic materials are those developed by using inspiration from nature, as the term derives from the Greek *bio* ("life") and *mimetikos* ("imitative"). These probes comprise both *in vitro*-assembled biological "bricks" or synthetic molecules with the aim to mimic the biorecognition capabilities of antibodies.

1.2.1 Aptamers

As one of the drawbacks in developing contaminants biosensors is the synthesis of antibodies for these highly toxic targets, the use of biomimetic receptors has recently become an interesting alternative. Due to this, novel specific ligands like aptamers are emerging, as they have shown themselves to be good candidates as recognition elements in robust and stable biosensors [14].

Aptamers are short single-stranded DNA or RNA (ssDNA or ssRNA) sequences that are able to identify specific targets and bind to them by folding into unique secondary or tertiary structures [15]. The term "aptamer", which comes from the Latin *aptus* ("fit") and from the Greek *meros* ("part"), was chosen after these specific three-dimensional foldings, allowing them to bind tightly to a broad range of targets, ranging from large proteins to small molecules. An outstanding interest in aptamer technology triggered the development of the iterative *in vitro* process SELEX (Systematic Evolution of Ligands by EXponential enrichment), a highly-reproducible methodology that underwent several modifications since its introduction in 1990 [16–18]. Aptamers are isolated from a synthetic oligonucleotidic library (10^{15}–10^{16} individual sequences, which are flanked by constant 5'- and 3'-ends primer sequences) according to their affinity towards a target molecule, looking for the best selectivity and specificity (**Figure 1.2**) [19].

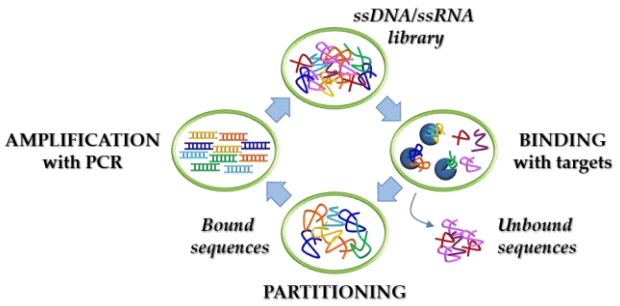

Figure 1.2. *Schematic representation of the SELEX process.*

During the SELEX process, the small fraction of the starting sequences able to interact with the target is immobilized on a solid support, while unbound sequences are separated *via* a washing step. Bound sequences are then eluted, amplified *via* polymerase chain reaction (PCR) and prepared for the following selection cycle. After a certain number (usually ranging from 8 to 15) of selection and amplification rounds, the enriched library is cloned and sequenced to obtain the sequence information of each oligonucleotide. Selected sequences are then truncated (in order to remove the primers needed for the PCR) and characterized with respect to the affinity towards the selected target [20]. Selected aptamers display low dissociation constants (K_d), often ranging within the nanomolar or picomolar range.

Compared to antibodies or aminoacid-based structures, aptamers offer several advantages, such as no need of animal immunization, high chemical and thermal stability in quite extreme conditions (*e.g.* high temperature or pH values), low cross reactivity and prolonged shelf life [21,22]. Moreover, aptamers are easy to be immobilized and/or labeled by adding different functional groups to the nucleotidic sequence [23].
Due to those features, aptamers have been used in diagnosis, therapeutics, target validation, drug industry, and as detection agents [24].

1.2.2 Engineered Protein Scaffold Molecules (Affibodies)

Parallel to aptamers, in order to overcome immunoglobulin limitations, another field of investigation is represented by the development of alternative binding proteins (based either on scaffold with the immunoglobulin fold or on completely different protein topologies), called collectively engineered protein scaffolds. Usually, this scaffold is derived from a robust and small soluble monomeric protein (such as the Kunitz inhibitors or the lipocalins) or from a stably folded extramembrane domain of a cell surface receptor (*e.g.* protein A, fibronectin or the ankyrin

repeat). Compared with antibodies or their recombinant fragments, these protein scaffolds often provide practical advantages including elevated stability, high production yield in *in vitro* systems and possibility to modulate desired properties (such as solubility, thermal stability, protease resistance, etc.) [25–27].

Among these classes of engineered proteins, affibodies received particular attention and found application in several studies especially for *in vivo* diagnostic imaging [28,29] and targeted therapy [30,31] applications. Affibody molecules are being developed by a Swedish biotechnology company (Affibody Medical AB, www.affibody.se) and are an engineered version of the Z domain (the immunoglobulin G-binding region) of staphylococcal protein A.

Affibody molecules are constituted by only 58 aminoacids (molecular weight ≈ 6.5 kDa) and are structured as a triple α-helix bundle: since they lack disulphide bridges, they can be produced in simpler organisms such as prokaryotes, rather than in the animal systems required for antibodies synthesis [32]. Moreover, due to their small size they can also be chemically synthesized using solid phase peptide synthesis (SPPS), which eliminates the need of biological systems for their production and allows specific site modification to be performed.

Affibodies can include specific labels, such as fluorophores, radioactive labels and other moieties, such as biotin, which can be used to couple the affibody to surfaces or other molecules, including enzymes [33].

1.2.3 Molecularly Imprinted Polymers

Another promising alternative to classical immunosensors is given by molecularly imprinted polymers (MIPs), due to their reliability in non-biological conditions (*e.g.* organic solvents, extreme pH values, high temperatures, etc.), in which antibodies exhibit poor stability, and low realization cost.

Molecular imprinting is a process used for preparing affinity polymers for various targets of analytical interest. It involves the formation of a complex through covalent or non-covalent interactions between a given target molecule (template) and functional monomers, which are then subject to polymerization to form a cast-like shell.
The subsequent removal of the template leaves binding sites within the polymer possessing both the correct shape and the correct orientation of functional groups to allow for selective recognition of the imprint species [34,35]. The molecular memory, imprinted on the polymer, is able to selectively bind the target [12,36].

MIPs can be prepared for any kind of substance, such as inorganic ions, drugs, nucleic acids, proteins, and so on. They possess a number of advantages in comparison with natural biomolecules [37], as they are stable, specific, low-cost, and easy to prepare and to miniaturize; all these features render them as promising alternatives to the natural bioreceptors used in sensor technology [38]. Numerous analytes which have no optical or electrochemical properties can also be detected by exploiting MIPs capacity of generating optical or electrochemical signals in response to template binding with the functional groups in the imprinting site [39,40].

One of the limitations associated with the development of MIP sensors is the difficulty in integrating them with the transducers; the most direct and smart way for overcoming this drawback is the electropolymerization, in which the MIP can be synthesized *in situ* at an electrode surface by simply controlling the layer's thickness by the amount of charge passed. This approach is particularly attractive for making small devices for clinical diagnostics, environmental control, and for pharmaceutical industries [12,41,42].

For the successful application of MIPs in sensors, it is necessary to improve their binding kinetics, to decrease the analysis time, and to remove most of the template. It has been demonstrated that the possibility

of designing MIPs at the nanoscale has a key effect on these issues by enhancing the surface-to-volume ratio, thus making binding sites more accessible to analytes. Different MIP nanostructures have been prepared and incorporated in the design of sensing devices; among these, MIP nanoparticles (NPs) have been prepared through several strategies and successfully applied in different analytical fields [43,44].

1.3 Aptamer Assay Formats

Many different designs were applied in the development of electrochemical aptasensors: usually, the most common scheme consists in a device composed of a DNA (or RNA) oligonucleotide, used as the molecular probe and able to recognize the analyte, and an electrochemical transducer, used to convert the chemical reaction resulting from the interaction of the target with the aptamer probe (*e.g.* production of electroactive molecules, conformational changes, electrochemical mediators release) into an electronic signal that can be elaborated by a computer.

The first step of the aptasensor development is represented by the immobilization of the aptamer capture probe onto a substrate.
A great variety of methods for aptamer immobilization (*e.g.* biotin/streptavidin or thiols/gold affinity, as the most used techniques [45]) has been reported in literature. The probe immobilization step plays the major role in determining the overall performance of an aptasensor. The achievement of high sensitivity and selectivity requires maximization of the binding efficiency and minimization of non-specific adsorption, respectively.

Control of the immobilization process is essential for assuring high reactivity, proper orientation, accessibility and stability of the surface-confined aptamer probe as well as for minimizing non-specific adsorption events. The choice of the immobilization method is dependent on both the

assay format and the detection principle and strictly influences the ability of the aptamer to bind the target analyte. The most successful approaches are the covalent bond, the affinity reaction and the self-assembled layer. In particular, to guarantee suitable stability, surface coverage and maintaining the same binding affinity as showed in solution, various molecules (such as tri(ethylene glycol), TEG, or -$(CH_2)_6$-, etc.) acting as arm spacers were introduced.

After a proper blocking step, in order to avoid the non-specific adsorption of interfering substances, the affinity reaction with the target is performed. The assay format and the aptasensing strategy are largely determined by the size of the target ligand [46].

1.3.1 Sandwich Assay

Labeled methods usually offer high sensitivity and specificity.
In the sandwich format, the target molecule is captured between two aptamers, or between an aptamer and an antibody that binds different regions of the target. The capture aptamer is anchored to the sensor surface, while the other labeled biorecognition element is used for detection. Labels include various kinds of molecules, such as enzymes (*i.e.* alkaline phosphatase or peroxidase, often conjugated with streptavidin to exploit its high binding affinity with biotin) or electroactive compounds (*i.e.* ferrocene, gold nanoparticles, In(II) salts), which can be directly bound to the secondary aptamer sequences during their synthesis.
The sandwich approach allows the decrease of the non-specific signal in complex samples but the cost and the time of assay increase [18,47,48].

1.3.2 Competitive Assay

Since a DNA or RNA aptamer is able to bind its complementary sequence by hybridization reaction, aptamer-based displacement assays have also been reported [48–50]. In these assays, after the immobilization

of the aptamer, a hybridization reaction with a labeled (*i.e.* with an enzyme, a redox mediator, etc.) complementary oligonucleotide sequence was performed. The subsequent incubation with the analyte, for which the aptamer possesses a higher affinity with respect to the complementary sequence, leads to the displacement of the labeled complementary DNA/RNA probe with the consequent decrease of the analytical signal.

1.3.3 Switch-on/-off Assay

Exploiting the 3D folding-based structure, two labeled strategies, named switch-on and switch-off, are described in literature. In both approaches, an aptamer functionalized with an electroactive molecule (*i.e.* ferrocene, methylene blue, etc.) is immobilized on the electrode surface.

In the switch-on assay, after the binding reaction with the analyte, the conformational change of the aptamer structure decreases the distance between the redox molecule and the electrodic surface, leading to an increase of the measured electrochemical signal. In the case of switch-off strategy, the distance between the electroactive molecule and the electrode surface increases and, thus, a decreasing of the electrochemical signal is observed [18,49,50].

1.3.4 Label-free Assays

In the label-free approach, the aptamer-analyte binding modifies the interfacial properties of the aptasensor surface [48,51,52].
Label-free displacement assays using unlabeled complementary sequences were also reported. In this approach, the changing of the molecules bound to the aptasensor leads to an increase of the recorded capacitance or resistance values because of steric hindrance and electrostatic interactions. The advantage of the label-free strategy is the real-time evaluation of the analyte-bioreceptor binding [53–55].

1.4 New Approaches for Electrochemical Aptasensors based on Screen-Printed Transducers

The combination between aptamers and electrochemistry offers the possibility to develop a huge number of simple-to-use devices with a low cost, fast and sensitive response and a high selectivity. These features make them particularly suitable for on-field screening analysis, being easily coupled to portable devices, especially when the use of screen-printed electrodes (SPEs) is exploited as an advantageous alternative with respect to classical solid electrodes.

Screen-printing technology is based on a layer-by-layer deposition of a peculiar ink mixed with a conductive powder (*e.g.* graphite or a metal like gold, silver or platinum) on a polymeric support; the printing process makes use of proper screens or meshes, in order to define the size and the shape of the disposable electrochemical cells, usually produced in a three-electrodes configuration. This technology owns the advantages given from the flexibility of the design, the automation of the process, a good reproducibility and a wide choice of materials, which determine the selectivity, the sensitivity and the adequacy of their use in certain kinds of analysis [56].

The low cost and ease of mass production represent the main advantages of SPEs, combined with the possibility of miniaturization and lowering the sample volume, allowed by their reduced dimensions: all these features are the primary element to be taken into account when developing small and portable devices for on-field analysis [57].
Even in the context of the laboratory routine, SPEs can represent the solution to some drawbacks given by solid electrodes, like memory effect or long cleaning procedures, which can affect also the reproducibility of the measurements [58].

Some limitations can be observed in case of the use of organic

solvents, as they may dissolve the insulating ink used to protect electric contacts, thus being a source of damage for SPEs structure [59]; nevertheless, examples of SPEs compatible with the use of organic solvents are reported [60]. Moreover, in some cases, small dimensions can cause low sensitivity, due to the low-rate electron transfer [61].

To solve these issues (even if some works still report the use of unmodified electrodes [62]), electrochemical and biochemical modifications can be exploited to improve their performance: in the case of SPEs, these modifications are simpler if compared to those being done on ordinary electrodes, which need several polishing, preparation and refreshment steps. In this way, SPEs characteristics were adapted to those required by different classes of analytes [56–58]; the most recent developments are connected with the use of nanostructured materials, which represent the most promising field to be used in SPEs functionalization [63].

2. Food Contaminants

The presence of harmful chemicals and microorganisms in food is often addressed ad food contamination, which can cause consumer illness at different levels of severity. Food security has the challenge of assuring food to be safe from a chemical, physical and biological point of view.
This aspect of food security is called food safety (an umbrella term that encompasses many facets of handling, preparation and storage of food to prevent illness and injury) including chemical, microphysical and microbiological aspects of food quality [64]. In fact, unsafe food containing harmful bacteria, viruses, parasites or chemical substances causes more than 200 diseases — ranging from diarrhea to cancer [65].
Specifically, chemical contamination of food is opposed to microbiological contamination, which is normally found under foodborne illness. Chemical contaminants, unlike foodborne pathogens, are often unaffected by thermal processing [66]: for this reason, the impact they may exert over consumer health could be also manifested only after many years of processing and prolonged exposure at low levels. A classification of food contaminants can be made according to the contamination source and to the mechanism by which they enter the food products: in fact, food contamination could be due both to naturally occurring environmental contaminants or to substances artificially introduced by humans.
Product mislabeling, accidental cross-contamination or intentional adulteration with low quality or unsafe ingredients for economic purposes could also constitute a serious drawback. Therefore, to help manufacturers improve the quality of their food production in terms of hazard analysis of critical control points (HACCP) risk assessment and good manufacturing practice (GMP), sensitive analytical methods are required.

Food quality control is essential for consumer protection as well as for food industry. Regulatory agencies as the United States Food and Drug Administration (US FDA) and the European Food Safety Authority

(EFSA) are laying some strict guidelines containing the maximum levels accepted for certain contaminants in foodstuff to maintain a high standard of human health and consumer protection [67]. Potential hazardous residues in food include several different substances: natural and environmental contaminants (*e.g.* toxins, heavy metal ions), agrochemicals pollutants like pesticides, human and veterinary drugs, growth promoters, packaging components, and others [68]. The detection of contaminants is then of utterly importance in food safety and environmental analysis; thus, it requires highly sensitive and easy-to-use analytical procedures to be developed.

Conventional analytical methods used for this kind of analysis include separation techniques (*e.g.* high-performance liquid chromatography, tandem mass spectrometry), which often provide sensitive and selective results [69]. Despite the advantages of these techniques, the high costs, the expensive instrumentation, the technical skills needed for users and the complex pretreatment processes are pushing scientists to find out rapid, low cost, highly sensitive and simple alternative analytical methods [70]. In the actual context of intensive agriculture, the assessment of food quality requires fast screening of contaminants: in this perspective, the development of biosensors for this aim has gained increasing interest, as these devices come to meet the aforementioned requirements [71].

2.1 Pesticides

Agrochemicals are chemicals used in agricultural practices and animal husbandry with the aim to increase crop yields; such agents include pesticides, plant growth regulators and veterinary drugs.
Among these, pesticides are those substances or mixture of substances used to limit the growth of infesting species (*e.g.* insects, weeds, little mammals, fungi, etc.) that can compromise the agricultural production

[72]. As stated by Food and Agriculture Organization (FAO), a pesticide is usually intended to control pests; nevertheless, for the actual purposes, this term embraces also some materials used to modify pests or crops behavior or physiology (*e.g.* insects repellents, germination inhibitors) [73]. The recent history of agricultural production has been characterized by the use of different kinds of chemical substances to control pests, starting with inorganic compounds (*e.g.* sulphur, arsenic, mercury, lead) and it viewed a great change after the discovery of dichlorodiphenyltrichloroethane (DDT) as an insecticide in 1939 by Paul Müller, that became soon widely used [74].

Approximately 3 billion kg of pesticides are spread each year around the world, about 45% of which in Europe, 25% in USA and 25% in other countries: this poses a serious threat, as the chemicals contaminate the raw sources of food [75,76]. Besides the prevention of crop losses gained with their use, pesticide residues may get access to the food chain through air, water and soil and cause acute and delayed effects on the health of exposed people, such as cancer, sterility, deformation in fetuses, allergies, asthma, neurological diseases and acute intoxication [77]. The worldwide estimation of pesticides poisoning accounts for millions of people, with more than 300'000 deaths every year due to this poisoning [78].

Pesticides are characterized by a great diversity of chemical structures, action mechanisms and usages, therefore they can be listed according to many different criteria, such as their application purpose, their chemical structure, or others as their stability and their penetration into the organisms [79]. Among the several classes of pesticides (*e.g.* herbicides, fungicides, bactericides, virucides, nematicides and so on), insecticides, which are used to kill infesting insects, are claimed to be a major factor in causing the increase of the agricultural productivity in the 20th century [80].

2.1.1 Organophosphorus Pesticides

Organophosphates (*e.g.* phorate, profenofos, isocarbophos, chlorpyrifos, parathion) are a large class of contact insecticides with the same target of the class of carbamates, as they irreversibly inhibit acetylcholinesterase and other cholinesterases, which are essential enzymes for the proper function of the central nervous system both in humans and insects. This inhibition causes an accumulation of the neurotransmitter acetylcholine in nerves, which affects the normal functioning of muscles and vital organs, thus leading to severe symptoms or even death; chemical warfare nerve agents act in the same way [81]. Over the last years, compounds and formulations characterized by a fast biodegradation and low persistence, as organophosphorus pesticides (OPPs) are, began to replace some of the oldest types of compounds (*e.g.* organochlorines), whose active molecules can persist in the environment for more than 30 years [82]. Thus, the analysis of pesticide residues is an important concern due to their bioaccumulation effect, high toxicity and long-term damage risk to environment and human health security.

The chemical structures of some OPPs are shown in **Figure 2.1**.

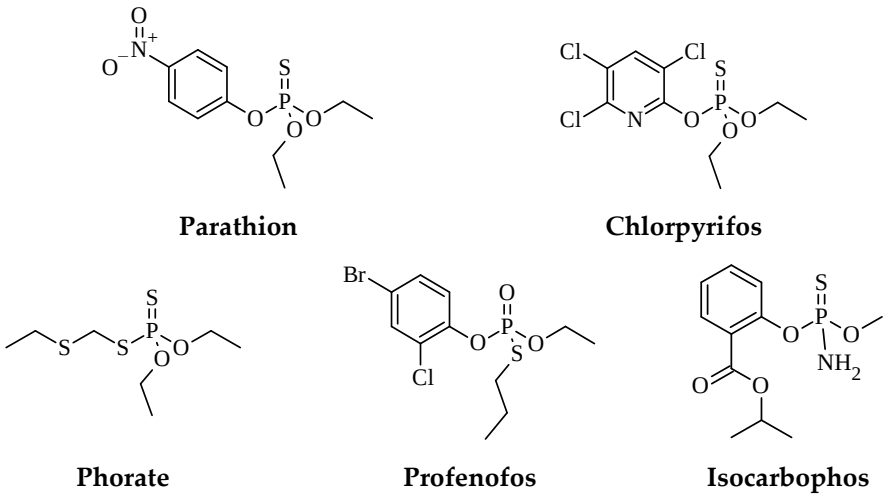

Figure 2.1. *Chemical structures of the most commonly used organophosphorus pesticides.*

2.2 Mycotoxins

The term "toxin" refers to a poisonous substance produced within living cells or organisms (*e.g.* small molecules, peptides, proteins) [83] capable of causing a disease upon contact or absorption by body tissues. The toxicity of these substances owns a great variability, ranging from minor (as a bee sting) to deadly (as botulinum toxin). Among these, mycotoxins (from the Greek *mykes*, "fungus" and *toxini*, "toxin") are defined as toxic secondary metabolites, of wide ranging structural diversity but low molecular weight, produced by organisms belonging to the fungus kingdom which are able to cause both diseases and even death in humans and other animals [84]. The reason for the production of mycotoxins is not yet known, as they are not necessary either for fungi growth or development [85]. This term is often used for those toxic chemical products that promptly colonize crops [86] and other foodstuffs (*e.g.* coffee, dried fruits, spices, etc.) both at field and postharvest stages of production.

As estimated by FAO, about 25% of the world's food crops are contaminated with mycotoxins to a certain degree: they can be commonly found in wine and beer from contaminated grapes, cereals but also meat and other animal products (*e.g.* eggs, milk, cheese) due to the food chain. One of the main obstacles about these molecules is their high chemical stability, as they cannot be destroyed even during high-temperature cooking processes [87]. To add complexity, a single species of fungi may produce multiple different mycotoxins, and several species can be present simultaneously: therefore, the multi-exposure to various mycotoxins may lead to enormously augmented toxicity due to possible synergistic effects [88,89]. Moreover, the severity of their adverse impact on human health (*e.g.* gastrointestinal diseases, kidney damage, immune suppression — generally defined as mycotoxicosis) depends on the intrinsic toxicity of the mycotoxins themselves, the extent of the exposure, the age and the

nutritional status of the individual and to combined effects with other chemicals to which the individual is exposed [90]. As a consequence, the US FDA has determined the lowest levels of mycotoxins that can be consumed in food [91,92]. Although in nature there are about 300 known mycotoxins with wide ranging structural diversity, many of them are still not identified and classified. The most relevant mycotoxins groups under a toxicological and a legislative point of view include aflatoxins, ochratoxins and some trichothecenes (fumonisins, deoxynivalenol, T-2, HT-2 and zearalenone); others such as patulin, citrinin, moniliformin, tremorgenic mycotoxins and ergot alkaloids fall outside these families but are still of significant importance [93,94].

2.2.1 Aflatoxins

Aflatoxins form one of the major grouping of mycotoxins and are mainly produced by fungi of the species *Aspergillus*, such as *A. flavus* (from which the term "aflatoxin" was coined around 1960, after its discovery as the source of "Turkey X disease" [95]) and *A. parasiticus*. This class includes four main types of mycotoxins produced: aflatoxin B_1 (AFB_1), aflatoxin B_2 (AFB_2), aflatoxin G_1 (AFG_1) and aflatoxin G_2 (AFG_2). Letters B and G derive from the terms "blue" and "green", respectively, which indicate the fluorescence type emitted from these substances when irradiated by UV light at 360 nm [96]. These basic aflatoxins are not soluble in water, and the liver can metabolize them to reduce their toxicity by adding an OH-group to form hydroxylated metabolites, such as aflatoxin M_1 (AFM_1), aflatoxin M_2 (AFM_2), aflatoxin P_1 (AFP_1), aflatoxin Q_1 (AFQ_1) and aflatoxicol (AFL), which are water soluble and can be excreted from the body through milk (from which the M letter comes from) [97,98].

The chemical structure of these molecules is shown in **Figure 2.2**.

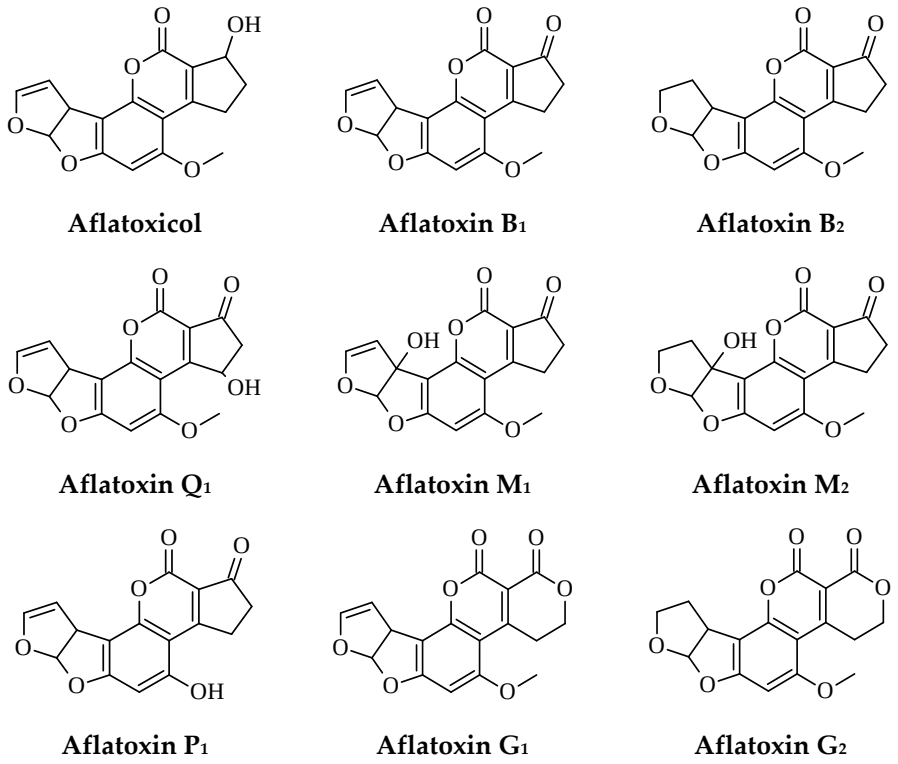

***Figure* 2.2.** *Chemical structures of basic aflatoxins and their hydroxylated metabolites.*

2.2.2 Trichothecenes

Trichothecenes constitute a family of more than sixty sesquiterpenoid metabolites produced by a number of fungal genera, including *Fusarium*, *Myrothecium*, *Phomopsis*, *Stachybotrys*, *Trichoderma*, *Trichothecium*, and others. The term "trichothecene" is derived from "trichothecin", which was the one of the first members of the family to be identified.

All trichothecenes contain a common 12,13-epoxytrichothene skeleton and an olefinic bond with various side chain substitutions; moreover, they are classified as macrocyclic or nonmacrocyclic, depending on the presence of a macrocyclic ester or an ester-ether bridge between C-4 and C-15 [99]. Nonmacrocyclic trichothecenes can in turn be classified into two

subgroups: type A, whose elements have a hydrogen or ester type side chain at the C-8 position, and includes T-2 toxin, neosolaniol, and diacetoxyscirpenol (DAS), while type B subgroup contains elements bearing a ketone in the same position, and include fusarenon-x, nivalenol (NIV), and deoxynivalenol (DON). They are commonly found as food and feed contaminants, and their consumption can result in alimentary hemorrhage and vomiting; direct contact causes dermatitis [100].

The chemical structure of these molecules is shown in **Figure 2.3**.

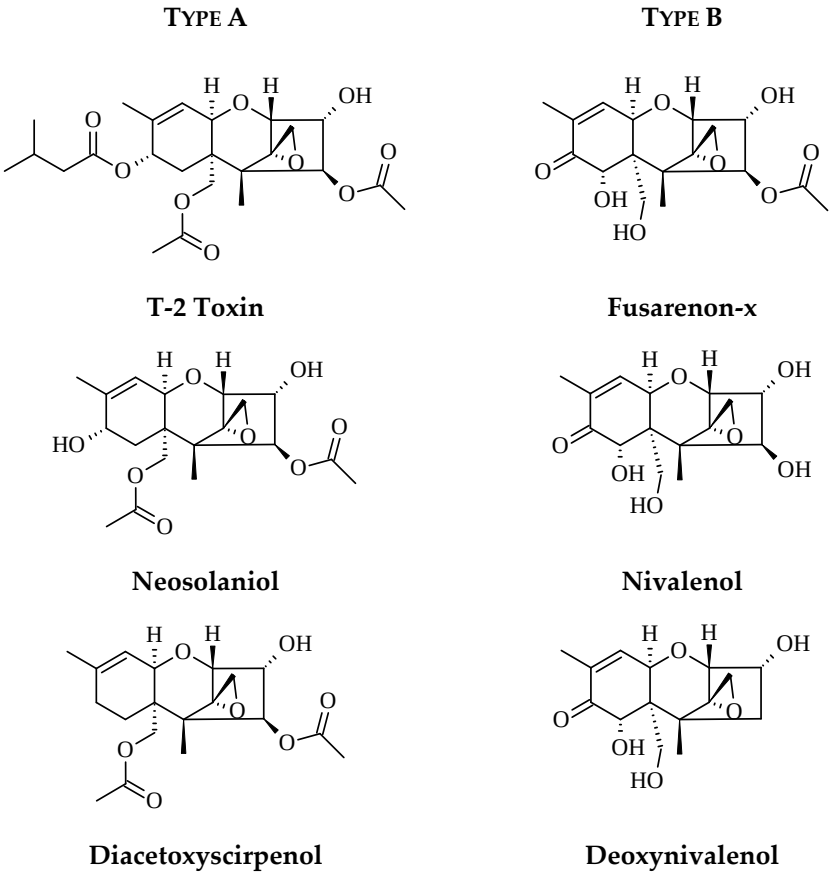

Figure 2.3. *Chemical structures of the most common nonmacrocyclic trichothecenes.*

2.3 Allergens

The National Institute of Allergy and Infectious Diseases (NIAID) of the United States defines food allergy as "an adverse health effect arising from a specific immune response that occurs reproducibly on exposure to a given food" [101]. Food allergens are recognized by the Codex Alimentarius as foods or ingredients that are known for causing hypersensitivity and hence shall always be declared. These group of substances comprises proteins from peanuts, tree nuts, fish [102–105], crustaceans, mollusks, wheat and gluten-based cereals, soy [106–108], eggs [109], milk [110–112], celery, mustard, sesame, lupin [113] and also sulphites at concentrations of 10 mg/kg or more [114]. All these trigger an immunologic mechanism represented almost exclusively by IgE-mediated severe adverse reactions [115].

Adverse reactions to foods are in fact divided into non-toxic and toxic reactions, whereas the first ones are subdivided into immune- and non-immune-mediated reactions [116]. Symptoms of an immunological reaction depend from person to person and can involve digestive disorders, circulatory or respiratory symptoms or skin irritations, among others; besides, an allergic reaction can also provoke in some cases life-threatening situations as anaphylactic shocks [117].

No current treatment or vaccine can be a cure for hypersensitive immune responses to food: for this reason, allergic individuals must strictly avoid the consumption of the allergenic food to prevent possible life-threatening reactions. Nevertheless, many patients could experience an accidental exposure to a known allergen, due to the complexity of food preparation methods in the modern diet, despite the careful effort put forth by manufacturers. Hence, food allergic patients are still at high risk of unintentionally consuming trace amounts of allergens that may have contaminated food products during the production line. For these reasons, allergic consumers are limited in the consumption by food products

labeled with "may contain", that are being completely avoided for safety concerns [118]. Moreover, allergens may not always be identified by the consumer, both for unintentional reasons (such as product mislabeling) or even intentional ones (such as adulteration with low quality or unsafe ingredients for economic purposes) [119–121].

In this perspective, it becomes clear that to establish an appropriate analytical methodology for detection of traces of allergens is of outstanding importance; moreover, the investigation on the effect of food processing on both allergenicity and detectability needs to be carried out.

2.3.1 Milk Allergens

Milk is a complex matrix in the form of an emulsion of butterfat globules within a water-based fluid that contains many nutrients, as dissolved carbohydrates (*e.g.* lactose) and protein aggregates with minerals. A study carried out in 2014 by Nwaru and collaborators about the incidence of the most popular food allergies throughout Europe [122] revealed that allergy to cow's milk is, nowadays, the most frequent food allergy, especially in early-age children: it implies a percentage of around 6% in the youngest population [123,124] and about 2–3% of infants [125]. Although milk is one of the food ingredients which should be listed on the label of commercial food products, most of the immunoreactions in consumers occurs because of an unexpected exposure to milk proteins even in "non-dairy" preparations, which might contain unlabeled additives or milk-based contaminants.

Cow's milk allergy (CMA) can be defined as any immuno-mediated adverse reaction to cow's milk proteins, with symptoms usually occurring within 2 h after milk intake [126]. Cow's milk contains more than 25 different proteins, but only some of them have been identified as allergens: whey proteins alpha-lactalbumin (α-LA), beta-lactoglobulin (β-LG), bovine serum albumin (BSA), lactoferrin (LF) [127], four caseins [128].

3. Electrochemical Set-Up

3.1 Techniques

Among all the electrochemical techniques used for labeled assay, voltammetry (in which the current is measured in relation to a potential variation) plays a special role. In particular, because of the increasing of the signal-to-noise ratio (due to the reduction of the background and capacitive current), which leads to an increase of the sensitivity, pulsed voltammetric techniques (such as DPV and SWV) have been widely applied.

The use of a label-based approach, coupled with pulsed voltammetric techniques, allows the decreasing of the non-specific signal (with the consequent increasing of the sensitivity) but with an increase of the cost and of the working time of the assay [129,130].

In the label-free approach, the aptamer-analyte binding modifies the interfacial properties of the aptasensor surface. Different electrochemical techniques, such as CV, potentiometry, and EIS can be used.

3.1.1 Cyclic Voltammetry

Cyclic voltammetry (CV) is a powerful and popular electrochemical technique commonly employed to investigate the reduction and oxidation processes of molecular species [131] and largely applied for the determination of their thermodynamic and kinetic parameters [9].
CV can be also applied for the characterization of the electrodic surface, fast determination of the redox potentials of electroactive targets and comparisons between different media effects on redox processes.

In CV, the electrode potential ramps linearly versus time in cyclical phases (**Figure 3.1**). The changes that do appear on repetitive cycles are important keys to unlock information about reaction mechanisms [132].

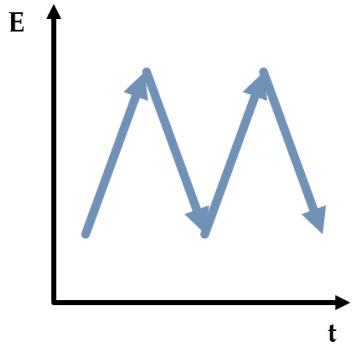

Figure 3.1. *Potential waveform applied in cyclic voltammetry.*

The potential is measured between the working electrode and the reference electrode, while the current is measured between the working electrode and the auxiliary electrode. The results of this measurement are commonly reported as current (i) versus applied potential, or voltage (E), in a plot called voltammogram (**Figure 3.2**).

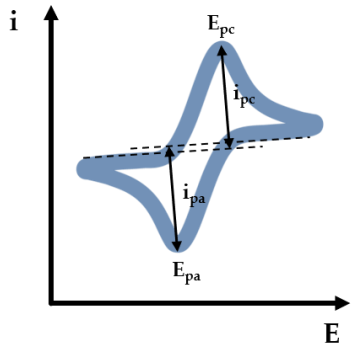

Figure 3.2. *Example of a cyclic voltammogram for a reversible redox process.*

By the analysis of a cyclic voltammogram, it is possible to determine the cathodic peak potential (E_{pc}), related to the reduction process and the anodic peak potential (E_{pa}), related to the oxidation process. Both processes define their characteristic peak current, indicated as i_{pc} for the cathodic peak and i_{pa} for the anodic one.

The analyte may display a reversible CV wave, which is observed when all of the initial amount of the analyte can be recovered after a forward and reverse scan cycle. The more reversible this process is, the more similar the oxidation peak will be in shape to the reduction peak.

Reversibility implies that the system is at equilibrium at all potentials, which means that the Nernst equation is valid at these potentials. The peak current for a reversible system at 298 K is given by the Randles-Sevcik equation [133] (*Equation 3.1*)

$$i_p = (2.69 \times 10^5)\, n^{3/2}\, AcD^{1/2} v^{1/2} \qquad (3.1)$$

where:

- i_p is the peak current (A);
- A is the electrode area (cm^2)
- D is the diffusion coefficient (cm^2/s)
- c is the concentration of the analyte (mol/cm^3)
- v is the scan rate (V/s).

The peak current is directly proportional to the concentration and it increases with an increase in the square root of the scan rate ($v^{1/2}$).
For a simple reversible couple, the magnitude of i_{pa} is equal to that of i_{pc} and, for a monoelectronic process, ΔE_p = 0.059 V.

3.1.2 Differential Pulse Voltammetry

Differential pulse voltammetry (DPV) is a voltammetry method used to make electrochemical measurements, with a series of regular voltage pulses superimposed on a linear potential sweep or stairsteps (**Figure 3.3**) [134].

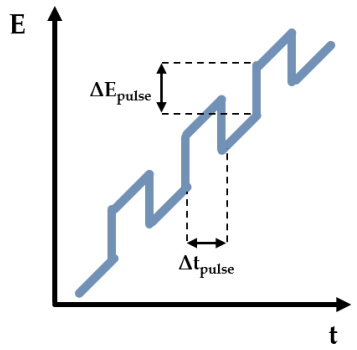

Figure 3.3. *Potential waveform applied in differential pulse voltammetry.*

The system of this measurement is usually the same as that of standard voltammetry. The potential between the working electrode and the reference electrode is changed from an initial potential to an interlevel potential by a pulse of a defined magnitude, the pulse amplitude (ΔE_{pulse}), which remains constant for a defined time (Δt_{pulse}); then it changes to the final potential, which is different from the initial potential. The value of the current between the working electrode and auxiliary electrode is sampled before the pulse application and before the pulse ending.
The difference between these values is plotted against the potential, obtaining a peak-shaped voltammogram (**Figure 3.4**) with the peak height and area being directly proportional to the analyte concentration, while the peak position (defined by the peak potential) is related to the redox potential of different electroactive species.

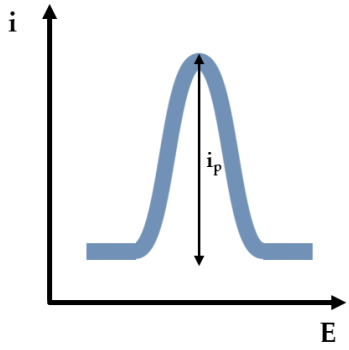

Figure 3.4. *Example of a typical differential pulse voltammogram.*

The main advantages of DPV, as well as other pulsed voltammetric techniques, consist in increasing the signal-to-noise ratio because of the reduction of background currents and in reducing the interference of capacitive currents, as their decay is faster than that of faradaic currents. Compared to other non-pulsed voltammetric techniques, DPV relies on a higher sensitivity and lower LODs; moreover, the peak-shaped response allows the determination of species with a small separation in their redox potentials, making this technique to be particularly useful for mixture analysis.

3.1.3 Electrochemical Impedance Spectroscopy

Electrochemical impedance spectroscopy (EIS) is an analytical method that can provide information about the characteristics of an electrodic surface and about changes of bulk solution properties [135].
EIS measurements are generally carried out in two different modes.

- *Galvanostatic mode.* A sinusoidal alternating current (AC) is superimposed to a selected direct current (DC), giving a phase-shifted AC voltage as the response.
- *Potentiostatic mode.* A sinusoidal AC voltage is superimposed to a selected direct DC potential, giving a phase-shifted AC current as the

response.

By the variation of the frequency of the applied signal, the impedance (Z) of the electrode surface can be determined by the ratio between the time-dependent function of the applied AC potential *E(t)* and the related AC current *i(t)* in potentiostatic mode (*Equation (*3.2)

$$Z = \frac{E(t)}{i(t)} = \frac{E_0 \sin(2\pi\upsilon t)}{i_0 \sin(2\pi\nu t + \varphi)} = Z_0 \frac{\sin(2\pi\upsilon t)}{\sin(2\pi\nu t + \varphi)} \qquad (3.2)$$

where:

- E_0 is the potential value at t = 0;
- i_0 is the current value at t = 0;
- Z_0 is the impedance value at t = 0;
- ν is the frequency;
- φ is the phase shift between the potential time function and the current time function (**Figure 3.5**).

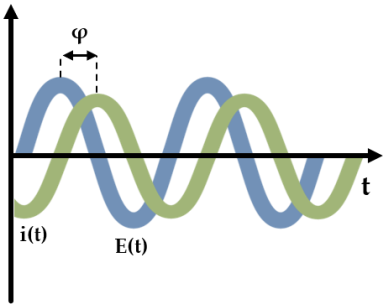

Figure 3.5. *Phase-shifted potential and current time functions.*

Although impedance is only present in AC systems, it works in a similar manner as the resistance as it represents the total electron opposition within a circuit and takes into account contributions from resistors, capacitors and inductors; therefore, it is often presented as a

complex number (*Equation* (3.3)

$$Z = Z_0(\cos\varphi + j\sin\varphi) = Z' + jZ'' \qquad (3.3)$$

where:

- j is the imaginary unit;
- Z' is the real part of the impedance, or resistance (R);
- Z'' is the imaginary part of the impedance, or reactance (X).

Results of EIS measurements are generally reported in the form of a Nyquist plot in which the opposite of the imaginary component is plotted against the real one (**Figure 3.6**).

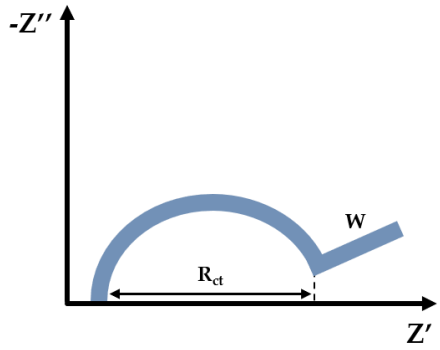

Figure 3.6. *Example of a Nyquist plot.*

An equivalent circuit (*i.e.* Randles circuit) is then properly selected to define the analytical information, mainly expressed in terms of double-layer capacitance (C_{dl}, related to the charging of the double layer at the electrode interface), charge transfer resistance (R_{ct}, that depends from the current flow produced by the redox reaction at the interface) or Warburg diffusion element (W, that models the diffusion process).

In biosensor application, EIS spectroscopy can be used to characterize each electrode modification step (*e.g.* surface conductivity modification,

self-assembly of monolayers, probe immobilization), as well as to perform label-free quantitative measurements (*e.g.* interaction between the immobilized probe and the target, enzymatic production of insoluble species [136,137]). In comparison with other techniques, EIS allows a proper sensitivity for the evaluation of the bioreceptor-analyte interaction, despite the use of a specific instrumentation and data analysis [138,139].

3.2 Apparatus

Voltammetric measurements were performed with PalmSens2 portable potentiostat/galvanostat (PalmSens BV, Houten, The Netherlands) controlled by PSTrace 5.8 software for data acquisition and elaboration. Impedimetric measurements were performed with an Autolab PGSTAT 30(2) potentiostat/galvanostat (Metrohm Autolab BV, Utrecht, The Netherlands) equipped with a FRA2 module and controlled by NOVA 2.1 software for data acquisition and elaboration.
The experimental data were fitted by using OriginPro 2020 software (OriginLab, Northampton, USA).

Screen-printed electrochemical cells based on a graphite working electrode, a graphite counter electrode and a silver pseudo-reference electrode (EcoBioServices, Florence, Italy), in both single-cell (**Figure 3.7**) and 8-cells array configurations, were used for the electrochemical experiments.

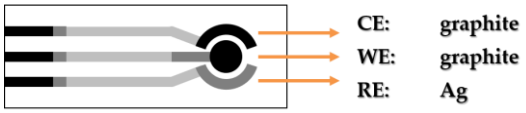

Figure 3.7. *Schematic representation of a screen-printed electrochemical cell. CE: counter electrode; WE: working electrode; RE: reference electrode.*

4. Nanostructured Platforms

In the last years, the introduction of nanostructured systems in sensor devices has highlighted the possibility to obtain analytical systems characterized by high sensitivity, selectivity and reliability.
Because the common biological systems (such as proteins, viruses, membranes, etc.) are nanostructured and their interactions take place at nanometric scale, nanomaterials become ideal candidates for the development of advanced biosensing devices.

Nanostructures present several advantages in analytical applications and can be mainly used as transducers (due to their unique optical, chemical, electrical, and catalytic properties) or as a component of the recognition element of a biosensing device (due to the high surface-to-volume ratio that increases the number of bioreceptors attached to the sensing surface) [140]. Finally, their dimensional scale (1–100 nm) allows the miniaturizing of the sensor, which is a very crucial point in the realization of portable devices.

4.1 Conductive Polymers

Traditionally, polymers were seen as good electrical insulators and most of their applications had relied on their insulating properties [141]. However, until three decades ago, researchers showed that certain classes of polymers exhibit semiconducting properties. Such materials can combine the high conductivity of metals with the mechanical properties of polymers, such as flexibility and the ease of thin film formation. Conductive polymers, also known as "fourth generation of polymeric materials", have become competitive materials for biosensing applications and have recently attracted a lot of attention in this field [142,143].
Some features like light weight, low cost, flexibility, biocompatibility and process ability made conductive polymers an ideal platform for the

immobilization of bioreceptors.

Conductive polymers can be prepared by electrochemical or chemical oxidation of corresponding monomers in various organic solvents and/or in aqueous media [144]. In particular, electrodeposited polymers have several advantages, including the ease of preparation of uniform films with a well-controlled thickness and a peculiar conductivity directly onto the electrodic surface [145–148]; in fact the electrochemical process allows to control such film properties by the synthesis parameters as the current density, the pH, and the nature and concentration of the electrolyte.

The first time that a polymer was electrochemically prepared and characterized was in 1862 by Letheby [149], who carried out the electrolytic oxidation of a sulphatic solution of aniline (ANI) obtaining polyaniline (PANI), thus probably the earliest known synthetic polymer [150]. Since then, conducting polymers have been broadly used to modify electrodes for the development of electrochemical sensors and biosensors, as they also provide an increase of the effective superficial area [145]. Several polymer systems have been reported [151], being PANI [152], polyacetylene (PAc) [153], polypyrrole (PPy) [154], poly(3,4-ethylenedioxythiophene) (PEDOT) [155] and polythiophene (PTh) among the most intensively studied and thus widely used (**Figure 4.1**) [156].

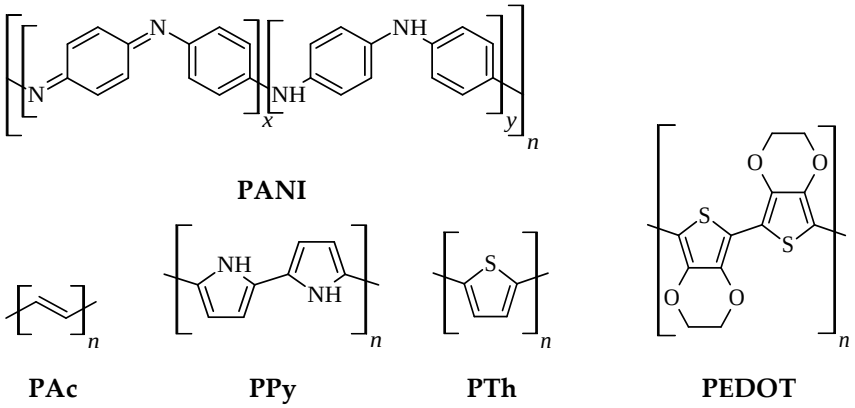

Figure 4.1. *Chemical structures of the most commonly used conductive polymers.*

4.1.1 Polyaniline

PANI, historically called "aniline black" [157], is one of the pioneering conducting polymers, which can be synthesized both chemically and electrochemically. It has been found that PANI can exist in three different and isolable oxidation states at the molecular level; other oxidation states are the result of a physical mixture of these ones [158].

- *Leucoemeraldine*. Completely reduced form, composed of solely reduced base units — formula $(C_6H_4NH)_n$;
- *Emeraldine*. Intermediate oxidation state, composed of equal amounts of alternating reduced and oxidized base units — formula $([C_6H_4NH]_2[C_6H_4N]_2)_n$;
- *Pernigraniline*. Completely oxidized form, composed of solely oxidized base units — formula $(C_6H_4N)_n$.

PANI is popular among organic conjugated polymers because of its ease of synthesis, low cost, uniform conductive mechanism, and superior environmental stability in the presence of oxygen and water [159].
In general, PANI has a high electrical conductivity only under acidic conditions due to its redox state associated with protonation of nitrogen atoms in the polymer backbone. Thus, one cannot expect a sufficient conductivity of PANI under neutral or alkaline conditions [160].
As a consequence, the best charge stabilizing agents for PANI are strong acids, which are sometimes called "doping agents" as they introduce charge carriers into polymer chains [161].

PANI can not only be used as an immobilization platform for biomolecules owing to its favorable storage ability, film-forming ability and biocompatibility, but also act as electron mediator in redox or enzymatic reactions due to its excellent conductivity and inherent electroactivity [162]. Therefore, since PANI shows peculiar conductive features only in acidic pH values, which makes its application in sensing

a big deal, it is often doped with something that can increase these properties, such as noble metal NPs or conjugate carboxylic acids [143]. Incorporation of metals and metal oxides into conductive polymers can enhance electron transfer, improving their conductivity and their stability. The obtained composite materials with a well-controlled composition and electrochemical properties provide rapid and accurate sensing due to their selectivity, high sensitivity, many active sites, homogeneity, and strong adherence to the electrode. Specifically, PANI doped with gold nanoparticles (AuNPs) has been already characterized and successfully applied as an electrochemical platform for the biosensing of pesticides in the environmental field [72,163,164].

4.1.2 Poly(Aniline-*co*-Anthranilic Acid)

A large variety of PANI derivatives can be prepared through substitutions in the ring or on the nitrogen atoms. Anthranilic acid (AA), a carboxylated aniline-based polymer capable of self-doping, is of interest as a soluble derivative of PANI that had been already used in clinical analysis [165]. The obtained copolymer combines conductive properties of ANI with the ability of AA to bind the biocomponents through its carboxylic groups.

4.1.3 Poly-L-Lysine

Apart from the aforementioned aniline-based polymers, another polymer that has attracted attention is poly-L-lysine (PLL), due to its versatility, good biocompatibility, stability and good solubility in water [166,167]. It can be quickly prepared by electropolymerization of L-lysine, an essential aminoacid usually employed in protein biosynthesis [168]. This polymer was firstly described in 1977 by Shima and Sakai as a product of a fermentation of *Streptomyces* [169], and widely used as food preservative. PLL presents a great potential as an electrode modifier in electrochemical biosensors [170], as the related monomer does not exhibit

carcinogenic effects and thus can represent a more user-friendly alternative to ANI.

4.2 Gold Nanoparticles

Over the past few decades, metal NPs have attracted much attention due to their fascinating physical, chemical, optical and electronic properties, which are significantly different from those of the bulk materials [171].

Among metal nanomaterials, gold plays a special role, as one the most studied and applied nanomaterial. AuNPs are a colloidal suspension of gold particles of nanometric dimensions. Even if the first application of AuNPs can be dated to the Roman Age to color glasses (for instance, the famous Lycurgus cup), the modern evaluation of colloidal gold began with the study of Faraday in the 1850s, which revealed that a colloidal gold solution shows different properties with respect to bulk gold (*i.e.* an intense red/purple color, in contrast with the bright yellow color of massive gold, **Figure 4.2**).

Figure 4.2. *Solutions of gold nanoparticles of increasing size.*

This phenomenon is due to their unique interaction with light called localized surface plasmon resonance (LSPR). When the oscillating electric field of incident light interacts with AuNPs, the free electrons of metal NPs undergo an oscillation with respect to the metal lattice. At a particular frequency, this process is resonant and allows the absorption of a specific photon (with an energy comprised in the visible range of the spectrum),

that confers the characteristic intense color of AuNPs dispersions [172].

The peculiar properties of AuNPs coupled to their easy synthesis, high compatibility with biological systems, and enhanced scattering and absorption have drawn particular attention in their application for developing sensors and biosensors [173].

In general, controlling the size of NPs is a key factor in the development of electrochemical sensing systems. An electrode surface can be easily modified by the direct electrodeposition of AuNPs, which was generally performed starting from an aqueous solution of $HAuCl_4$ prepared in acidic medium. Subsequently, Au(III) was reduced to Au(0) in the form of cluster aggregates by the application of a constant negative potential (or step potential) for a fixed time or by varying the potential for a different number of cycles at an optimal scan rate [174,175].

Exploiting the high affinity between gold and thiol groups, AuNPs have been successfully coupled with different thiolated biorecognition elements (such as aptamers/DNA probes, antibodies, enzymes, etc.) and extensively used in a wide range of sensing/signal amplification approaches, both in sandwich and label-free assays.

Moreover, the inclusion of AuNPs in conductive polymers can enhance electron transfer through a direct or mediated mechanism with improved conductivity and enhanced stability [14].

4.3 Nanocomposite Conductive Materials

As already sketched previously (***Section 4.1***), the properties of conductive polymers may be enhanced by the addition in the polymerization mixture of conjugate carboxylic acids or by the incorporation of noble metal NPs inside their porous matrix.
Three different platforms were then developed and studied by combining these two elements:

1. AuNPs/PANI/GSPE, obtained by depositing gold nanoparticles onto a polyaniline-modified GSPE;
2. P(ANI-co-AA)/GSPE, obtained by electropolymerizing aniline and anthranilic acid in a single step onto a bare GSPE;
3. AuNPs/PLL/GSPE, obtained by depositing gold nanoparticles onto a poly-L-lysine-modified GSPE.

Apart from the conductivity enhancement achieved, the polymer is used to provide protection against fouling of the surface and a scaffold for dispersing and anchoring the metal particles [143], which could be subsequently used for the immobilization of bioreceptors.

The nanostructured platforms were then employed in the development of different electrochemical aptasensors to detect compound of interest in food and environmental analysis, as described in the following chapters. The sensors were considered as single use, so, after each measurement, the electrodes were discarded.

4.3.1 Polymerization and Deposition Protocols

- *Polyaniline*. Electropolymerization of aniline was performed by following the optimized procedure described by Saberi *et al*. [143]. 50 μL of a 2.5 mM ANI solution in 50 mM $HClO_4$ were dropped onto the electrochemical cell and cyclic voltammograms were registered

for 10 scans from −0.4 V to +0.8 V at 50 mV/s scan rate. The modified cell was washed with 50 μL of a 0.5 M H_2SO_4 solution or Milli-Q water, depending on the subsequent modification.

- *Poly(aniline-co-anthranilic acid)*. Electropolymerization of aniline and anthranilic acid was performed by following the optimized procedure described by Lettieri *et al* [113]. 50 μL of a 2.5 mM equimolar solution of ANI and AA in 50 mM $HClO_4$ were dropped onto the electrochemical cell and cyclic voltammograms were registered for 10 scans from −0.2 V to +1.0 V at 50 mV/s scan rate. The modified cell was washed with 50 μL of Milli-Q water.
- *Poly-L-lysine*. Electropolymerization of L-lysine was performed by following a procedure described by Kuralay and collaborators with some modifications [176]. 50 μL of a 10 mM L-lysine solution in 50 mM phosphate buffer saline (PBS), 0.1 M NaCl, pH 7.5 were dropped onto the electrochemical cell and cyclic voltammograms were registered for 15 scans from −0.5 V to +1.5 V at 100 mV/s scan rate. The modified cell was washed with 50 μL of a 0.5 M H_2SO_4 solution or Milli-Q water, depending on the subsequent modification.
- *Gold nanoparticles*. Electrodeposition of gold nanoparticles was performed by following the optimized procedure described by Saberi *et al* [143]. 50 μL of a 0.5 mM $HAuCl_4$ solution in 0.5 M H_2SO_4 were dropped onto the electrochemical cell and cyclic voltammograms were registered for 15 scans from −0.2 V to +1.2 V at 100 mV/s scan rate. The modified cell was washed with 50 μL of Milli-Q water.

The polymerization profiles of PANI and P(ANI-*co*-AA) show a similar behavior (**Figure 4.3**). For potential values around +0.65 V and +0.72 V for PANI and the copolymer, respectively, the formation of the radical monomers decreases with the number of cycles: this is probably due to the fact that the polymer formed during the first cycles prevents the monomers from reaching the surface of the electrode. Thus, the

phenomenon that is mainly occurring is the growth of already formed chains, instead of the formation of new chains from the monomers. The profiles also show the redox peaks corresponding to the oxidation and the reduction of the polymer being deposited onto the surface: in this case, the current height increases with the number of cycles during the polymerization process.

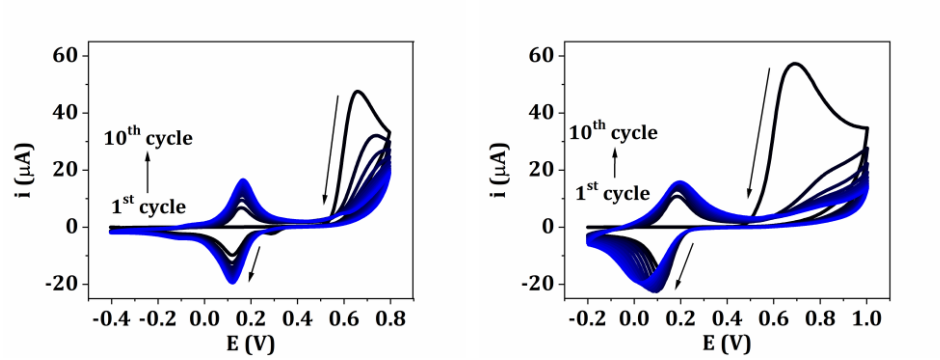

Figure 4.3. *Cyclic voltammograms of* ***(a)*** *aniline and* ***(b)*** *aniline/anthranilic acid electropolymerization at a GSPE surface.*

The number of cycles for the electropolymerization was optimized by considering the growth of the current peak height after each cycle.
No significant differences in the redox peaks were found in both cases by using 10 cycles and thus this value was used for the following experiments. These CV patterns are consistent with previous studies of electropolymerization of PANI [72] and PAA [165], since the redox peaks of the copolymer are located at potential values which are intermediate between the ones of the individual polymers.

When AuNPs were electrodeposited onto the PANI-modified GSPEs, the current peak increased dramatically; moreover, the signals related to the redox behavior of PANI are becoming less visible in the voltammogram related to gold deposition and this confirms that the polymeric layer is progressively being covered by AuNPs (**Figure 4.4**).

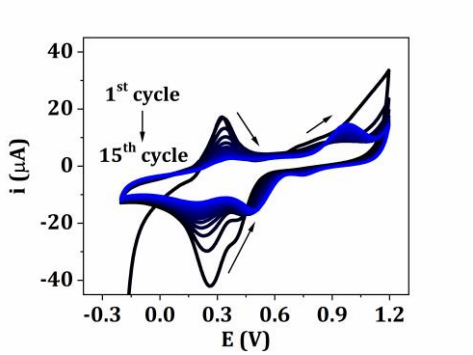

Figure 4.4. *Cyclic voltammogram of gold nanoparticles electrodeposition at a PANI/GSPE surface.*

After having performed all the modification steps, the sensors were stored at 4 °C in dry conditions for further experiments.

4.3.2 Electrochemical Characterization of the Platforms

Bare and nanostructured GSPEs were characterized in all their modification steps by means of CV at different scan rates (25, 50, 75, 100, 125, 150 mV/s) by dropping onto the SPEs 50 μL of 5 mM $[Fe(CN)_6]^{-4/-3}$ redox probe (equimolar solution in 0.1 M KCl) and by scanning the potential from −0.5 V to +0.8 V. The current peak height was taken as the electrochemical signal and plotted against the square root of the scan rate. The obtained curve was fitted with the Randles-Sevcik equation [131] (*Equation 3.1*). The platform containing PANI and AuNPs was further characterized in presence of 1 mM $[Ru(NH_3)_6]^{+2/+3}$ redox probe (equimolar solution in 0.1 M KCl) by scanning the potential from −0.55 V to +0.05 V. The choice of using two differently charged redox probes was done in order to understand the effect of the charge itself on the interaction of the redox probe with the modified electrodic surfaces. EIS measurements were also performed for this platform (frequency range: from 100 kHz to 10 mHz, amplitude: 10 mV, DC potential: +0.13 V) in presence of 5 mM $[Fe(CN)_6]^{-4/-3}$ redox probe (equimolar solution in 0.1 M KCl).

Redox peaks were observed at the modified electrodes: PANI/GSPEs, AuNPs/GSPEs and AuNPs/PANI/GSPEs gave higher current response compared to bare GSPE (**Figure 4.5** and **Figure 4.6**).

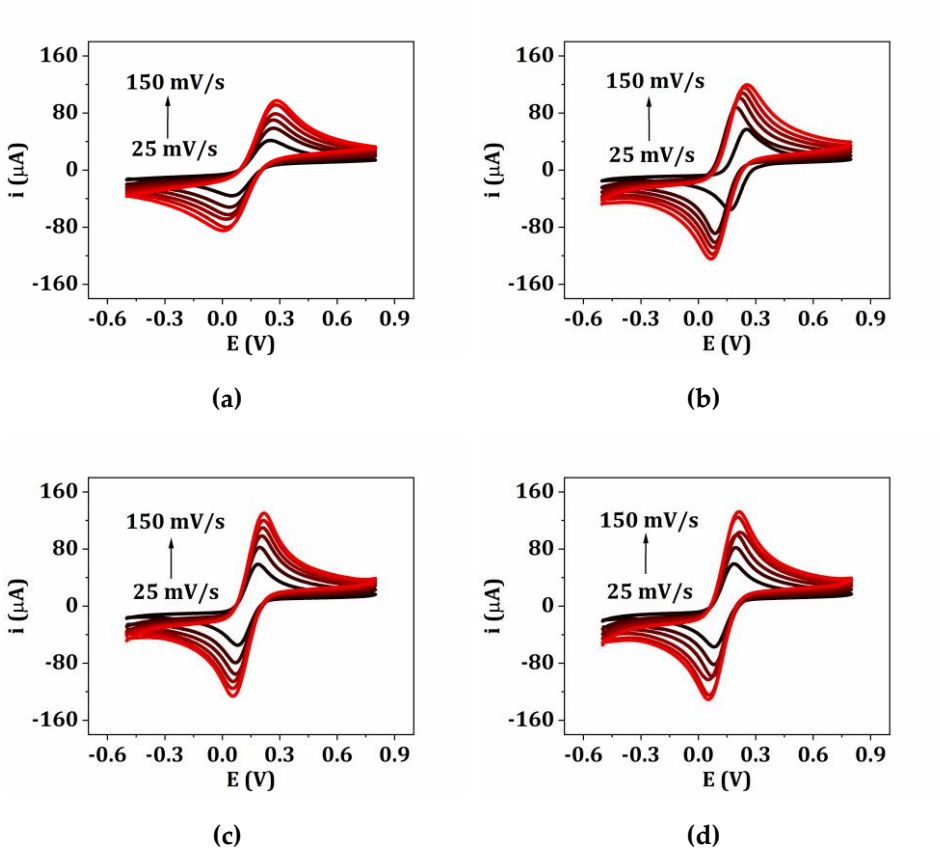

Figure 4.5. *Cyclic voltammograms of bare and nanostructured GSPEs in presence of 5 mM* $[Fe(CN)_6]^{-4/-3}$ *redox probe (equimolar solution in 0.1 M KCl).*
(a) *GSPE;* ***(b)*** *PANI/GSPE;* ***(c)*** *AuNPs/GSPE;* ***(d)*** *AuNPs/PANI/GSPE.*

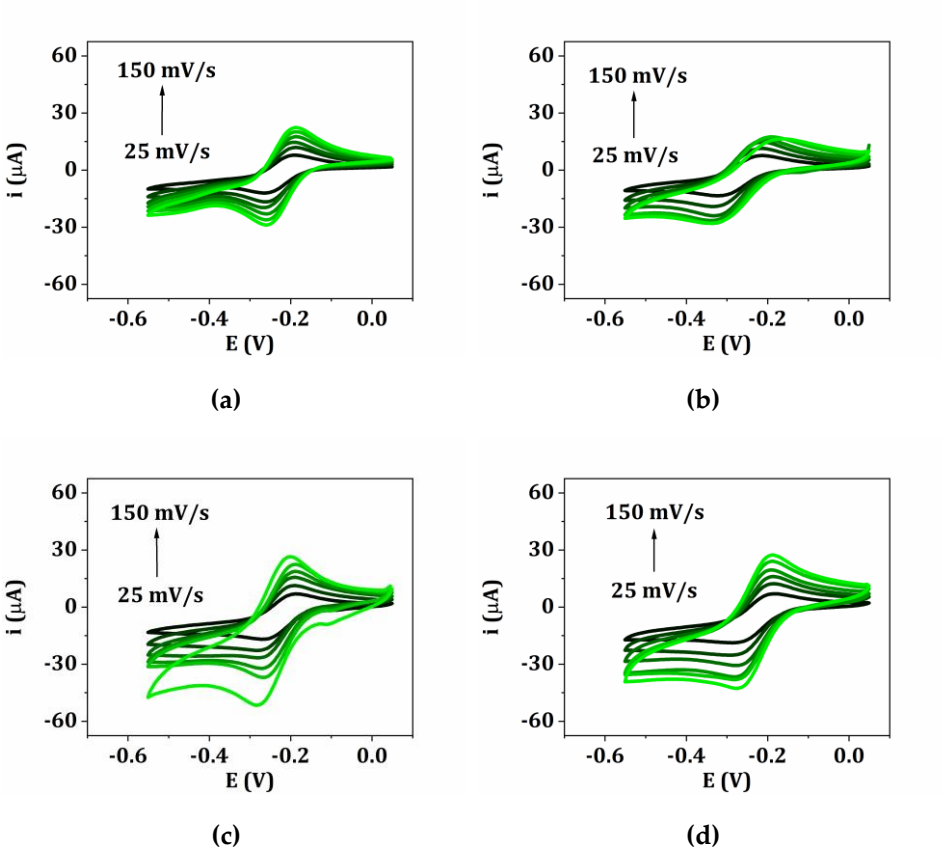

Figure 4.6. *Cyclic voltammograms of bare and nanostructured GSPEs in presence of 1 mM $[Ru(NH_3)_6]^{+2/+3}$ redox probe (equimolar solution in 0.1 M KCl).*
(a) *GSPE;* ***(b)*** *PANI/GSPE;* ***(c)*** *AuNPs/GSPE;* ***(d)*** *AuNPs/PANI/GSPE.*

Thus, the modified electrodes demonstrated a faster charge transport behavior, which was due to an increase of the effective surface area of the electrodes modified with different configurations. The scan rate study shows that both the anodic current (i_{pa}) and cathodic current (i_{pc}) increased with an increase in the scan rate (25–150 mV/s). The cooperation of PANI and AuNPs in the modified film amplified the peak current and reversibility of redox peaks, which can be related to the larger electroactive surface area of AuNPs/PANI/GSPE and electrocatalytic behavior of AuNPs, thus demonstrating the deposition of the nanostructured

materials. AuNPs are excellent electrical conductor; their incorporation generated multiple active sites, which facilitated the electron transfer across the PANI matrix during the electrochemical processes. A similar behavior was also observed for the P(ANI-*co*-AA) and the AuNPs/PLL platforms: the obtained results show that the cathodic and anodic current intensity peaks increase with increasing the scan rate [1], suggesting that the electron exchange of the redox probe towards the copolymer and the nanocomposite containing PLL is controlled by diffusion.

Regarding the electroactive surface area, a different behavior was observed for the two different redox probes used for characterizing the platform containing PANI and gold (**Table 4.1**).

Table 4.1. *Electroactive areas of the different platforms (in mm²), calculated from the CV scans performed in $[Fe(CN)_6]^{-4/-3}$ and $[Ru(NH_3)_6]^{+2/+3}$ redox probes. The percentage of variation was calculated with the average values ($\bar{A}$) with respect to the unmodified GSPE.*

		A_{anodic}	$A_{cathodic}$	$\bar{A}$	%RSD	Variation (%)
$[Fe(CN)_6]^{-4/-3}$	GSPE	6.8	6.2	6.5	7	-
	PANI/GSPE	7.8	8.3	8.0	5	+23
	AuNPs/GSPE	9.1	8.9	9.0	2	+38
	AuNPs/PANI/GSPE	9.3	9.2	9.2	1	+42
	P(ANI-*co*-AA)/GSPE	7.0	7.4	7.2	4	+11
	PAA/GSPE	6.4	7.2	6.8	7	+5
	GSPE*	3.6	3.8	3.7	5	-
	PLL/GSPE*	4.9	4.4	4.7	7	+27
	AuNPs/PLL/GSPE*	5.9	5.3	5.6	8	+51
$[Ru(NH_3)_6]^{+2/+3}$	GSPE	1.8	2.1	2.0	10	-
	PANI/GSPE	0.8	1.4	1.1	36	–45
	AuNPs/GSPE	2.3	3.1	2.7	22	+35
	AuNPs/PANI/GSPE	2.1	2.4	2.3	8	+15

*The characterization was conducted with a different batch of GSPEs.

[1] For the sake of conciseness, only the voltammograms related to the AuNPs/PANI nanocomposite building steps are shown.

In the case of the negatively charged redox couple ($[Fe(CN)_6]^{-4/-3}$), the value increased following the order GSPEs < PANI/GSPEs < AuNPs/GSPEs < AuNPs/PANI/GSPEs, as the negative charge of the complex is probably being attracted by the positively charged amino groups of PANI polymeric backbone. The same trend was observed with the nanocomposite platform containing PLL. Regarding the copolymer, the value increased following the order GSPEs < PAA/GSPEs < P(ANI-*co*-AA)/GSPEs and the extent of the increase is lower, probably due to the presence of the carboxylic groups of AA monomers. In the case of the positively charged redox couple ($[Ru(NH_3)_6]^{+2/+3}$), the value increased following the order PANI/GSPEs < GSPEs < AuNPs/PANI/GSPEs < AuNPs/GSPEs; even if the use of PANI gave a more reproducible surface, the presence of the polymer established a charge repulsion with the redox probe, which led to a decrease of the electroactive area value with respect to GSPEs and AuNPs/GSPEs. EIS measurements confirmed the above findings about the AuNPs/PANI platform, as the obtained results are complementary to those given by CV: in fact, the diameter of the circular part of the Nyquist plots (related to R_{ct}) of the electrodes modified with different configurations decreased in the order GSPE > PANI/GSPE > AuNPs/PANI/GSPE (**Figure 4.7**).

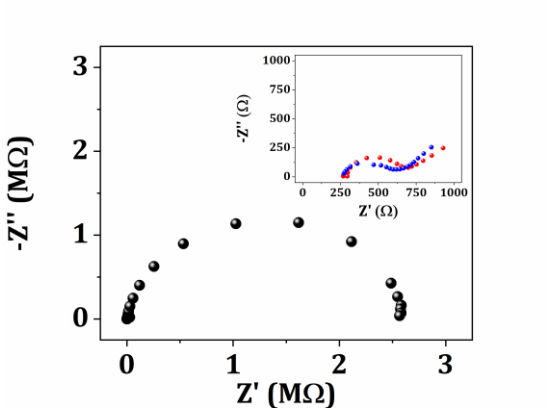

Figure 4.7. *Nyquist plots of bare and modified GSPEs in presence of 5 mM* $[Fe(CN)_6]^{-4/-3}$ *(equimolar solution in 0.1 M KCl):* • *GSPE,* • *PANI/GSPE,* • *AuNPs/PANI/GSPE.*

sensors

MDPI

5. Electrochemical Nanocomposite Single-Use Sensor for Dopamine Detection

Sensors, **2019**, *19*(14), 3097 — **DOI**: 10.3390/s19143097

5.1 Abstract

In this work, we report the development of a simple and sensitive sensor based on graphite screen-printed electrodes (GSPEs) modified by a nanocomposite film for dopamine (DA) detection. The sensor was realized by electrodepositing polyaniline (PANI) and gold nanoparticles (AuNPs) onto the graphite working electrode. The sensor surface was fully characterized by means of the cyclic voltammetry (CV) technique using $[Fe(CN)_6]^{-4/-3}$ and $[Ru(NH_3)_6]^{+2/+3}$ as redox probes. The electrochemical behavior of the nanocomposite sensor towards DA oxidation was assessed by differential pulse voltammetry (DPV) in phosphate buffer saline (PBS) at physiological pH. The sensor response was found to be linearly related to DA concentration in the range 1–100 μM DA, with a LOD of 0.86 μM. The performance of the sensor in terms of reproducibility and selectivity was also studied. Finally, the sensor was successfully applied for a preliminary DA determination in human serum samples.

Keywords: dopamine; conducting polymer; gold nanoparticles; serum; electrochemical.

5.2 Introduction

5.2.1 State of the Art

The understanding of the chemistry of the brain, its structure, functions and, in particular, the neurotransmission process, has been a long-term goal. The brain plays a major role as both an information storage and a processing system. Neurotransmission is the process of exchanging and using of this information, and it occurs within a discrete group of highly specialized cells called neurons. Neurotransmitters are substances that aid in transmitting the impulses between the nerve cells, or between a nerve and a muscle, acting as messengers in the synaptic transmission process [177]. They are essential for human health and any imbalance in their activities can cause serious mental disorders. Neurotransmitters are present in various biological fluids, including serum, plasma, platelets, cerebral spinal fluid, urine, and saliva.

Designed electrochemical sensors and micro-sensors have demonstrated a great potential for rapid, real-time measurements with high spatial resolution [178–181]. Therefore, they can facilitate the study of the role and action mechanism of neurotransmitters. Moreover, they can find potential uses in biomedicine because real-time monitoring of extracellular neurotransmitters concentration offers great benefits for the diagnosis and treatment of neurological disorders and diseases [182,183]. The use of electrochemical sensors for DA determination represents a perfect analytical approach considering their low cost and the short time required for the analysis. Moreover, they can be suitable for a routine chair-side test represented by a point-of-care testing (POCT) device. Different strategies have been employed to realize the modification of electrode surfaces for improving the selectivity, sensitivity, and accuracy [184–191]. Nanocomposite films involving conducting polymers have already been applied in DA detection. For instance, Zablocka *et al*. [192] reported the modification of a gold electrode with a PPy-mesoporous

silica molecular sieves nanostructured film, while Ali *et al*. [193] presented a PANI-carbon nanotubes composite applied *via* a nonoxidative approach. Many electrochemical approaches with low LODs for DA have been already presented [194–197] and most of them make use of glassy carbon, carbon paste [198], or gold electrodes, which are not disposable and whose surface is sometimes difficult to be properly cleaned or regenerated.

5.2.2 Target Analyte

DA is a neurotransmitter belonging to the catecholamine family. DA plays a crucial role in motor coordination, motivational behavior and the regulation of cognitive processes such as attention and working memory; it is also involved in reward pathways, which is important in mediating the effects of abusive drugs, and owns a peculiar importance also in the functioning of renal, hormonal and cardiovascular systems [199].
DA acts on a range of receptors located in various brain regions and in the periphery. Alterations in the optimal DA concentration have been associated with different neurodegenerative (Parkinson's) and psychotic (Schizophrenia, addiction) disorders [200]. Parkinsonian symptoms appear when dopaminergic neuronal death exceeds a critical threshold of 70–80%. The decreased level of DA is directly associated with an uncontrolled motor function, which leads to an inability in neutralizing the imbalance in neurotransmitters.

5.2.3 Strategy

In this work, we combined the features of a conductive polymer and metallic NPs into an AuNPs/PANI nanocomposite film, directly realized onto the GSPEs surface, in order to detect DA neurotransmitter.
The novelty of the realized sensor compared to those reported in literature was the use of a fast and easy-synthesizable nanocomposite film coupled with SPEs for faster, more sensitive, disposable and cost-effective

detection, which are features that could be all suitable in future POCT analysis. In order to assess the suitability of the developed sensor for a possible integration in an easy-to-use kit, and to evaluate the influence of the matrix effect, preliminary experiments were performed in certified human serum samples.

5.3 Materials and Methods

5.3.1 Chemicals

Aniline (C_6H_7N), perchloric acid ($HClO_4$), tetrachloroauric acid ($HAuCl_4$), sulfuric acid (H_2SO_4), dopamine hydrochloride ($C_8H_{11}NO_2 \cdot HCl$), serotonin ($C_{10}H_{12}N_2O$), uric acid ($C_5H_4N_4O_3$), di-sodium hydrogen phosphate (Na_2HPO_4), sodium di-hydrogen phosphate di-hydrate ($NaH_2PO_4 \cdot 2H_2O$), sodium chloride (NaCl), potassium chloride (KCl), potassium ferrocyanide ($K_4[Fe(CN)_6]$), potassium ferricyanide ($K_3[Fe(CN)_6]$), hexammineruthenium(II) chloride ($[Ru(NH_3)_6]Cl_2$), hexammineruthenium(III) chloride ($[Ru(NH_3)_6]Cl_3$) and human male serum (type AB) were purchased from Merck KGaA (Darmstadt, Germany). Milli-Q water was used for all preparations. The buffer solution used in this work was 0.1 M PBS, 0.1 M NaCl, pH 7.0.

5.3.2 Sensor Development

In this study, an electrochemical nanocomposite sensor for DA determination was proposed. As illustrated in **Figure 5.1**, the protocol involves the following steps: (a) electropolymerization of ANI onto GSPEs; (b) AuNPs electrodeposition; (c) DA determination by DPV measurements.

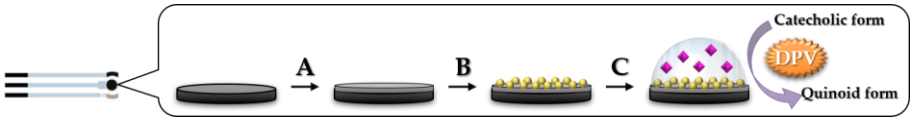

Figure 5.1. *Scheme of the nanocomposite sensor for dopamine detection. (A) Electropolymerization of aniline; (B) electrodeposition of gold nanoparticles; (C) DA detection in 0.1 M PBS pH 7.0.*

A calibration curve was obtained by dropping various DA solutions at different concentrations (ranging from 1 μM to 100 μM) in PBS onto the nanocomposite sensor. DA, as an electroactive compound, was oxidized and detected by means of DPV by scanning the potential from +0.005 V to +0.6 V at 4 mV/s (2 mV step potential, 50 mV pulse potential, 0.05 s pulse time). The current peak height was taken as the electrochemical signal and plotted versus DA concentration. The obtained curve was fitted with a linear equation. Preliminary experiments for the determination of DA in human serum were also performed. The real samples were diluted at a proper ratio in PBS buffer and then spiked with standard addition of DA. The sensor response was then determined by DPV measurements, under the same conditions used for DA calibration curve.

5.4 Results and Discussion

5.4.1 Study of Dopamine Oxidation by CV

As previously shown in ***Subsection 4.3.2***, the electrode surface successfully modified with AuNPs and PANI provided the necessary conduction pathways, besides acting like a nanoscale electrode in promoting the electron transfer between the analyte and the electrode surface. The scan rate study was then performed in presence of DA to assess for the suitability of the nanostructured platform in the analysis of this neurotransmitter. DA was chosen as a model analyte because it can be easily determined by electrochemical analysis, oxidizing it at the electrode surface and measuring the related anodic peak current.

Cyclic voltammetry was performed using 50 μM DA in PBS at different scan rates (25, 50, 75, 100, 125 and 150 mV/s). The redox peak current height increased with increasing the scan rate from 25 mV/s to 150 mV/s, as shown in **Figure 5.2**.

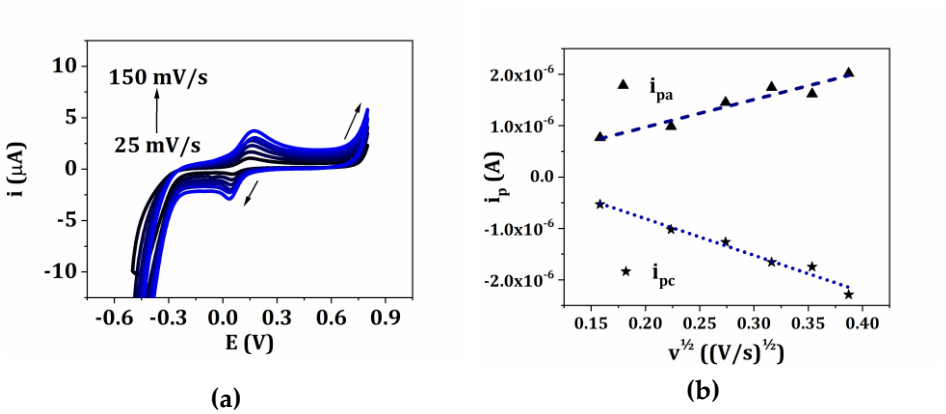

Figure 5.2. (a) *Cyclic voltammograms of AuNPs/PANI/GSPE performed with 50 μM dopamine in 0.1 M PBS pH 7.0 at different scan rates;* ***(b)*** *linear relationship between* i_p *vs.* $v^{1/2}$.

A good linearity was obtained between the redox peak current and the square root of the scan rate with correlation coefficients of 0.93 and 0.97 for i_{pa} vs. $v^{1/2}$ and i_{pc} vs. $v^{1/2}$, respectively. The obtained results suggest that the electron transfer reaction at the electrode surface was controlled by diffusion processes. The linear relationship of the plot confirmed that the nanocomposite film was electroactive, conducting and confined to the surface. Since the developed AuNPs/PANI/GSPEs demonstrated a good electrochemical response towards DA, they were applied for its determination.

5.4.2 Dopamine Calibration Curve

A calibration curve of DA in buffered solutions was obtained by DPV technique. An increase of the current peak height was recorded by increasing the DA concentration in the range from 0 μM to 100 μM (**Figure 5.3**, a panel) and a linear relationship was obtained ($i_{ox} = 0.015\ [DA] + 0.007$) with a good regression value of 0.998 (**Figure 5.3**, b panel).
The LOD, calculated as 3.3 S_{blank}/slope, was found to be 0.86 μM.

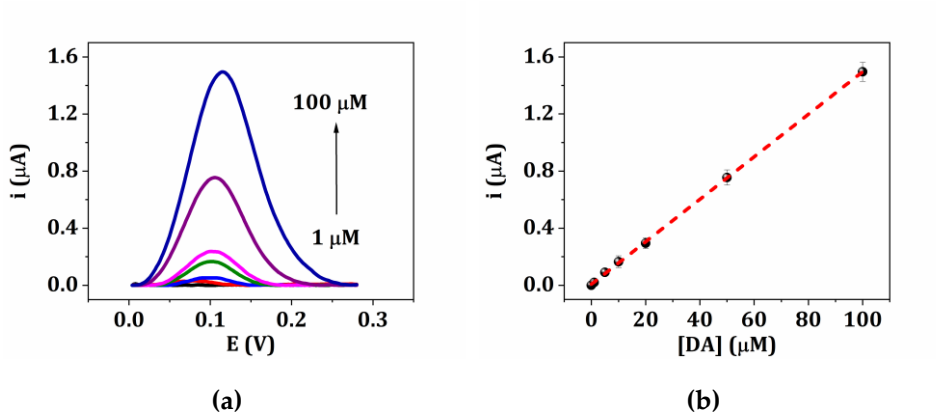

Figure 5.3. *Dopamine detection at AuNPs/PANI/GSPE.* ***(a)*** *Differential pulse voltammograms performed with different DA concentrations;* ***(b)*** *calibration curve for DA. Each measurement was repeated at least five times using different sensors.*

The selectivity of the sensor was investigated by detecting 50 μM of DA solution in presence of possible interfering substances, such as uric acid and serotonin. These molecules coexist in biological fluids and their selective determination can be useful from a clinical point of view.
In non-pathological conditions, the concentrations of uric acid and serotonin are in the micromolar range in serum, for this reason the 300 μM uric acid and 50 μM serotonin solutions were tested. The potential peak values were well separated resulting at +84 mV for DA, +251 mV for serotonin and +367 mV for uric acid (**Figure 5.4**). Therefore, DA can be successfully measured even in the presence potential interferents by the AuNPs/PANI/GSPEs sensor, while at bare, unmodified electrodes, their

selective determination is not possible because of the proximity of their oxidation potentials [201].

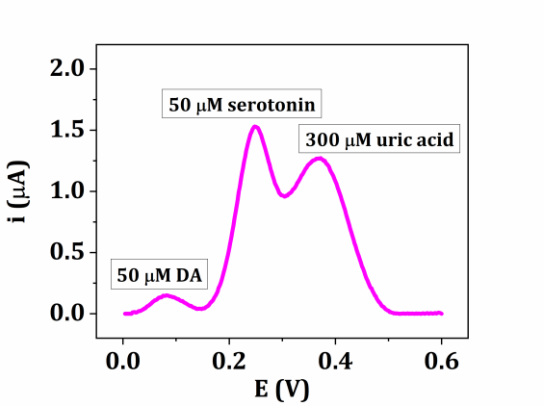

Figure 5.4. *Differential pulse voltammograms performed with 50 μM dopamine, 300 μM uric acid and 50 μM serotonin in 0.1 M PBS pH 7.0.*

5.4.3 Serum Samples Analysis

In order to evaluate the operability of the proposed sensor, some preliminary experiments in human serum samples were performed.
With this aim, commercial serum was diluted with PBS and then spiked with DA standard solutions, without any other pretreatment. The DA response was then determined by DPV measurements, in the same conditions used for the calibration curve of DA buffered solutions.

In order to choose the proper dilution ratio, preliminary experiments were performed by spiking with 50 μM DA the serum samples diluted at different ratios and by comparing the obtained signals (i_{sample}) with that of 50 μM DA in PBS (i_1). The results are shown in **Table 5.1**.

Table 5.1. *Measurements of 50 μM dopamine current peak height by varying the dilution ratio of serum samples in 0.1 M PBS pH 7.0. Each measurement was repeated at least five times using different sensors.*

Dilution ratio	i_{sample}/i_1	%RSD
1:5	0.10	1.2
1:10	0.07	1.5
1:20	0.16	0.8
1:40	0.23	0.7

The obtained results showed that by increasing the dilution ratio, the i_{sample}/i_1 value increases, as the matrix effect was less significant on the sensor response, so a 40-fold dilution was chosen. DA was then spiked at different concentrations in the as-diluted serum and a linear calibration curve (i_{ox} = 0.006 *[DA]* + 0.439, R^2 = 0.992) was obtained (**Figure 5.5**).

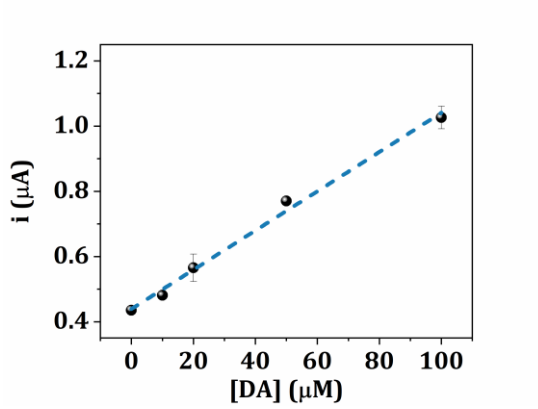

Figure 5.5. *Calibration curve for dopamine in 40-fold diluted serum. Each measurement was repeated at least five times using different sensors.*

The %RSD, calculated using at least five measurements with different SPEs, was 2%. These results confirmed the suitability of the use of the proposed nanocomposite sensor for the determination of DA in serum analysis.

5.5 Conclusions

In this work, we have designed a fast and easy strategy for the modification of GSPEs with PANI and AuNPs for DA electrochemical detection. The nanocomposite sensor facilitates the electron transfer, which leads to an increase in sensitivity towards DA oxidation at the sensor surface. A good linear relationship between the current peak values and the DA concentration in the range from 1 μM to 100 μM, with a LOD of 0.86 μM, was obtained. Good sensitivity and reproducibility were achieved for DA detection, with a linear response that meets clinical needs. The sensor was then preliminarily applied to measure DA in human serum. Even if *in vivo* studies should always be performed to test the actual applicability of the device, the easiness of this nanocomposite sensor building procedure combined with the use of a portable instrument confer upon it a great potential to be used as a disposable, cost-effective, and fast device for DA detection in point-of-care analysis.

sensors

MDPI

6. DNA-based Sensor for the Detection of an Organophosporus Pesticide: Profenofos

Sensors, **2018**, *18*(7), 2035 — **DOI**: 10.3390/s18072035

6.1 Abstract

In this work, we propose an electrochemical DNA aptasensor for the detection of profenofos, an organophosphorus pesticide (OPP), based on a competitive format and disposable graphite screen-printed electrodes (GSPEs). A thiol-tethered DNA capture probe, that results to be complementary to a portion of the chosen aptamer sequence, was immobilized on gold nanoparticles/polyaniline composite film-modified electrodes (AuNPs/PANI/GSPE). Different profenofos solutions containing a fixed amount of the biotinylated DNA aptamer were dropped onto the realized aptasensors. The hybridization reaction was measured by using a streptavidin-alkaline phosphatase (ALP) enzyme conjugate, which catalyzes the hydrolysis of 1-naphthyl phosphate (1-NPP).

The enzymatic product 1-naphtol (1-NPOH) was detected by means of differential pulse voltammetry (DPV). The aptasensor showed itself to work as a signal-off sensor, according to the competitive format used.

A dose response curve was obtained between 0.10 μM and 10 μM with a LOD of 0.27 μM.

Keywords: screen-printed electrodes; aptasensor; nanoparticles; organophosphorus pesticide; profenofos.

6.2 Introduction

6.2.1 State of the Art

To date, the detection and the quantification of pesticides are generally based on conventional chromatographic techniques coupled with mass spectrometry [69], which provide sensitive and selective detection. In particular, profenofos detection had been carried out both through a gas-liquid chromatographic method using a flame-ionization detector [202] and a HPLC-based method using a diode array detector [203].

Chromatographic techniques commonly require highly skilled personnel and are not suitable for screening analysis. Thus, biosensors development for pesticide analysis represents a rapid, cost-effective, and easy alternative to conventional techniques for environmental monitoring, including *in situ* analysis [70]. The main drawback in developing biosensors for detecting pesticides consists in the synthesis of antibodies for these highly toxic targets. In this perspective, the use of biomimetic receptors such as DNA aptamers has recently become an interesting alternative, since they have shown themselves as good candidates as recognition elements in robust and stable biosensors for pesticide detection [14,76,164].

Recently, some aptamer-based biosensors have been developed for the determination of OPPs. A colorimetric assay was developed employing AuNPs modified with an aptamer for the detection of omethoate. The aptamer showed high selectivity towards omethoate, resulting in the disconnection of aptamer molecules from AuNPs and in their aggregation. Using the OPP-binding aptamer and target-induced color changes in AuNPs, this biosensor showed a good linearity between 0.1 μM and 10 μM, with LOD of 0.1 μM [204]. A similar approach was developed for the colorimetric detection of malathion employing an

aptamer, a cationic peptide and unmodified AuNPs. The biosensor was found to be linear in the range 0.01–0.75 nM with a LOD of 1.94 pM [205].

An electrochemical aptasensor based on copper oxide nanoflowers and single walled carbon nanotubes nanocomposite for chlorpyrifos detection was developed from Huo *et al*. A good linearity for chlorpyrifos ranging from 0.1 ng/mL to 150 ng/mL, with a low LOD of 70 pg/mL was obtained [206].

Different optical and photoelectrochemical affinity sensors for profenofos detection, based on MIPs and calixarenes, were also reported in literature [207–209].

6.2.2 Target Analyte

Profenofos, O-(4-bromo-2-chlorophenyl)-O-ethyl-S-propyl phosphorothioate, is a liquid with a color ranging from pale yellow to amber and a garlic-like odor which was first registered in the United States in 1982 and is extensively used nowadays for efficient control of insect pests. Its mechanism of action can induce significant inhibitory effects on acetylcholinesterase activity, as well as instability of erythrocyte membrane [210]. Although it is used in the form of a racemate, the S(−) isomer is a more potent inhibitor. As of 2015, it is no longer approved in the European Union [211].

6.2.3 Strategy

In this work, we developed for the first time an electrochemical DNA aptasensor for profenofos based on a competitive assay format.
The DNA aptamer was selected from a library of aptamers, built by SELEX, as it proved itself to show one of the highest ability to bind profenofos (K_d = 1 μM) among three other OPPs [212]. A thiol-tethered DNA capture probe, that results to be complementary to a portion of the

chosen aptamer sequence, was immobilized on the surface of AuNPs/PANI composite film-modified GSPEs. Different profenofos solutions containing a fixed amount of the biotinylated DNA aptamer were dropped onto the realized aptasensors. The hybridization reaction was measured by using a streptavidin-ALP enzyme conjugate, which catalyzes the hydrolysis of 1-NPP to 1-NPOH. The enzymatic product was detected by means of DPV. The aptasensor showed itself to work as a signal-off sensor, according to the competitive format used.
This innovative method combines the portability of screen-printed electrochemical cells and of a computer-controlled instrument to ensure the possibility of a disposable and cost-effective *in situ* analysis.

6.3 Materials and Methods

6.3.1 Chemicals

Aniline (C_6H_7N), perchloric acid ($HClO_4$), tetrachloroauric acid ($HAuCl_4$), sulfuric acid (H_2SO_4), DL-dithiothreitol ($C_4H_{10}O_2S_2$), 6-mercapto-1-hexanol ($C_6H_{14}OS$), profenofos, paraoxon, bovine serum albumin, streptavidin-alkaline phosphatase enzyme conjugate, 1-naphthyl phosphate disodium salt ($Na_2C_{10}H_7O_4P$), *p*-nitrophenyl phosphate disodium salt hexahydrate ($Na_2C_6H_4NO_6P{\cdot}6H_2O$), ethanol ($C_2H_6O$), tris(hydroxymethyl) aminomethane ($C_4H_{11}NO_3$), di-sodium hydrogen phosphate (Na_2HPO_4), sodium di-hydrogen phosphate di-hydrate ($NaH_2PO_4{\cdot}2H_2O$), diethanolamine ($C_4H_{11}NO_2$), potassium chloride (KCl), magnesium chloride hexahydrate ($MgCl_2{\cdot}6H_2O$), potassium ferrocyanide ($K_4[Fe(CN)_6]$), potassium ferricyanide ($K_3[Fe(CN)_6]$) were purchased from Merck KGaA (Darmstadt, Germany). Pear juice was purchased in a local market. Milli-Q water was used for all preparations.

The DNA sequences were purchased from Eurofins Genomics GmbH (Ebersberg, Germany) and are listed below.

- Thiol-tethered complementary oligonucleotide sequence (oligo-SH): 5'-(SH)-(CH_2)$_6$-CCG ATC AAG AAT CGC TGC AG-3';
- Biotinylated DNA aptamer (apt-BIO): 5'-(biotin)-TEG-AAG CTT GCT TTA TAG CCT GCA GCG ATT CTT GAT CGG AAA AGG CTG AGA GCT ACG C-3'.

Prior to immobilization, the thiol-modified DNA sequence was treated with DTT, purified by elution through a NAP-5 column of Sephadex G-25 DNA grade resin (Cytiva, Little Chalfont, UK) and then quantified by measuring UV absorption at 260 nm.

The buffer solutions used in this work are:

1. storage buffer: 10 mM TRIS buffer, pH 8.0;
2. immobilization buffer: 0.5 M phosphate buffer, pH 7.0;
3. detection buffer: 0.1 M DEA buffer, 0.1 M KCl, 1 mM $MgCl_2$, pH 9.6.

6.3.2 Apparatus

UV absorption measurements were carried out with a Varian Cary 100 Bio UV spectrophotometer equipped with a 6+6 peltier thermostatable multicell holder and built-in temperature probes. The results were analyzed with Thermal application provided in the Cary 100 Bio software suite. Secondary structures of both the DNA sequences were predicted through the MFold algorithm [213].

6.3.3 DNA Melting Curve Studies

The hybridization reaction between the DNA capture aptamer (apt-BIO) and the selected complementary sequence (oligo-SH) was assessed by recording melting curves; melting temperatures were obtained as first-order derivative plot of absorbance versus temperature.

100 µL of 1 µM oligonucleotide solutions in immobilization buffer were placed into quartz microcuvettes (1 cm path length) and the temperature was increased from 25 °C to 95 °C at constant rate of 1 °C/min directly inside them through the immersed probe into the sample solutions. At the same time, the absorbance at 260 nm was monitored at 1 nm spectral bandwidth. Immobilization buffer was used as a blank solution. The entity of the interaction between the DNA aptamer and the target pesticide was also investigated in the same conditions.

6.3.4 Aptasensor Development

The developed DNA aptasensor assay was based on a competitive approach as reported in **Figure 6.1**.

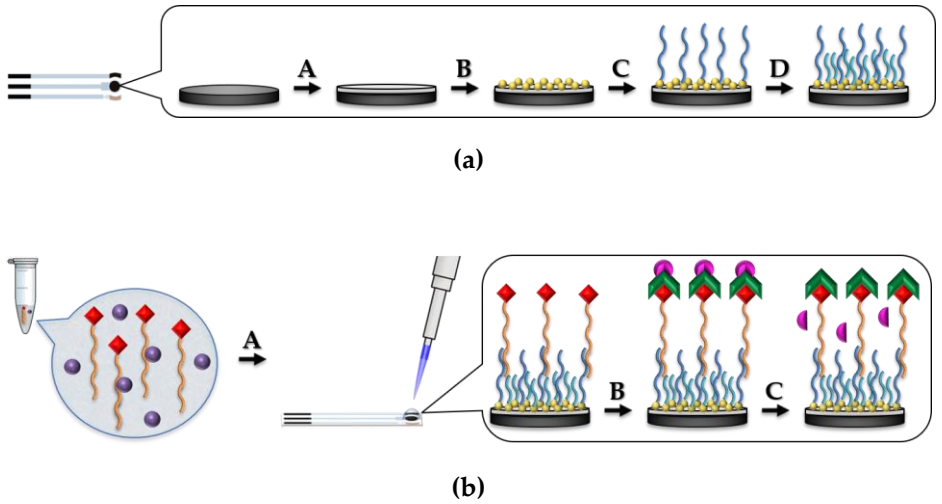

Figure 6.1. *Scheme of the DNA-based sensor assay for profenofos detection.* ***(a)*** *GSPE surface modification: A) electropolymerization of aniline; B) electrodeposition of gold nanoparticles; C) thiolated DNA capture probe immobilization; D) mixed SAM formation with 6-mercapto-1-hexanol.* ***(b)*** *Hybridization and detection: affinity reaction between profenofos at different concentrations and biotinylated DNA aptamer sequence in solution; A) hybridization reaction between DNA aptamer and the immobilized DNA capture probe; B) coupling with streptavidin-alkaline phosphatase enzyme conjugate; C) incubation with 1-naphthyl phosphate enzymatic substrate and detection of 1-naphthol enzymatic product.*

6.3.4.1 DNA Probe Immobilization

The nanostructured GSPEs were modified by self-assembly of a mixed monolayer of thiolated DNA capture probe (oligo-SH) and 6-mercapto-1-hexanol (MCH) [214]. The purified thiolated complementary sequence was subjected to a thermal treatment by heating it at 90 °C for 5 min and cooling it down to room temperature.

7 μL of 2 μM capture probe solution were then deposited onto the modified surface of the working electrode and chemisorption was allowed to proceed overnight (≈ 16 h). During this period, the sensors were stored in petri dishes at 4 °C to protect the solution from evaporation. To remove unbound oligonucleotide sequences, the surface was washed three times with 15 μL of immobilization buffer.

This immobilizations step was followed by the formation of a self-assembled monolayer (SAM) by incubation with 7 μL of 1 mM MCH aqueous solution for 60 min. Finally, the aptasensors were washed with 15 μL immobilization buffer for three times.

6.3.4.2 Profenofos Detection

To obtain a dose-response calibration curve, profenofos detection was performed by dropping a solution containing a proper concentration of biotinylated DNA aptamer (apt-BIO) and the target pesticide onto the sensor surface and by allowing the competitive reaction to proceed.
In particular, the affinity reaction between 0.5 μM biotinylated DNA aptamer and the target pesticide in the concentration range 0–10 μM was first performed in solution; then, after 40 min, 7 μL of these solutions were incubated for other 30 min onto the sensors surface. The aptasensors were then rinsed for three times with 15 μL detection buffer.

6.3.4.3 Enzymatic Labeling and Electrochemical Measurements

The biotinylated hybrids formed onto the developed aptasensor surface were further incubated with 15 µL of a solution containing 1 U/mL of streptavidin-ALP conjugate and 8 mg/mL of BSA in detection buffer. After 10 min, each sensor was washed three times with 100 µL detection buffer for two cycles of washings.

Then, after this labeling step, 50 µL of 1 mg/mL 1-NPP solution in detection buffer were placed onto the disposable aptasensors.
After 20 min, the electroactive enzymatic product thus formed (1-NPOH) was detected by DPV by scanning the potential from 0 V to +0.6 V at 40 mV/s (5 mV step potential, 70 mV modulation amplitude) [215].

The current peak height was taken as the electrochemical signal.
The signal is expressed in relative percent units as S_x/S_0 (*i.e.* ratio between measured signal to blank signal) and plotted against profenofos concentration. The obtained curve exhibits the typical sigmoidal shape of a competitive assay and was fitted with a Boltzmann-type sigmoidal equation [216] (*Equation (6.1)*):

$$S_x/S_0 = A_2 + \frac{A_1 - A_2}{1 + e^{([Profenofos] - x_0)/dx}} \qquad (6.1)$$

where A_1 is the y value at the top plateau at the curve, A_2 is the y value at the bottom plateau, x_0 is the x value at which y is halfway between bottom and top and dx is the slope of the linear part of the curve.

6.4 Results and Discussion

6.4.1 Studies on the Affinity of the DNA Aptamer for the Target Pesticide

The selective binding of targets is strongly influenced by the secondary structures of DNA sequences, since aptamers themselves are subjected to conformational changes that create many weak bonds, in order to capture the target molecule. The secondary structures thus formed were predicted by using the MFold algorithm and are shown in **Figure 6.2**.

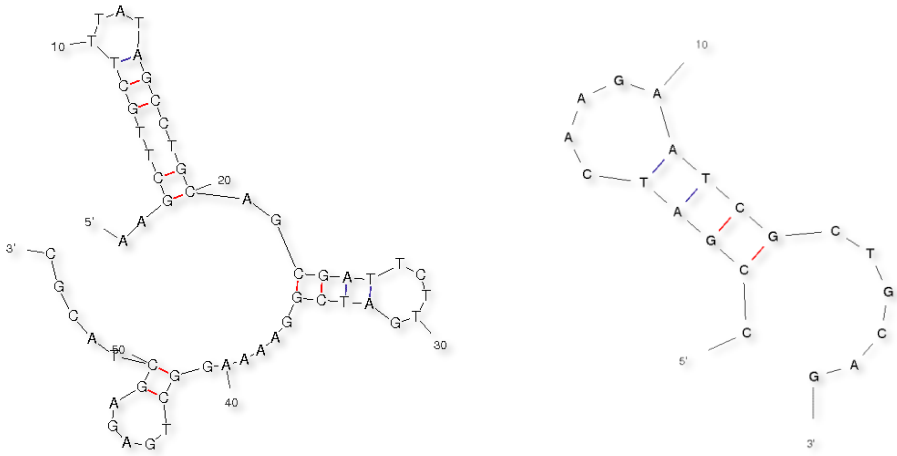

(**a**) (**b**)

Figure 6.2. *Secondary structures of* ***(a)*** *apt-BIO and* ***(b)*** *oligo-SH sequences as predicted with MFold algorithm at 25 °C in 0.5 M phosphate buffer, pH 7.0 ([Na⁺] = 0.8 M). The bond between G and C is shown in red to indicate its stability.*

The prediction temperature was set at 25 °C and the ionic strength was regulated according to the immobilization buffer solution used.
The drawing mode was set to untangle with loop fix, while the other parameters were left as default settings. From the predicted conformations, apt-BIO prevalently shows a single-stranded structure characterized by three differently-sized loops, while oligo-SH shows a

single-loop structure in the same conditions, because of its shorter length. For this reason, the hybridization reaction between the two DNA strands is more efficient compared to the one that would occur in presence of any other sequence with a more stable secondary structure.

The affinity of the receptor for the analyte and for the chosen complementary sequence was assessed by comparing these structures with preliminary studies on the melting temperatures of the aptamer alone and in presence of its complementary sequence or the pesticide (**Table 6.1**).

The obtained T_m values for the biotinylated aptamer in presence of the thiolated capture probe or profenofos are close to the one related to the aptamer alone; moreover, the overlapping region of the two oligonucleotides is located on the medium-size loop. This suggests that also the interaction with profenofos takes place in the same region.

Table 6.1. *Melting temperature (T_m) values, as obtained from analyzing melting curves.*

Sample*	T_m (°C)
Apt-BIO	54.0
Apt-BIO + oligo-SH	58.0
Apt-BIO + profenofos	57.0

*Concentration: 1 μM each.

6.4.2 Aptasensor Development

6.4.2.1 Competitive Assay

In order to develop the competitive aptamer-based assay for profenofos detection, the thiolated DNA capture probe was immobilized on modified graphite screen-printed working electrodes and the hybridization reaction with increasing concentrations of the biotinylated aptamer sequence was performed in accordance with previously reported studies [7,14]. Apt-BIO is functionalized with biotin in 5'-end, in order to

interact with streptavidin-ALP enzyme conjugate. The current peak height increased linearly with apt-BIO concentration up to 0.5 μM, where a plateau was reached (**Figure 6.3**).

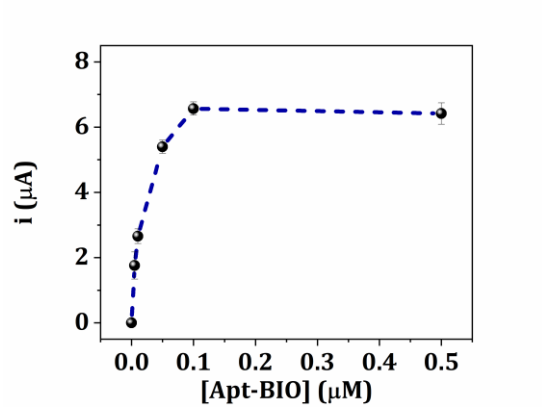

Figure 6.3. *Hybridization curve between immobilized oligonucleotide sequence (2 μM) and biotinylated aptamer sequence (0.005–0.5 μM) in immobilization buffer. Each measurement was repeated at least five times using different sensors.*

This behavior is due to the limited number of biorecognition sites that were bound onto the sensor surfaces. The concentration of 0.5 μM apt-BIO was thus used for all experiments involving profenofos, since to perform the competitive assay it is necessary to work in saturation conditions to obtain the maximum signal value in absence of the analyte.

6.4.2.2 Profenofos Detection

The pesticide detection was performed by competitive assay. In order to check if the pesticide itself, as an organophosphorus compound, could constitute an inhibition element for the phosphatase enzyme used in the labeling step, spectrophotometric measurements were carried out. Absorbance at 405 nm was collected for the biotinylated aptamer sequence, profenofos and the enzyme in presence of *p*-nitrophenyl phosphate colorimetric enzymatic substrate). No significantly different values were obtained compared to the ones collected without profenofos,

confirming that the pesticide is not interfering with the enzymatic activity (data not shown).

Different solutions containing a fixed concentration (0.5 μM) of apt-BIO and increasing profenofos concentrations were thus analyzed.
A decrement of the current peak height was recorded by increasing the concentration of the pesticide and a dose-response curve for profenofos was obtained in the range 0.1–10 μM. The signal is reported as S_x/S_0 percent units, that is the percentage of the signal decrease with respect to the blank value (**Figure 6.4**).

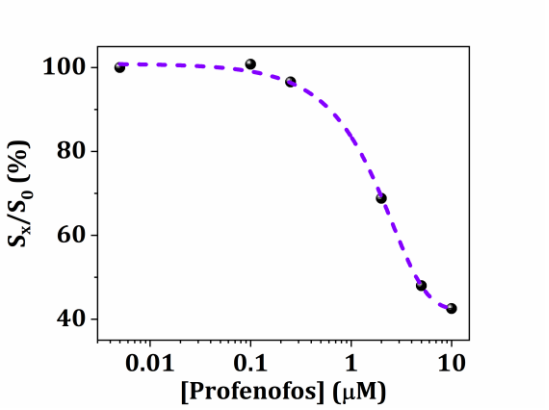

***Figure 6.4**. Profenofos dose-response curve. Each measurement was repeated at least five times using different sensors.*

The fitting of experimental data values gives the *Equation (6.2*:

$$S_x/S_0 = 42.2 + \frac{127.2}{1 + e^{([Profenofos]+0.3)/1.7}} \qquad (6.2)$$

showing a correlation coefficient R^2 of 0.997. The LOD was calculated as previously reported by Taylor *et al*. [217] and a value of 0.27 μM was obtained. The reproducibility of the aptasensor was also evaluated by multiple analysis of each standard profenofos solution.

Aptamer cross-reactivity with another OPP, paraoxon, was tested: paraoxon is the active metabolite of parathion, a molecule with a strong insecticidal and acaricidal effect, and the exposure to this molecule produces high mortality [218]. Paraoxon solutions at different concentrations (1 μM and 5 μM) were tested: the results are in accordance with the inhibition ratios obtained for nine structurally similar pesticides (*e.g.* acetamiprid, chlorpyrifos, parathion, etc.) [212], indicating that the aptamer sequence displays weak affinity with the above molecules, and thus to paraoxon. The described aptasensor was confirmed as a promising analytical tool for pesticide detection, since the tested concentrations gave an average 0.2% RSD value for five repetitions of each standard solution.

6.4.2.3 Fruit Juice Samples Analysis

Once verified the suitability of the aptasensor for detecting profenofos in standard solutions, preliminary experiments on spiked commercially available pear juice samples were carried out after their dilution (1:10) in immobilization buffer. The aptasensor response was then determined by DPV measurements, in the same conditions used for the pesticide calibration curve (**Figure 6.5**).

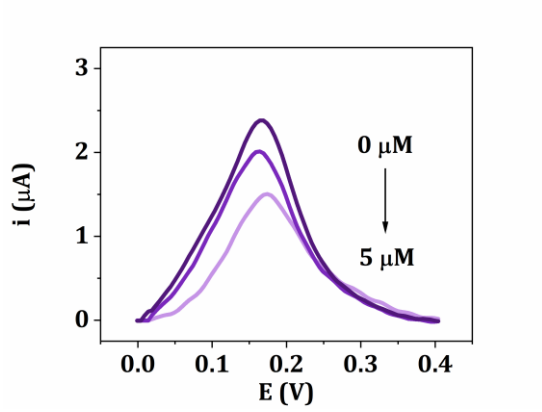

Figure 6.5. *Differential pulse voltammograms performed in pear juice samples spiked with profenofos standard solutions (final concentrations: 1.0 μM and 5.0 μM).*

The signal was found to decrease by increasing the profenofos spiked concentration in the analyzed samples. A stronger matrix effect was observed by increasing the pesticide spiked concentration, resulting in a decrease of the recovery value. The results obtained for the spiked samples with standard addition of profenofos are shown in **Table 6.2**.

Table 6.2. *Recovery values obtained from the analysis of profenofos-spiked pear juice samples. Each measurement was repeated at least five times using different sensors.*

Profenofos spiked (μM)	Profenofos found (μM)	Recovery (%)	%RSD
1.0	0.87	87%	7
5.0	2.45	49%	8

6.5 Conclusions

Affinity-based biosensing can contribute to pesticide detection as a valid and innovative analytical approach. In this work, we developed for the first time a simple and cost-effective aptasensor for the direct determination of profenofos pesticide, based on a competitive format and disposable screen-printed electrochemical cells. From the obtained results, this analytical tool has proven itself to be promising for application in real samples analysis, since it involved low amounts of reagents and easy-to-prepare portable aptasensors. All these features make it suitable for the realization of a commercial kit.

Contents lists available at ScienceDirect

Talanta

journal homepage: www.elsevier.com/locate/talanta

7. Electrochemical Enzyme-Linked Oligonucleotide Array for Aflatoxin B_1 Detection

Talanta, **2019**, *203*, 49 — **DOI**: 10.1016/j.talanta.2019.05.044

7.1 Abstract

In this work, an electrochemical enzyme-linked oligonucleotide array to achieve simple and rapid detection of aflatoxin B_1 (AFB_1) is presented. The assay is based on a competitive format and disposable screen-printed cells (SPCs). Firstly, the electrodeposition of poly(aniline-*co*-anthranilic acid) copolymer (P(ANI-*co*-AA)) on graphite screen-printed working electrodes was performed by means of cyclic voltammetry (CV).

AFB_1 conjugated with bovine serum albumin (AFB_1-BSA) was then immobilized by covalent binding on P(ANI-*co*-AA) copolymer.

After performing the affinity reaction between AFB_1 and the biotinylated DNA-aptamer (apt-BIO), the competition was carried out on the modified SPCs. The biotinylated complexes formed onto the sensor surface were coupled with a streptavidin-alkaline phosphatase (ALP) conjugate.

1-naphthyl phosphate (1-NPP) was used as the enzymatic substrate; the electroactive product was detected by differential pulse voltammetry (DPV). The response was signal-off, according to the competitive format used. A dose-response curve was obtained between 0.1 ng/mL and 10 ng/mL with a LOD of 0.086 ng/mL. Finally, preliminary experiments in maize flour samples spiked with AFB_1 were also performed.

Keywords: aptasensor; aflatoxin; conductive polymer; screen-printed electrode; mycotoxin.

7.2 Introduction

7.2.1 State of the Art

In the actual context of intensive agriculture and food industry growth, food safety is progressively becoming a global issue; the assessment of food quality in agrifood field requires nutrients monitoring and fast screening of contaminants. In this perspective, the increasing interest of developing biosensors for food quality control is justified by the fact that they come to meet the requirements of fast and on-field analysis; moreover, compared to conventional methods used for these analysis (such as spectrophotometric or chromatographic methods), biosensors have the incontestable advantages of selectivity, which allows direct detection with minimal sample pretreatment, low cost and portability [71].

There is a growing interest to apply aptamer-based approaches for food analysis in response to most significant challenges posed by food industry. Most approaches to analyze toxins are still limited to ochratoxin A (OTA), considered as a model target among mycotoxins [219].
However, in recent years, increasing efforts have been focused on the development of aptamer-based sensors for AFB_1 [220], which mostly exploit optical techniques as the transduction element [221].
In the work of Sabet *et al*., aptamer-conjugated quantum dots (QDs) were adsorbed to AuNPs leading to a quenching effect on QDs fluorescence, which was being recovered upon addition of AFB_1, resulting in a nanobiosensor with a LOD of 3.4 nM to be applied in rice and peanut samples [222]. A similar approach was reported by Chen *et al*. for the analysis of infant rice cereal, in which the binding of AFB_1 to its specific fluorescein-labeled aptamer caused the release of a complementary DNA strand bearing a quencher moiety; the LOD was found to be 1.6 ng/mL [223]. Conversely, a surface plasmon resonance (SPR) aptasensor in a direct assay format was developed by Sun *et al*. by immobilizing the aptamer onto a commercial sensor chip, which can be regenerated by

passing a flow of buffer over it. The sensor showed a LOD of 0.4 nM; it was applied in the analysis of diluted red wine and beer [224].
A dual lateral flow aptasensor was developed by Zhu *et al*. using AFB_1 as the model target and was validated using 11 kinds of food and feedstuff samples (*e.g.* protein powder, rice, cake flour, cottonseed meal) with a simple aqueous extraction protocol [225]. Among various biosensors for AFB_1 detection, electrochemical biosensors for the detection of aflatoxins play a prominent role due to their sensitivity, selectivity, low cost, simplicity and, in some cases, portability [226]. The sensing strategy proposed by Abnous *et al*. was based on the π-shape structure formed by an aptamer and its complementary strands, which acts as a physical barrier. In absence of the target mycotoxin, the structure remained intact and a weak peak current was obtained; upon the addition of AFB_1 the structure was disassembled, and a strong current was recorded.
The aptasensor was then applied for the analysis of human serum and grape juice [227].

According to our knowledge, only few biosensors based on competitive approaches using AFB_1-BSA are reported in literature.
An electrochemical immunosensor based on the immobilization of AFB_1-BSA onto magnetic NPs was developed by Piermarini *et al*. The LOD and the sensitivity of the assay were calculated to be 0.6 ng/mL and 1.5 ng/mL, respectively [228]. To date, two examples of optical aptamer assays exploiting AFB_1-BSA as the immobilized element have been reported [229,230].

7.2.2 Target Analyte

Among all known aflatoxins, AFB_1 (which was first described in the early 1960s) is considered the most toxic and listed as a potent human carcinogen: according to the International Agency of Research on Cancer (IARC) classification, it is designated as first hazard class and is primarily

responsible for hepatocellular carcinoma in humans [220].
In animals, AFB_1 has also been shown to be mutagenic, teratogenic and to cause immunosuppression [231–233]. The contamination of this toxin often occurs in cereals (*e.g.* maize, rice, barley), wine, spices, nuts (*e.g.* peanuts), soy products as well as animal feeds [230]. Aflatoxins are most commonly ingested; however, AFB_1 retains the ability to permeate through skin [234].

7.2.3 Strategy

In this work, we present an innovative electrochemical enzyme-linked oligonucleotide array for AFB_1 detection based on a competitive assay format, in which an AFB_1-BSA conjugate was immobilized on modified GSPEs. The DNA aptamer used in this work was selected from a library of aptamers, built by SELEX, and proved itself to have the best affinity for AFB_1 [235]. The AFB_1-BSA conjugate was covalently immobilized on P(ANI-*co*-AA) conductive film, directly electropolymerized onto the GSPEs surface by means of CV. Different AFB_1 solutions, containing a fixed amount of the biotinylated oligonucleotide, were placed onto the realized sensors to let the competition between bound and free AFB_1 molecules for the binding with the biotinylated DNA aptamer to take place. The competition reaction was traced by a streptavidin-ALP enzyme conjugate. The enzymatic substrate 1-NPP was then added. The enzymatic product 1-NPOH was detected by DPV. The developed assay showed a signal-off behavior, according to the competitive format used. Finally, preliminary experiments in maize flour samples spiked with AFB_1 were also performed. The portability of SPCs and a computer-controlled instrument are combined in this assay to make it suitable for a rapid and cost-effective *in situ* analysis.

7.3 Materials and Methods

7.3.1 Chemicals

Aniline (C_6H_7N), anthranilic acid ($C_7H_7NO_2$), perchloric acid ($HClO_4$), 1-ethyl-3-(3-dimethylaminopropyl) carbodiimide hydrochloride ($C_8H_{17}N_3 \cdot HCl$), N-hydroxysuccinimide ($C_4H_5NO_3$), aflatoxin B_1, aflatoxin G_1, aflatoxin B_1-bovine serum albumin conjugate, L-lysine hydrochloride ($C_6H_{14}N_2O_2 \cdot HCl$), bovine serum albumin, streptavidin-alkaline phosphatase enzyme conjugate, 1-naphthyl phosphate disodium salt ($Na_2C_{10}H_7O_4P$), methanol (CH_4O), ethanol (C_2H_6O), tris(hydroxymethyl) aminomethane ($C_4H_{11}NO_3$), di-sodium hydrogen phosphate (Na_2HPO_4), sodium di-hydrogen phosphate di-hydrate ($NaH_2PO_4 \cdot 2H_2O$), diethanolamine ($C_4H_{11}NO_2$), sodium chloride (NaCl), potassium chloride (KCl), magnesium chloride hexahydrate ($MgCl_2 \cdot 6H_2O$), potassium ferrocyanide ($K_4[Fe(CN)_6]$), potassium ferricyanide ($K_3[Fe(CN)_6]$) were purchased from Merck KGaA (Darmstadt, Germany). Maize flour was purchased in a local market. Milli-Q water was used for all preparations.

The biotinylated DNA aptamer sequence (apt-BIO) used in this work was purchased from Eurofins Genomics GmbH (Ebersberg, Germany) and is reported as the following: 5'-(biotin)-TEG-GTT GGG CAC GTG TTG TCT CTC TGT GTC TCG TGC CCT TCG CTA GGC CCA CA-3'.

The buffer solutions used in this work are the following:

1. storage buffer: 10 mM TRIS buffer, 0.1 M KCl, pH 8.0;
2. immobilization buffer: 0.1 M phosphate buffer, 0.1 M NaCl, pH 7.4;
3. activation buffer: 0.1 M phosphate buffer, 0.1 M NaCl, pH 5.0;
4. detection buffer: 0.1 M DEA buffer, 0.1 M KCl, 1 mM $MgCl_2$, pH 9.6.

7.3.2 Apparatus

Scanning electron microscopy (SEM) analysis was carried out using Gaia 3 microscope (Tescan a.s., Brno, Czech Republic). SEM images were acquired using the following parameters: acceleration voltage 5 kV, view field 89.2 μm, magnification 3.10 kx.

7.3.3 Aflatoxin B_1 Standard Solutions

Standard solutions of AFB_1 (0.2, 1.0, 2.0, 10.0 and 20.0 ng/mL) were prepared daily by diluting a stock solution (0.25 mg/mL prepared in methanol) in immobilization buffer. The dilution ratio was chosen to make the solution contain the lowest percentage of methanol as possible.
In fact, high percentages of the organic solvent constitute a drawback in the use of this kind of SPCs, as their insulating layer could be dissolved and interfere in the electrochemical analysis.

7.3.4 Enzyme-linked Oligonucleotide Array Development

The developed enzyme-linked oligonucleotide array is based on a competitive approach, as reported in **Figure 7.1**. GSPEs were modified by electrodeposition of P(ANI-*co*-AA) copolymer by means of CV.
To immobilize the AFB_1-BSA complex, the carboxylic groups onto the polymeric surface were activated through EDC/NHS chemistry, so that they could react with the amino groups of the BSA protein (**Figure 7.1**, a panel). The competition between immobilized AFB_1 molecules onto the electrode surface and free AFB_1 molecules into sample solutions for the binding with the biotinylated aptamer was then carried out.
The biotinylated complexes formed onto the sensor surface were then labeled with a streptavidin-ALP enzyme conjugate, which catalyzes the hydrolysis of the 1-NPP enzymatic substrate into 1-NPOH.
The enzymatic product was then detected by DPV (**Figure 7.1**, b panel).

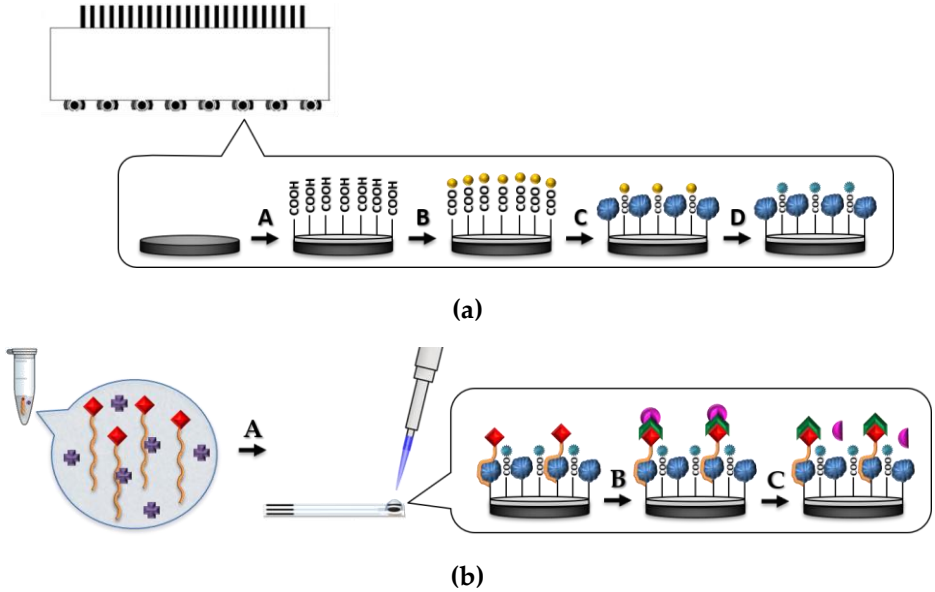

Figure 7.1. *Scheme of the enzyme-linked oligonucleotide array for aflatoxin B_1 detection.* ***(a)*** *GSPE surface modification: A) electrocopolymerization of aniline and anthranilic acid; B) activation of the carboxylic groups; C) AFB_1-BSA conjugate immobilization; D) blocking of the unreacted activated carboxylic groups with L-lysine.* ***(b)*** *AFB_1 detection: affinity reaction between AFB_1 at different concentrations and biotinylated DNA aptamer sequence in solution; A) competition between free and immobilized AFB_1 molecules; B) coupling with streptavidin-alkaline phosphatase enzyme conjugate; C) incubation with 1-naphthyl phosphate enzymatic substrate and detection of 1-naphthol enzymatic product.*

7.3.4.1 Aflatoxin B_1-BSA Immobilization

The P(ANI-*co*-AA)/GSPEs (previously described in ***Subsection 4.1.2***) were used as platform for the covalent immobilization of AFB_1-BSA.

An activation step was performed to increase the reactivity of the carboxylic groups of the AA component inside the copolymer. 8 µL of a mixture of 0.2 M NHS and 0.4 M EDC in activation buffer were dropped onto the electrodes surface and let react for 30 min at 4 °C. After this time, the cells were washed for three times with 100 µL immobilization buffer. The AFB_1-BSA conjugate was dissolved in Milli-Q water at a concentration of 1 mg/mL as stock solution and then diluted at 2 µg/mL in

immobilization buffer. 15 μL of this solution were deposited onto the modified surface of the working electrodes and chemisorption was allowed to proceed overnight (≈ 16 h). During this period, the sensors were stored in petri dishes to protect the solution from evaporation.
To remove unbound AFB_1-BSA molecules, the surface was washed for three times with 15 μL of immobilization buffer. A blocking step was then performed by adding 8 μL of 0.1 mg/mL L-lysine solution in immobilization buffer for 30 min, which was then washed again for three times with 15 μL of immobilization buffer. Modified GSPEs were stored in dry conditions at 4 °C before use.

7.3.4.2 Aflatoxin B_1 Detection

To obtain a dose-response calibration curve, AFB_1 detection was performed by dropping AFB_1 solutions containing a proper concentration of the biotinylated DNA aptamer (apt-BIO) onto the sensor surfaces and by allowing the competitive reaction to proceed.
Specifically, the competition for the binding with the aptamer between AFB_1-BSA, immobilized onto the electrode surface, and free aflatoxin, contained in the sample, was performed in two steps. In the first step, the affinity reaction between target mycotoxin in the concentration range 0.1–10 ng/mL and 20 nM apt-BIO is allowed to proceed in microtubes for 15 min; in the second step, 8 μL of these mixtures were dropped onto the modified sensors for 30 min. The sensors were then rinsed for three times with 15 μL of detection buffer. Control experiments were performed using AFG_1 solutions, in order to test the selectivity of the developed biosensors.

7.3.4.3 Enzymatic Labeling and Electrochemical Measurements

The biotinylated complexes formed on the sensor surface were further incubated with 15 µL of a solution containing 1 U/mL of streptavidin-ALP enzyme conjugate and 8 mg/mL of BSA in detection buffer.
Each sensor was washed two times with 50 µL of detection buffer. 50 µL of 1 mg/mL enzymatic substrate (1-NPP) in detection buffer were then dropped onto the disposable sensor surface. The electroactive enzymatic product, 1-NPOH, was detected after 20 min *via* DPV by scanning the potential from 0 V to +0.6 V at 4 mV/s (5 mV step potential, 70 mV pulse potential, 0.05 s pulse time, 0.15 s interval time) in accordance with a previously reported protocol [215].

The current peak height was taken as the electrochemical signal.
The signal is expressed in relative percent units as S_x/S_0 (*i.e.* ratio between measured signal to blank signal) and plotted against AFB_1 concentration. The obtained curve showed the typical sigmoidal shape of a competitive assay and was fitted with a dose-response sigmoidal equation (*Equation (7.1)*):

$$S_x/S_0 = A + \frac{B - A}{1 + 10^{[\log C - c(AFB_1)]^{Hillslope}}} \qquad (7.1)$$

where *A* and *B* are the Y values at the top and at the bottom plateau of the curve, respectively; *C* is related to the target concentration necessary to reduce the signal at the 50%; *Hillslope* is the slope of the linear part of the curve.

7.3.4.4 Maize Flour Samples Analysis

For the analysis of real samples, 25 g of maize flour were weighed and mixed with 50 mL of a 50% (%v/v) ethanol/water solution for 5 min with a high-speed blender. This mixture was centrifuged at 5000 rpm for 5 min;

the supernatant was then collected and evaporated to dryness under a nitrogen stream. The dried extracted sample was then suspended in immobilization buffer. To assess the matrix effect and the suitability of the extraction procedure, different batches of maize flour were spiked before or after the extraction procedure, so that the effect of the contamination was tested both on maize flour and on the extracted samples. The response was then determined by DPV measurements, under the same conditions used for AFB_1 calibration curve.

7.4 Results and Discussion

7.4.1 Modification of GSPEs

SEM analysis was exploited to investigate the morphology of ANI and AA copolymerization onto the GSPEs surface. **Figure 7.2** (a panel) shows that the unmodified GSPE surface appears rougher than in the case of the obtained P(ANI-*co*-AA acid)-modified GSPE surface (**Figure 7.2**, b panel). This confirms the fact that the polymerization was successfully carried out.

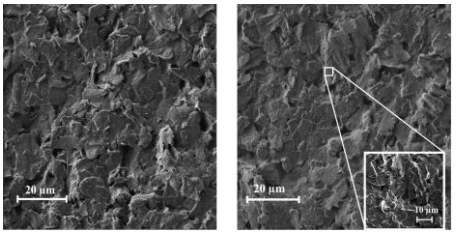

(a) **(b)**

Figure* 7.2.** *SEM images of* ***(a) *unmodified GSPE and* ***(b)*** *poly(aniline-co-anthranilic acid) copolymer-modified GSPE.*

The P(ANI-*co*-AA)/GSPEs were then used for covalent immobilization of AFB_1-BSA: in fact, in our case, the polymer is used for the multiple purposes of providing a higher electroactive area compared

to the bare electrode, of protecting the latter versus its fouling, and of working as a scaffold to anchor the AFB$_1$-BSA conjugate by exploiting the binding between the carboxylic groups of the copolymer and the amine groups of the protein. EIS and CV measurements were performed to assess the modification of the GSPEs surface and the immobilization of AFB$_1$-BSA using $[Fe(CN)_6]^{-4/-3}$ as the redox probe.

The Nyquist plots after each assembly step, under optimized conditions, are shown in **Figure 7.3** (a panel); while the values of the charge transfer resistance (R_{ct}) obtained by EIS are reported in **Figure 7.3** (b panel). As it can be seen from the first panel, the electrode conductivity increases after the electropolymerization of P(ANI-*co*-AA) onto the graphite surface, while the reproducibility growth shown in the second panel is due to the improved uniformity of the surface determined by the electrodeposition of the copolymer nanolayer. The immobilization of the AFB$_1$-BSA was confirmed by EIS measurements observing an increase of R_{ct} to a mean value of (151±10) kΩ, with respect to the P(ANI-*co*-AA) modified electrodes. CV measurements confirm the above results, as the current peak height increases after the electropolymerization of the copolymer onto the graphite surface, while it is decreasing after the immobilization of AFB$_1$-BSA (**Figure 7.3**, c panel).

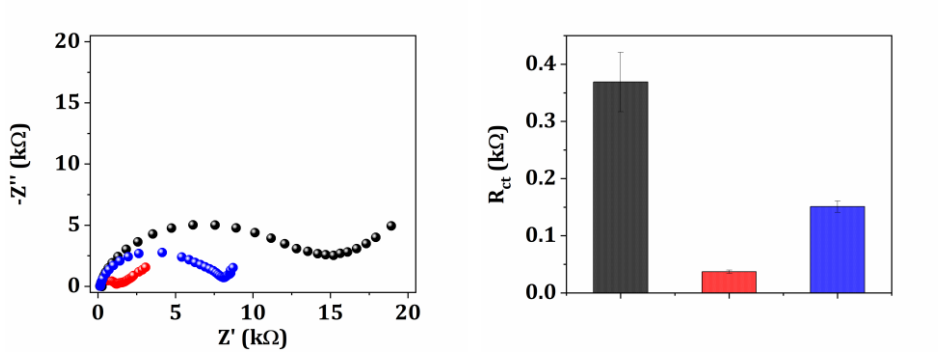

(a) **(b)**

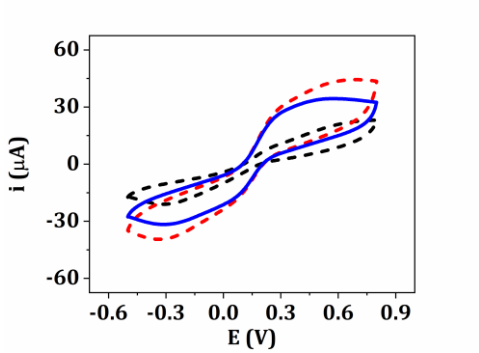

(c)

Figure 7.3. *Electrochemical characterization of bare and modified GSPEs in presence of 5 mM $[Fe(CN)_6]^{-4/-3}$ redox probe (equimolar solution in 0.1 M KCl): • GSPE, • P(ANI-co-AA)/GSPE, • AFB1-BSA/P(ANI-co-AA)/GSPE.* ***(a)*** *Nyquist plots;* ***(b)*** *average and standard deviation of R_{ct} values. Each measurement was repeated at least five times using different sensors.* ***(c)*** *cyclic voltammograms (scan rate: 50 mV/s).*

For estimating the shelf life of the developed sensors, a batch of AFB1-BSA-modified P(ANI-*co*-AA)/GSPEs was stored in dry conditions at 4 °C. The stability of the developed biosensors was tested by EIS analysis in regular time intervals up to one month. 30 biosensors were assayed over this period and the R_{ct} value and the average %RSD were calculated.
The results showed good reproducibility with a 10% coefficient of variation. This property of the modified sensors ensures reliable measurement for on-field application.

7.4.2 Selected Oligonucleotide Sequence for Aflatoxin B1

The 3-dimensional structure of the aptamer sequence is of paramount importance for capturing selectively the analyte. The various aptamer conformations are due to weak bonds, such as hydrogen bond interactions, van der Waals interactions and π-stacking interactions.
To predict the secondary structure of the selected oligonucleotide sequence the algorithm MFold [213] was used. Oligonucleotide structures prediction was obtained by setting up the temperature to 20 °C, by

regulating the ionic strength according to the used immobilization buffer and by selecting untangle with loop fix as drawing mode; other parameters were left as default settings. From the theoretical conformations, the oligonucleotide sequence shows a prevalent single-stranded structure at 20 °C in solution characterized by two different sized loops as shown in **Figure 7.4**.

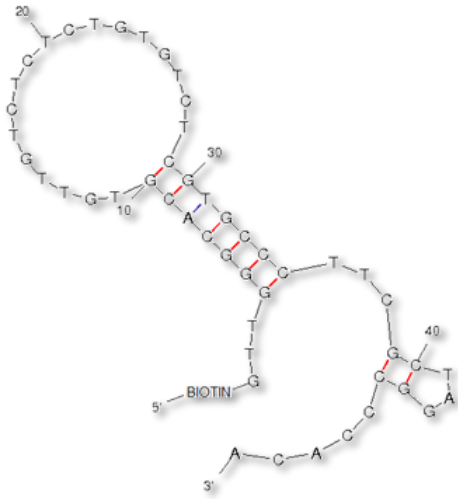

Figure 7.4. *Secondary structure of apt-BIO sequence as predicted with MFold algorithm at 20 °C in 0.1 M phosphate buffer saline, pH 7.4 ($[Na^+]$ = 0.26 M). The bond between G and C is shown in red to indicate its stability.*

7.4.3 Aflatoxin B_1 Competitive Assay

AuNPs and PANI-modified SPEs were initially chosen for developing our assay in accordance with the optimized procedure reported previously [72]. 2 µg/mL AFB_1-BSA conjugate were immobilized by chemisorption on the NPs through the interactions between the thiol groups of the protein aminoacids (*e.g.* cysteine) and gold.

The sensors were incubated with 0.1, 0.2 and 0.5 ng/mL AFB_1 solutions containing 20 nM apt-BIO and the response was determined through DPV

by following the labeling procedure already described. The signal variation with respect to the blank ($(S_x-S_0)/S_0$) in percent units is reported in **Table 7.1** for each AFB_1 concentration. The obtained results did not follow the expectations, as they showed a different trend from that of a competitive assay with a high standard deviation.

Table 7.1. *Signal variation with respect to the blank ($(S_x-S_0)/S_0$) in percent units obtained with different concentrations of aflatoxin B_1 onto the platform made of polyaniline and gold nanoparticles (AuNPs/PANI/GSPE). Each measurement was repeated at least five times using different sensors.*

AFB_1 (ng/mL)	$(S_x-S_0)/S_0$ (%)	%RSD
0.1	+30.4	14.4
0.2	−7.4	31.3
0.5	+1.2	14.2

This is due to the fact that chemisorption of the protein complex did not happen in an ordered and oriented way, eventually because of a low accessibility of the protein thiol groups. Thus, another path was followed, that is the doping PANI with PAA.

To find the best conditions for the competitive assay, key experimental parameters such as the AFB_1-BSA and apt-BIO concentrations and the target incubation time were studied.

In order to optimize the AFB_1-BSA immobilization, P(ANI-*co*-AA) sensors were incubated overnight with different AFB_1-BSA solutions (15.0, 5.0, 2.0, 0.002 μg/mL). The assay was then carried out for each AFB_1-BSA concentration by incubating the biosensors with a solution containing 3 ng/mL AFB_1 and 20 nM apt-BIO (S_3). These signals were put into comparison with those obtained from the blanks (S_0), which contain the aptamer only. The signal decrease (S_3/S_0) in percent units is reported in **Table 7.2**. The best data in terms of highest signal decrease and reproducibility were achieved when a concentration of 2 μg/mL of the

AFB_1-BSA conjugate was used; thus, this concentration was chosen for the following experiments.

Table 7.2. *Aflatoxin B_1-BSA concentration optimization. The peak current ratio between 3 ng/mL AFB_1 and the blank (S_3/S_0) is reported in percent units. Each measurement was repeated at least five times using different sensors.*

AFB_1-BSA (μg/mL)	S_3/S_0 (%)	%RSD
15.0	88	10
5.0	93	7
2.0	68	8
0.002	95	12

Experiments for the optimization of the apt-BIO concentration were performed by incubating the biosensors with 0 ng/mL (S_0) and 3 ng/mL AFB_1 (S_3) solutions containing different apt-BIO concentrations. The signal variation $(S_3-S_0)/S_0$ in percent units is reported in **Figure 7.5**.

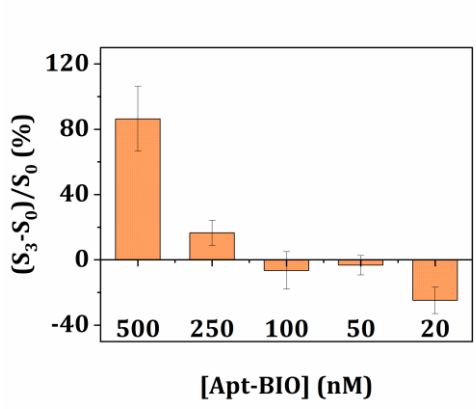

Figure 7.5. *Aptamer concentration optimization. The signal is reported as $(S_3-S_0)/S_0$ percent units, that is the signal variation obtained with 3 ng/mL aflatoxin B_1 with respect to the blank. Each measurement was repeated at least five times using different sensors.*

As the assay follows a competitive format, the addition of AFB_1 should cause a decrease of the current peak height in presence of the analyte with respect to the blank. However, by varying apt-BIO

concentration, this behavior was not always observed; the signal in presence of the target is increasing with respect to the blank with 500 nM and 250 nM of the biotinylated aptamer. This is probably due to the fact that higher concentrations of the aptamer could increase its non-specific adsorption in presence of the target molecules, and thus the current increases. With lower concentrations, this did not happen and the highest signal decrease with respect to the blank was obtained for 20 nM, thus this value was used for the following experiments.

Experiments for the optimization of apt-BIO incubation time were also performed by incubating the SPCs with 3 ng/mL target solution and 20 nM apt-BIO. The incubation times during which the apt-BIO was put into contact both with AFB_1 and with AFB_1-BSA were varied, since the use of different incubation times allows tuning the equilibrium of the binding between the aptamer and its target. The best performance of the assay in terms of highest signal decrease and reproducibility was observed when 15 min for affinity reaction between apt-BIO and AFB_1 in the microtubes and 30 min for the competition reaction onto the sensing surface were used (**Table 7.3**).

Table 7.3. *Assay time optimization. The peak current ratio between 3 ng/mL AFB_1 and the blank (S_3/S_0) is reported in percent units. Each measurement was repeated at least five times using different sensors.*

AFB_1-BSA (μg/mL)	Competition time (min)	S_3/S_0 (%)	%RSD
45	30	83	14
30	30	94	9
15	30	79	4
15	20	84	12
15	10	93	6

7.4.4 Aflatoxin B_1 Detection in Standard Solutions

Under the optimized experimental conditions, a calibration curve in AFB_1 buffered solutions was obtained by an indirect competitive format. Various solutions at different AFB_1 concentrations, containing a fixed amount (20 nM) of apt-BIO, were thus analyzed by DPV; the aptasensor response in buffered solutions only ($c(AFB_1) = 0$ ng/mL, [Apt-BIO] = 0 nM) was also tested (**Figure 7.6**, a panel). A decrease of the current peak height was recorded by increasing AFB_1 concentration in the range 0.1–10 ng/mL. The signal is reported as S_x/S_0 percent units, that is the percentage of the signal decrease with respect to the blank value (**Figure 7.6**, b panel). The obtained calibration curve shows a correlation coefficient $R^2 = 0.98$.
The LOD of the assay was calculated by the evaluation of the average response of the blank minus three times the standard deviation and a value of 0.086 ng/mL was achieved.

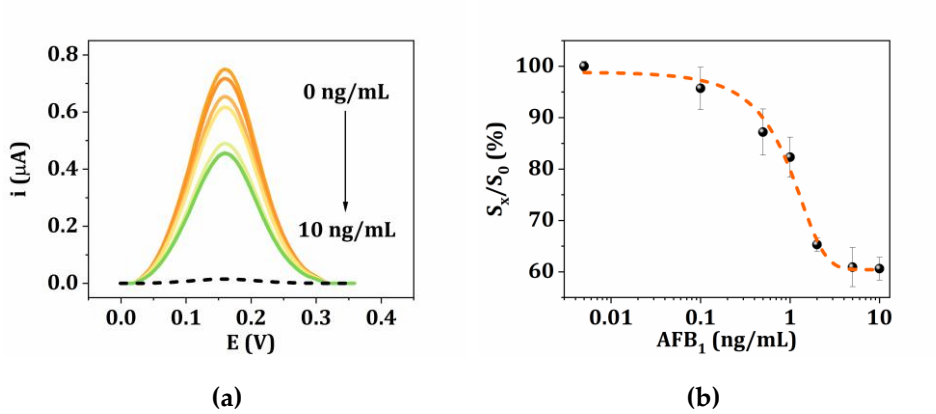

Figure 7.6. *Aflatoxin B_1 detection.* ***(a)*** *Differential pulse voltammograms obtained with different AFB_1 concentrations. The dotted scan corresponds to the signal registered in buffer solution containing 0 ng/mL AFB_1 and 0 nM apt-BIO;* ***(b)*** *calibration curve for AFB_1. Each measurement was repeated at least five times using different sensors.*

The described oligonucleotide assay was confirmed as a promising analytical tool for AFB_1 detection, since the tested concentrations gave an average 5% RSD value for five repetitions of each standard solution.

The assay selectivity was assessed in presence of AFG_1. When AFG_1 at different concentrations (1 ng/mL and 5 ng/mL) was added, a decrease lower than 7% with respect to the blank value was observed.

7.4.5 Aflatoxin B_1 Detection in Maize Flour Samples

In order to evaluate the operability of the assay, some preliminary experiments on maize samples were carried out. With this aim, two different batches of maize flour were contaminated by spiking with AFB_1 standard solutions before and after the pretreatment of samples.
The biosensor response was then determined by DPV measurements, in the same conditions used for the AFB_1 calibration curve. The signal was found to decrease with respect to the sample solution by increasing the AFB_1 spiked concentration in the analyzed samples (**Table 7.4**).

An acceptable bias was found for spiked maize flour samples confirming the possibility to use the biosensor in real samples.

Table 7.4. *Recovery values obtained from the analysis of aflatoxin B_1-spiked maize flour samples and extracts. Each measurement was repeated at least five times using different sensors.*

	AFB_1 spiked (ng/mL)	**AFB_1 found (ng/mL)**	**Recovery (%)**	**%RSD**
Extracted samples	1.0	0.80	80	7
	5.0	4.40	88	5
Maize flour	1.0	0.96	96	10
	5.0	4.20	84	8

7.5 Conclusions

In this work, we propose an electrochemical enzyme-linked oligonucleotide sensor, based on a competitive format, for the determination of AFB_1 in maize samples. The disposable screen-printed arrays make it simple and cost-effective, since it involves low amounts of reagents and mass-produced electrochemical cells. AFB_1 in solution competes with the AFB_1-BSA immobilized onto the electrode surface to bind the aptamer, which was labeled with ALP to generate signal for sensing. A dose-response curve was obtained between 0.1 ng/mL and 10 ng/mL and a LOD of 0.086 ng/mL was achieved. Preliminary experiments with maize samples were performed.

From the obtained results, the developed analytical tool has proven itself to be applicable for screening on-field analysis.

Contents lists available at ScienceDirect

Bioelectrochemistry

journal homepage: www.elsevier.com/locate/bioelechem

8. Mycotoxins Aptasensing: from Molecular Docking to Electrochemical Detection of Deoxynivalenol

Bioelectrochemistry, **2021**, *138*, 107691 — **DOI**: 10.1016/j.bioelechem.2020.107691

8.1 Abstract

This work proposes a voltammetric aptasensor to detect deoxynivalenol (DON) mycotoxin. The development steps of the aptasensor were partnered for the first time to a computational study to gain insights onto the molecular mechanisms involved into the interaction between a thiol-tethered DNA aptamer (80mer-SH) and DON.

The exploited docking study allowed to find the binding region of the oligonucleotide sequence and to determine DON preferred orientation.

A biotinylated oligonucleotide sequence (20mer-BIO) complementary to the aptamer was chosen to carry out a competitive format.

Graphite screen-printed electrodes (GSPEs) were electrochemically modified with polyaniline and gold nanoparticles (AuNPs/PANI) by means of cyclic voltammetry (CV) and worked as a scaffold for the immobilization of the DNA aptamer. Solutions containing increasing concentrations of DON and a fixed amount of 20mer-BIO were dropped onto the aptasensor surface: the resulting hybrids were labeled with an alkaline phosphatase (ALP) conjugate to hydrolyze 1-naphthyl phosphate (1-NPP) substrate into 1-naphthol (1-NPOH) product, which was detected by differential pulse voltammetry (DPV). According to its competitive format, the aptasensor response was signal-off in the range 5–30 ng/mL

DON. A LOD of 3.2 ng/mL was achieved within a 1-hour detection time. Preliminary experiments on maize flour samples spiked with DON yielded good recovery values.

Keywords: aptasensor; deoxynivalenol; molecular docking; screen-printed electrodes; mycotoxin.

8.2 Introduction

8.2.1 State of the Art

Mycotoxins detection by means of biosensors is mostly relying on the high affinity interactions between antigen and specific antibodies.
A DON-antibody had been widely used as the biorecognition element in detecting DON mycotoxin in the past decades [236], so that most approaches to analyze DON are still limited to immunosensors and immunoassays exploiting optical and electrochemical transduction techniques [237–240].

Among various biosensors for DON detection, electrochemical biosensors play a prominent role due to their sensitivity, selectivity, low cost, simplicity and, in some cases, portability [226]. A peptide-based immunosensor for green detection of DON was proposed by Yan *et al*. [241]. A selected DON mimotope (*i.e.* phage-displayed peptide) worked as a mimetic competing antigen for the binding with an anti-DON antibody, which was immobilized onto a 3-mercaptopropionic acid-modified gold electrode through EDC/NHS chemistry. The competition was traced by adding a horseradish peroxidase (HRP)-conjugated anti-phage antibody and the detection was carried out by means of SWV in presence of pyrocatechol and H_2O_2, resulting in a dynamic range of 0.1–10000 pg/mL and a LOD of 0.07 pg/mL. Another electrochemical approach was presented by Sunday *et al* [242]. A AuNPs-dotted 4-nitrophenylazo functionalized graphene (AuNP/G/$PhNO_2$) composite was used to develop a sensor platform by applying Nafion 117 as a binder and incorporating $[Ru(bipyridine)_3]^{+2}$ as a cationic reactant on a glassy carbon electrode. The modified electrode was then electrochemically reduced to generate aminophenyl surface, which was activated through EDC/NHS chemistry for the immobilization of the anti-DON antibody. The formation of the immunocomplexes after the interaction with DON molecules inhibited the electron flow and increased the charge transfer

resistance, resulting in a linear correlation towards DON concentration in the range 6–30 ng/mL with a LOD of 0.3 ng/mL. An electrochemical enzyme-linked immunomagnetic assay was developed by Romanazzo *et al*. based on the use of magnetic beads modified with a DON conjugate, which competes with free DON molecules in solution for the binding with a biotinylated recombinant Fab fragment [243]. The binding is traced by adding an avidin-biotin-HRP complex. The measurement is carried out onto magnetized graphite screen-printed working electrodes of an 8-cells array by adding the enzymatic substrate and measuring chronoamperometrically the enzymatic product. Using DON standard solutions, a working range between 100 ng/mL and 4500 ng/mL was obtained with an EC_{50} (*i.e.* the amount of DON needed to produce a 50% decrease in the signal) of 380 ng/mL and a LOD of 63 ng/mL. A similar approach was presented by Valera's group with an electrochemical immunosensor to detect DON residues in wheat samples [244]. The sensor relies on the competitive reaction between the mycotoxin and the antigen (DON-BSA) immobilized onto magnetic microparticles for the binding with an anti-DON antibody labeled with CdS nanoparticles (*CdS*NPs-AbDON). The *CdS*NPs were then dissolved in acidic medium and the released Cd(II) ions were detected by means of SWV. The LOD obtained in this case was as low as 0.348 ng/mL in buffered solution and of 342.4 ng/g in real samples.

Over the last years, aptamer-based biosensors (*i.e.* aptasensors) had exerted a strong interest in the sensing field and they have thus become a hot topic for researchers, as aptamers advantages over antibodies include high chemical and thermal stability, low-cost *in vitro* synthesis [21] and broad opportunities for modification and immobilization of various supports [22,245,246]. Consequently, various aptasensors have been developed for the analysis of a wide range of mycotoxins in the recent years [220,247,248]. To the best of our knowledge, only one electrochemical aptasensor for DON detection is reported in literature by

Ong group [249]. The study develops a biosensing system based on the use of iron nanoflorets graphene nickel foam as the transducer and an aptamer as the recognition element. The LOD attained with this approach is 2.11 pg/mL. Despite the low LOD value, the method exploits a long procedure of cleaning and biomodification of the nickel sponge, without mentioning the numerous washing steps between each immobilization/interaction step.

8.2.2 Target Analyte

DON, to be referred also as vomitoxin, is one of the best-known trichothecenes produced from *Fusarium graminearum* and *Fusarium culmorum* [250], which has been detected at high concentrations in cereals [251]. Trichothecenes are strong inhibitors of protein synthesis: in fact, exposure to DON causes the decrease of tryptophan uptake and, in turn, its synthesis of serotonin. DON assumption symptoms include loss of appetite, vomiting and weight loss, which are believed to be a consequence of reduced levels of this neurotransmitter [252,253].
The anorexic effects caused by DON manifests in animals as well as in humans; thus, vomitoxin contamination of food has a negative impact both for cattle breeders as well as for grain producers. Consequently, the detection of DON is of particular importance when considering its impact from both a health and an economic point of view [254].

8.2.3 Strategy

In this work, we present an electrochemical aptasensor for fast and sensitive DON screening analysis based on a competitive approach, which was developed on a disposable and cost-effective nanostructured sensing platform and coupled with a portable apparatus. Regarding the detection technique, the novelty of the realized biosensor compared to those reported in literature was primarily the use of a DNA sequence as the

receptor in a voltammetric enzyme-linked assay, which allowed a fast, sensitive and inexpensive detection. Moreover, the development of the aptasensor was coupled for the first time to a computational study.
The purpose of this research was in fact multiple: to gain insights on the competition mechanism exploited, to assess the suitability of the chosen format, and to apply a widely studied electrochemical platform [72,143,152,164] for the detection of new analytes. SPEs are applied as a platform for aptasensors development due to their advantages, such as rapid, simple and inexpensive manufacturing process, which lead to the possibility of a single usage to avoid contamination among different samples [72].

The aptamer was selected from a library of aptamers, designed by SELEX, as the one that showed to have the best ability to recognize DON [255]. In order to optimize the competitive format, the molecular interaction between the thiolated DNA aptamer and DON was firstly investigated by means of a docking study, which allows to verify the oligonucleotide sequence-binding region and to determine DON preferred orientation. A biotinylated oligonucleotide sequence (20mer-BIO), complementary to the aptamer region binding with DON, was then chosen to carry out the competitive format. The thiol-tethered DNA aptamer (80mer-SH) was immobilized by chemisorption onto graphite nanostructured electrode surface composed of AuNPs electrodeposited onto an electropolymerized PANI layer by means of CV. Solutions containing different concentrations of DON and a fixed amount of 20mer-BIO were placed onto the realized aptasensors to let the competition between DON molecules and the complementary oligonucleotide for the binding with the DNA aptamer to take place. The hybridization reaction was traced by a streptavidin-ALP conjugate, which catalyzes the hydrolysis of 1-NPP enzymatic substrate. The enzymatic product 1-NPOH was finally detected by DPV. The developed aptasensor showed a signal-off behavior, according to the competitive format used. The experimental

parameters involved in each step of the aptasensor design were studied and optimized. To test the aptasensor applicability, preliminary experiments in maize flour samples spiked with DON were finally performed. The easiness and rapidity of modification of SPEs, together with the stability of the DNA sequences used, allowed the preventive preparation and storage of multiple sensing platforms, which could then be transported and used as needed without a significant loss in their activity [22]. Moreover, the use of a Bluetooth®-controlled portable potentiostat in the electrochemical detection made the developed aptasensor a possible powerful tool for screening analysis.

8.3 Materials and Methods

8.3.1 Chemicals

Aniline (C_6H_7N), perchloric acid ($HClO_4$), tetrachloroauric acid ($HAuCl_4$), sulfuric acid (H_2SO_4), 6-mercapto-1-hexanol ($C_6H_{14}OS$), deoxynivalenol, aflatoxin B_1, aflatoxin G_1, bovine serum albumin, streptavidin-alkaline phosphatase enzyme conjugate, 1-naphthyl phosphate disodium salt ($Na_2C_{10}H_7O_4P$), methanol (CH_4O), ethanol (C_2H_6O), potassium ferrocyanide ($K_4[Fe(CN)_6]$), potassium ferricyanide ($K_3[Fe(CN)_6]$), tris(hydroxymethyl) aminomethane ($C_4H_{11}NO_3$), di-sodium hydrogen phosphate (Na_2HPO_4), sodium di-hydrogen phosphate di-hydrate ($NaH_2PO_4{\cdot}2H_2O$), diethanolamine ($C_4H_{11}NO_2$), sodium chloride (NaCl), potassium chloride (KCl), magnesium chloride hexahydrate ($MgCl_2{\cdot}6H_2O$) were purchased from Merck KGaA (Darmstadt, Germany). Maize flour was purchased in a local market. Milli-Q water was used for all preparations.

The DNA sequences used in this work were purchased from Eurofins Genomics GmbH (Ebersberg, Germany) and are listed as the following:

- 5′-(SH)-(CH_2)$_6$-GCA TCA CTA CAG TCA TTA CGC ATC GTA GGG GGG ATC GTT AAG GAA GTG CCC GGA GGC GGT ATC GTG TGA AGT GCT GTC CC-3′, as the thiolated DNA aptamer (80mer-SH);
- 5′-(biotin)-TEG-GGC ACT TCC TTA ACG ATC CC-3′, as the biotinylated complementary oligonucleotide (20mer-BIO).

The buffer solutions used in this work are the following:

1. storage buffer: 10 mM TRIS buffer, 0.1 M KCl, pH 8.0;
2. immobilization buffer: 0.1 M phosphate buffer, 0.1 M NaCl, pH 7.0;
3. affinity buffer: 0.1 M phosphate buffer, 0.1 M NaCl, pH 7.4;
4. detection buffer: 0.1 M DEA buffer, 0.1 M KCl, 1.0 mM $MgCl_2$, pH 9.6.

8.3.2 Aptamer-DON Interaction by Molecular Modeling Study

The MFold algorithm [256] was used to predict the DNA aptamer secondary structures, while DINAMelt Web Server [257] was used for the prediction of the Gibbs free energy of interaction between 80mer-SH and 20mer-BIO sequences. Oligonucleotide structures prediction was obtained by setting up the temperature at 25 °C and regulating at the concentration of the sodium ions at 0.26 M, according to the affinity buffer used ([Na_2HPO_4 + NaH_2PO_4] = 0.1 M, [NaCl] = 0.1 M, pH 7.4). Untangle with loop fix as drawing mode was selected, while other parameters were left as default settings. Starting from the aptamer sequence in FASTA format [258], a molecular docking approach using AutoDock4 program [259] was then applied, in order to define and visualize the interaction mechanism.

8.3.3 Aptasensor Development

The scheme of the realized aptasensor for DON determination based on a competitive approach is shown in **Figure 8.1**. The graphite screen-printed working electrode was progressively modified by ANI electropolymerization and by AuNPs electrodeposition. The 80mer-SH was then immobilized by chemisorption onto AuNPs. The immobilization step was followed by a mixed SAM formation by incubation with MCH. Solutions containing different concentrations of DON and a fixed amount of 20mer-BIO were analyzed. The biotinylated hybrids formed onto the aptasensor surface were labeled with a streptavidin-ALP conjugate. The enzyme catalyzes the hydrolysis of 1-NPP enzymatic substrate to 1-NPOH electroactive product, which was finally detected by DPV.

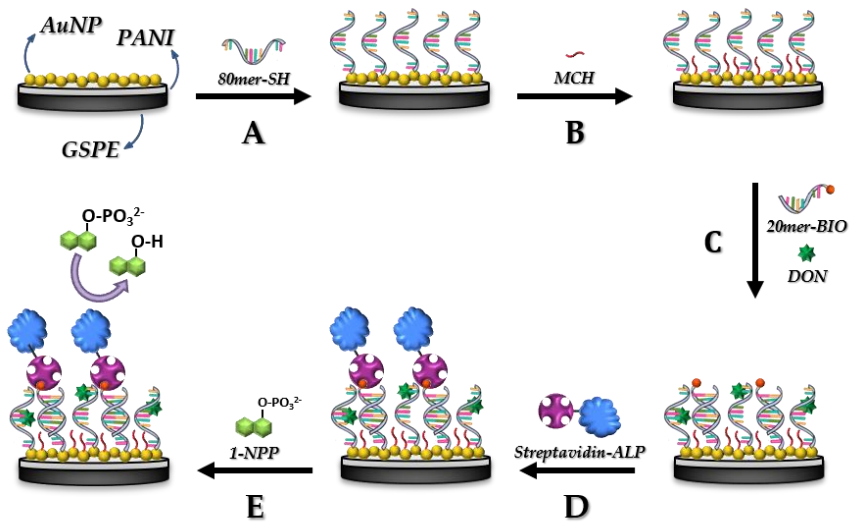

Figure 8.1. *Scheme of the developed aptasensor for deoxynivalenol detection.*
A) Thiolated DNA aptamer immobilization onto gold nanoparticles/polyaniline-modified working GSPE; B) blocking step with the addition of 6-mercapto-1-hexanol;
C) competitive reaction between DON molecules and the biotinylated complementary oligonucleotide; D) enzymatic labeling with streptavidin-alkaline phosphatase conjugate; E) incubation with 1-naphthyl phosphate enzymatic substrate and detection of 1-naphthol enzymatic product.

8.3.3.1 Aptamer Immobilization

The modification of the surface with AuNPs provided the basis for the immobilization of the thiolated aptamer. 10 μL of 80mer-SH solution (2 μM in immobilization buffer) were dropped onto the working electrode surface. Chemisorption was allowed to proceed overnight (≈ 16 h).
In the course of this period, the DNA-modified electrodes were kept in petri dishes as protection from any external factors, including the evaporation of the solution. The electrode surface was then washed with the immobilization buffer to remove any unbound aptamer sequence.
The immobilization step was followed by a mixed SAM formation by incubation with 1 mM MCH solution for 60 min. The aptasensors were stored under dry conditions at 4 °C before use.

8.3.3.2 Deoxynivalenol Detection

In this study, DON determination was provided by following a competitive format. DON is indirectly detected by electrochemically tracing the hybridization reaction between the immobilized 80mer-SH and the complementary 20mer-BIO. To achieve a dose-response calibration curve in this perspective, solutions containing a variable concentration of DON and a fixed amount of 20mer-BIO in affinity buffer were put together onto the aptasensor surface in order to achieve the competition for the limited number of binding sites constituted by the immobilized aptamer molecules. Specifically, DON standard solutions were prepared daily by diluting a stock solution (0.5 mg/mL prepared in methanol) in affinity buffer. The diluted solutions contain the lowest percentage as possible of methanol to avoid a deterioration of the insulating film of SPEs.
The competition was performed between DON in the concentration range between 0 ng/mL and 50 ng/mL and 1 nM 20mer-BIO for 30 min at room temperature. The aptasensors were then rinsed for three times with 50 μL of detection buffer.

8.3.3.3 Enzymatic Labeling and Electrochemical Measurements

The hybrids formed onto the aptasensor surface were marked with an enzymatic conjugate bearing a streptavidin moiety that binds with the biotin present on the complementary sequence. Therefore, each sensor was additionally incubated with 10 μL of a solution containing 1 U/mL of streptavidin-ALP enzyme conjugate and 8 mg/mL of BSA in detection buffer. After 20 min, all the sensors were washed three times with 50 μL detection buffer. The enzyme-labeled sensor surface was made to react with 50 μL of 1 mg/mL enzymatic substrate (1-NPP) in detection buffer for 20 min. The electroactive enzymatic product 1-NPOH was then detected *via* DPV by scanning the potential from 0 V to +0.6 V at 4 mV/s (5 mV step potential, 70 mV pulse potential, 0.05 s pulse time, 0.15 s interval time).

The current peak height was taken as the electrochemical signal. The signal is expressed in relative percent units as S_x/S_0 (*i.e.* ratio between measured signal to blank signal) and plotted against DON concentration. The obtained curve showed the typical sigmoidal shape of a competitive assay and was fitted with a dose-response sigmoidal equation (*Equation (8.1)*):

$$S_x/S_0 = A_1 + \frac{A_2 - A_1}{1 + 10^{(log\, X_0\, - c(DON))*p}} \qquad (8.1)$$

where A_1 and A_2 are the Y values at the bottom and at the top plateau of the curve, respectively; $logX_0$ is related to the target concentration necessary to reduce the signal at the 50%; p is the slope of the linear part of the curve.

8.3.3.4 Aptasensor Selectivity

The selectivity of the developed aptasensor was also studied. Solutions containing 25 ng/mL of AFB_1 or AFG_1 and a 1 nM fixed amount of 20mer-BIO were prepared and tested with the modified SPEs.
In addition, a solution containing 0 ng/mL of the mycotoxins and 1 nM of the biotinylated oligonucleotide sequence was tested as blank solution.

8.3.4 Maize Flour Samples Analysis

For the analysis of real samples, 25 g of maize flour were weighed and mixed with 50 mL of 50% (% v/v) ethanol/water solution for 5 min with a high-speed blender. This mix was centrifuged at 5000 rpm for 5 min; the supernatant was collected and then evaporated to dryness under a nitrogen flow. The dried extracted sample was then suspended in affinity buffer. The response was then determined by DPV measurements, under the same conditions used for DON calibration curve.

8.4 Results and Discussion

8.4.1 Aptamer-DON Binding Complex Study

8.4.1.1 Building 3D Structures for 80mer-SH

In aptasensors development, the selective capture of the analyte could be achieved by considering the role played by the 3-dimensional structure of the aptamer. Several types of interactions, including hydrogen bond interactions, van der Waals interactions and π-stacking interactions are giving rise to different conformations, which are of paramount importance in the binding with its target molecule.

In this work, MFold algorithm was used to determine primary and secondary folding forms of the aptamer; then, the molecular interaction between 80mer-SH and DON was investigated by molecular docking

study to verify the oligonucleotide sequence-binding region and to determine DON preferred orientation in the binding event. Using MFold algorithm, four structures, which present a folding energy value ranging from −2.67 kcal/mol to −1.98 kcal/mol, were obtained and are shown in **Figure S - 8.1**. In particular, structure A is characterized by the lowest folding energy (−2.67 kcal/mol), whereas structure D has the highest one (−1.98 kcal/mol); the structures indicated with B and C have intermediate folding energy values of −2.46 kcal/mol and −2.16 kcal/mol, respectively. Henceforth, these four structures will be reported in this ascending order of folding energy, from the more stable to the less one.

Since the folding energy differences are small (within 1 kcal/mol), it is not possible to select the most stable structure(s) to use for a 3D representation and for the following simulations: thus, all these four 2D structures were converted in 3D structures and used in the docking simulations by AutoDock4 program.

8.4.1.2 Molecular Docking Simulations

Docking simulations were carried out to study the interaction between DON and the four different 3D structures (A, B, C, D) obtained for 80mer-SH. These simulations allowed finding out the most probable binding regions of DON with the four aptamer structures mentioned above, also considering DON orientation. Moreover, the docking simulations allowed verifying whether the aforementioned binding regions were included in the aptamer sequence part which bound to the biotinylated complementary DNA oligonucleotide (20mer-BIO) chosen for the competitive assay. The aptamer structures were held rigid in the simulations, while the mycotoxin was fully flexible. Grid maps, one for each atom type present inside DON molecule, were calculated for several boxes to explore the whole aptamer structure.

A model of two input files used for docking analysis is reported in

Supplementary Material (***Section 8.6***).

The interaction between 80mer-SH and DON was studied on the whole oligonucleotide sequence, thus allowing to obtain the distribution of all docking conformations reported in **Figure 8.2**. Each panel shows one of the simulated aptamer structures (except for panel D, in which two different orientations are shown, as this 3D structure is more complex than the others) represented with a dark blue line, the complementary oligonucleotide represented with a white surface and all the interaction sites between DON and the aptamer represented with a sphere.
The spheres indicate the center (*i.e.* the average of the coordinates) of the mycotoxin and are displayed in a color scale representing the different values of the binding energy (from −6.0 kcal/mol to −0.9 kcal/mol) between DON and 80mer-SH. The blue spheres represent the positions of DON molecules in which the binding energy with the aptamer has the lowest value (around −6.0 kcal/mol). The histograms representing the distribution of the binding energy for the four aptamer structures are reported in **Figure S - 8.2** with the average value. The mean energy value of the aptamer structures is around −3.0 kcal/mol.

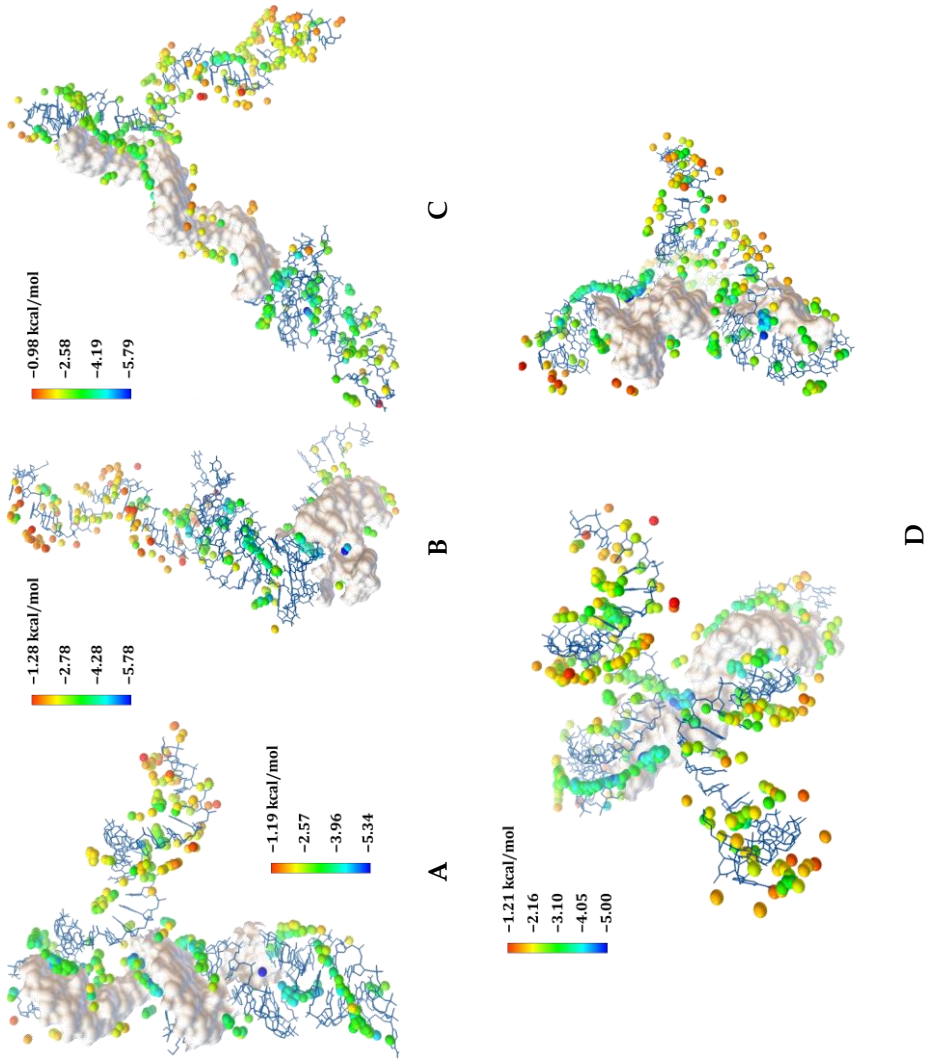

Figure 8.2. *Distribution of all the interaction sites between DON and the aptamer sequence for each aptamer structure (A, B, C, D). Each sphere corresponds to one DON docked orientation.*

For aptamer structures A, B and D, the strongest binding (binding energy values below −5.0 kcal/mol) is obtained when the position of the mycotoxin falls in the sequence part which binds to 20mer-BIO; conversely, for aptamer structure C the sequence part binding to 20mer-BIO interacts with DON less strongly, although all the correspondent energy values are around −4.0 kcal/mol.

Starting from these results, the complexes between DON and 80mer-SH with an associated binding energy lower than −4.8 kcal/mol were extracted for each structure and depicted in **Figure S - 8.3**. After the analysis of all the DON-aptamer complexes obtained for each structure (A, B, C and D), the nature of the interactions between the mycotoxin and the aptamer was analyzed for the DON-aptamer complex obtained for structure B, as it shows the highest stability with a binding energy value of −5.78 kcal/mol (**Figure 8.3**).

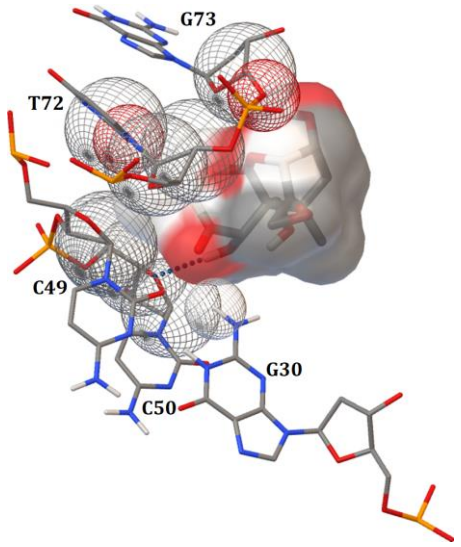

Figure 8.3. *Binding site of the aptamer (structure B) with DON. The complex with the lowest energy is shown. DON molecule is shown in solid surface representation, the interacting aptamer atoms are represented in wireframe: • carbon, • oxygen, • hydrogen, • nitrogen, • phosphorus. The dotted line represents the hydrogen bond. The interacting nucleosides are labeled.*

Hydrophobic interactions make the major contribution to the stability of DON-aptamer adduct, followed by electrostatic interactions. In this complex structure, H-bonds contribute to further stabilize the interaction; no π-stacking interactions are found, in agreement with DON structure.

On the basis of the folding energy values, more than one 3D structure could be possible for the aptamer in solution. Apart from this, the results obtained from docking study are very interesting and promising, as in most of the cases the DON-aptamer complexes with the lowest binding energy values show that the binding sites between the mycotoxin and 80mer-SH can be found in the sequence part which binds with the biotinylated complementary DNA oligonucleotide (20mer-BIO) selected for the competitive assay. In fact, the chosen aptamer is composed of two fixed end regions and a stochastic region of 35 bases. The two fixed end regions (5'-GCA TCA CTA CAG TCA TTA CGC ATC G and ATC GTG TGA AGT GCT GTC CC-3') are predefined and required to bind primers for the amplification step during the SELEX procedure; the 35-bases stochastic region (TA GGG GGG ATC GTT AAG GAA GTG CCC GGA GGC GGT) is responsible for the binding with the target [255]. Therefore, the results obtained from the docking study are not surprising but confirm that DON binds to the stochastic region. Nevertheless, this strategy could undoubtedly be considered as an useful tool to improve the aptasensor analytical performances, if the molecular docking study will be used to select an oligonucleotide with the proper length and sequence, rather than to verify the compatibility of an already chosen one.

8.4.2 Deoxynivalenol Competitive Assay

In order to perform DON analysis accurately with the developed aptasensor, method optimization studies were performed. As first point, the aptamer immobilization was investigated; the sensors were incubated with solutions at different concentrations of 80mer-SH.

Chemisorption was allowed to proceed overnight (≈ 16 h).
The immobilization step was followed by a mixed SAM formation by incubation with 1 mM MCH solution for 60 min. The sensors were then hybridized with 1 nM 20mer-BIO in absence of the target mycotoxin.
As a result, 2 μM in immobilization buffer was found to be the appropriate aptamer concentration, as above this concentration the current peak height rapidly approached a plateau, even increasing the amount of 80mer-SH immobilized on the surface (**Figure 8.4**, a panel). The selected concentration resulted to be a good compromise, as it gave the highest oxidation current without reaching the saturation of the electrode surface.

To appraise the influence of 20mer-BIO concentration, the hybridization reaction with solutions at different concentrations of 20mer-BIO was performed. After 20 min of incubation, the current peak height increased linearly with the oligonucleotide concentration up to around 7 nM, where a plateau was almost reached, as shown in **Figure S - 8.4**. However, for the competitive analysis, the oligonucleotide concentration was studied again in presence of DON and, as a result, the optimal DON binding performance was obtained with 1 nM concentration of the biotin-tagged oligonucleotide. Moreover, the chosen concentration value is lower than that corresponding to the beginning of the plateau (**Figure 8.4**, b panel), since working in saturation conditions, in this case, could have hampered somehow the competition reaction, as the complex between 80mer-SH and 20mer-BIO ($\Delta G = -28$ kcal/mol) is more stable than the aptamer-mycotoxin complex (-5.8 kcal/mol $< \Delta G < -5.0$ kcal/mol for the most stable complexes, as reported in **Figure 8.2**).

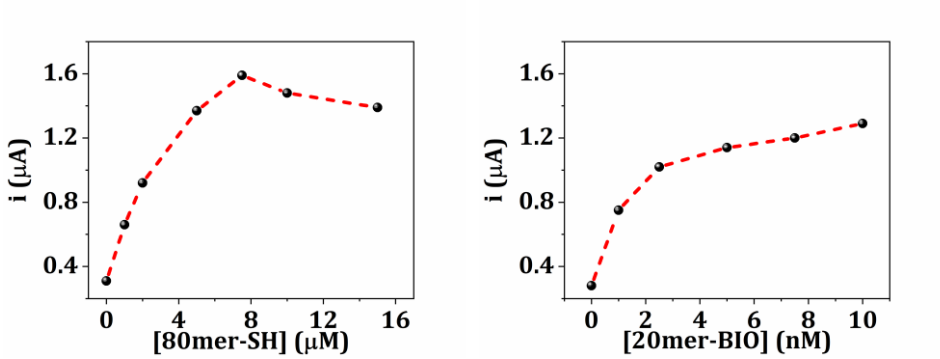

Figure 8.4. *Oligonucleotide sequences concentration optimization.* ***(a)*** *Hybridization curve between the immobilized aptamer (0–15 μM) and the biotinylated oligonucleotide (1 nM);* ***(b)*** *hybridization curve between 80mer-SH (2 μM) and 20mer-BIO (0–10 nM) in presence of deoxynivalenol. Each measurement was repeated at least five times using different sensors.*

Incubation time optimization study was conducted by adding solutions containing a specific DON concentration to the aptasensor surface immediately after the preparation. In fact, it has been noticed that the expected competition between 20mer-BIO and DON molecules for the binding with 80mer-SH could not be achieved if these elements were previously incubated in solution before being dropped onto the electrode surface. On the other hand, a competitive analysis was successfully achieved when performed directly on the aptasensor surface.

Therefore, freshly prepared solutions with a DON concentration of 20 ng/mL and containing 1 nM 20mer-BIO were kept on the aptamer-modified nanostructured electrode surface for 15, 30 and 45 min.

The obtained signals (S_{20}) were put into comparison with those obtained from the blanks (S_0), which contain 20mer-BIO only and which were incubated for the same periods of time. The best performance of the assay taking into consideration the highest signal decrease with respect to the blank and the related reproducibility was obtained when a competitive reaction time of 30 min was used (**Figure S - 8.5**).

8.4.3 Deoxynivalenol Detection in Standard Solutions

Under optimized experimental conditions, a calibration curve for DON was performed by competitive assay. Solutions containing 1 nM 20mer-BIO and increasing DON concentrations, were put on the surface of the aptasensors to provide competitive hybridization and analyzed by DPV; the aptasensor response in presence of 0 ng/mL DON and 0 nM 20mer-BIO was also evaluated (**Figure 8.5**, a panel). The obtained signal was reported as S_x/S_0 percent units, that is the percentage of the signal decrease with respect to the blank value. A decrease of the signal was observed by increasing DON concentration, thus a calibration curve with a correlation coefficient of $R^2 = 0.92$ was obtained in buffered solutions in the range 0–50 ng/mL of mycotoxin (**Figure 8.5**, b panel). The LOD of the assay was evaluated by taking into account the average response of the blank minus three times its standard deviation and, in this way, a value of 3.2 ng/mL was achieved. Thus, the developed aptasensor proved itself to be applicable in DON analysis, as all the tested mycotoxin concentrations gave an average 5% RSD for five repetitions of each standard solution.

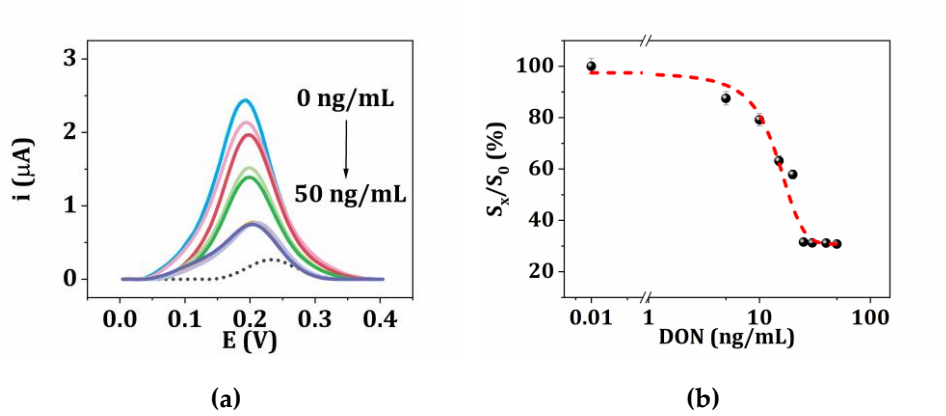

Figure 8.5. *Deoxynivalenol detection.* ***(a)*** *Differential pulse voltammograms obtained with different DON concentrations. The dotted scan corresponds to the signal registered in buffer solution containing 0 ng/mL DON and 0 nM 20mer-BIO;* ***(b)*** *calibration curve for DON. Each measurement was repeated at least five times using different sensors.*

8.4.4 Aptasensor Selectivity

The aptasensor selectivity was assessed by evaluating its response in presence of 25 ng/mL of each of the following mycotoxins: DON, AFB_1 and AFG_1. Accordingly, the obtained data show that the designed sensor interacts in a relevant way only with DON, as in presence of the target the signal decrease is of 60% with respect to the blank. On the other hand, the signal reduction against other mycotoxins is much lower. The obtained results are shown in **Figure 8.6**.

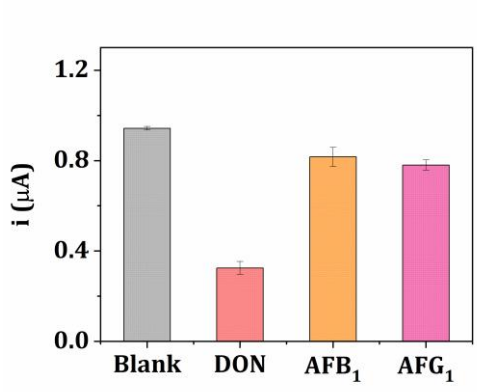

Figure 8.6. *Aptasensor selectivity. Current values obtained in buffer solutions containing 1 nM 20mer-BIO and • 0 ng/mL mycotoxins, • 25 ng/mL deoxynivalenol, • 25 ng/mL aflatoxin G_1, • 25 ng/mL aflatoxin B_1. Each measurement was repeated at least five times using different sensors.*

8.4.5 Deoxynivalenol Detection in Maize Flour Samples

Preliminary experiments on milled maize grains were performed in order to assess the operability of the developed aptasensor in real samples analysis. In this perspective, DON standard solutions (10–25 ng/mL) were used to contaminate different aliquots of maize flour after the pretreatment of the sample. The aptasensor response was then determined by DPV measurements, under the same conditions used for the mycotoxin calibration curve. The recovery values for maize extracts were calculated

by using the linear regression established in the range 10–25 ng/mL (**Figure S - 8.6**); the obtained results are showed in **Table 8.1**. This confirms the possibility for the developed aptasensor to be used in real samples analysis.

Table 8.1. *Recovery values obtained from the analysis of deoxynivalenol-spiked maize flour extracts. Each measurement was repeated at least five times using different sensors.*

DON spiked (ng/mL)	DON found (ng/mL)	Signal Decrease	Recovery (%)	%RSD
5.0	9.3	16	186	2
10.0	11.6	23	116	2
20.0	15.0	34	75	1
25.0	21.5	56	86	1

8.5 Conclusions

In this work, we report the development of an enzyme-labeled aptasensor, based on a competitive format and exploiting disposable SPEs and portable instrumentation, for the electrochemical determination of the non-electroactive DON molecule. The disposable SPEs make it simple and cost-effective, since it involves low amounts of reagents and mass-produced electrodes, that can be easily modified and stored prior to be used. The molecular interaction between DNA aptamer and DON was investigated by a docking study, which allows to verify if the complementary oligonucleotide sequence-binding region chosen for the competitive assay includes the interaction sites between the mycotoxin and the DNA aptamer, while also determining the preferred orientation assumed by DON in the binding event. The aptamer-DON complex with the highest stability (binding energy value below −5 kcal/mol) is obtained when the position of DON mycotoxin falls in the aptamer sequence part which binds the biotinylated DNA oligonucleotide used in the competition approach. This important result shows a good agreement

between computational and experimental approaches allowing to adopt docking study to obtain first relevant insights on the complementary sequence to be used. Therefore, it could be a valuable support in aptasensors development, allowing to rationalize an already chosen oligonucleotide sequence by describing the nature of the interactions involved and, as the final purpose, to select a complementary sequence of a proper length and primary structure to be used for improving the analytical performance of the developed aptasensors. Regarding the characterization of the aptamer itself, a detailed study about its affinity and selectivity towards DON (which has not been published before) was not performed yet but will be the topic of future research.

Under optimized experimental conditions, a dose-response curve was obtained between 5 ng/mL and 30 ng/mL DON and a LOD of 3.2 ng/mL was achieved within a 1-hour detection time. Preliminary experiments with maize samples were performed. Basing on the stability on the aptasensors and on the obtained results, the presented analytical tool has proven itself to be applicable for the development of an aptamer-based test kit for screening analysis.

8.6 Supplementary Material

File.gpf

```
npts 80 80 80
gridfld file.maps.fld
spacing 0.375
receptor_types A C HD N NA OA P SA
ligand_types A C HD OA
receptor file.pdbqt
gridcenter -16.676 -21.240 -2.378
smooth 0.5
map file.A.map
…
elecmap file.e.map
dsolvmap file.d.map
dielectric -0.1465
```

File.dpf

```
autodock_parameter_version 4.2
outlev 1
intelec
seed pid time
ligand_types A C HD OA
fld file.maps.fld
map file.A.map
…
elecmap test_structure1_AV.e.map
desolvmap test_structure1_AV.d.map
move ligand.pdbqt
about -0.1328 0.0186 -0.0356
tran0 random
quaternion0 random
dihe0 random
torsdof 4
rmstol 2.0
extnrg 1000.0
e0max 0.0 10000
ga_pop_size 150
ga_num_evals 2500000
ga_num_generations 27000
ga_elitism 1
ga_mutation_rate 0.02
ga_crossover_rate 0.8
ga_window_size 10
ga_cauchy_alpha 0.0
ga_cauchy_beta 1.0
set_ga
unbound_model bound
do_global_only 50
analysis
```

Model of two input files used for docking analysis.

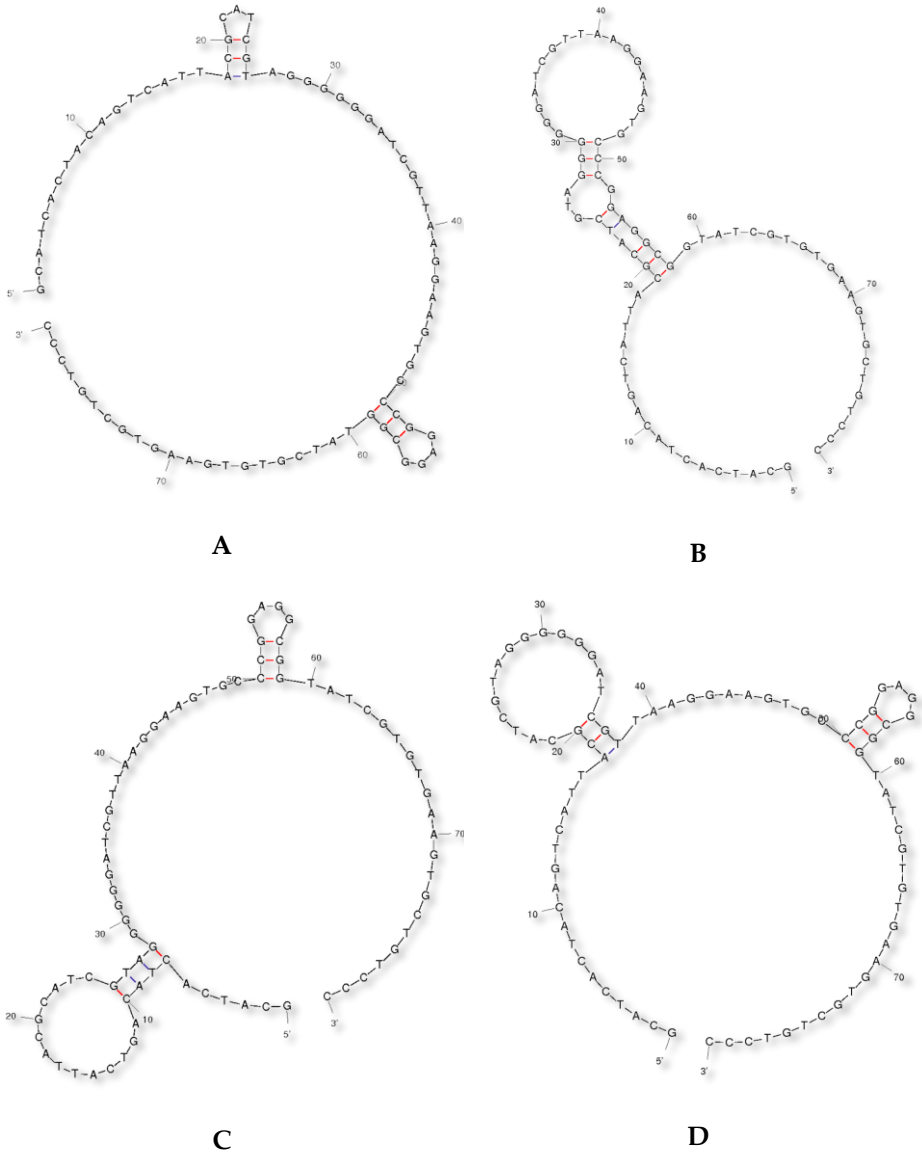

Figure S - 8.1. *Secondary structures of the aptamer (labeled with A, B, C, D) as predicted with MFold algorithm at 25 °C in 0.1 M phosphate buffer saline, pH 7.4 ([Na⁺] = 0.26 M). The bond between G and C is shown in red to indicate its stability.*

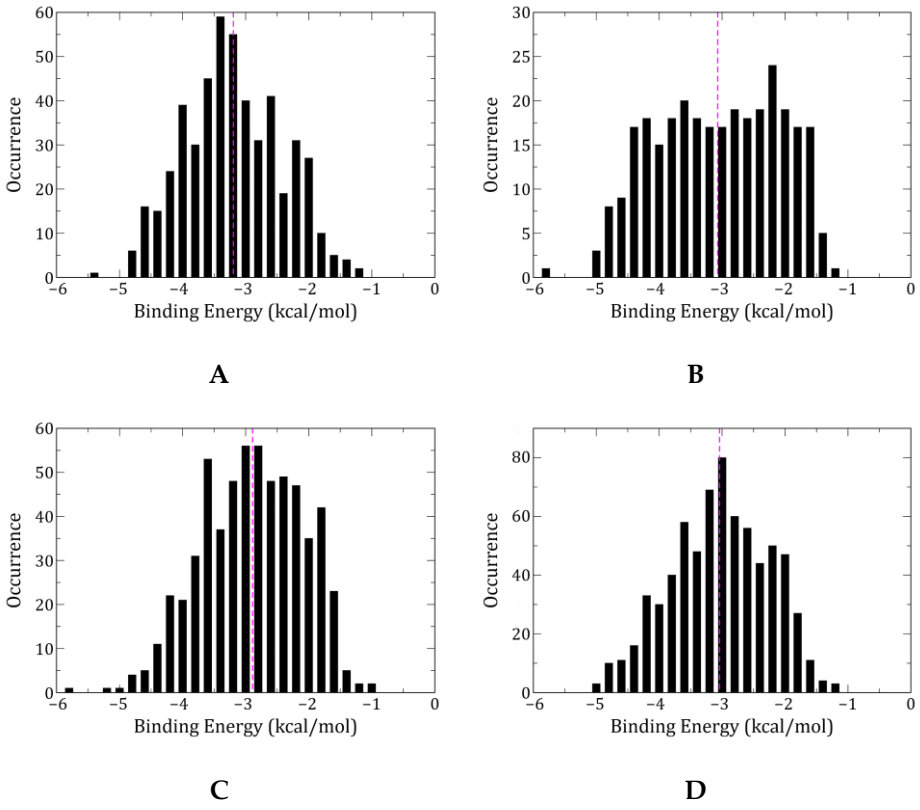

Figure S - 8.2. *Histograms of the DON-aptamer binding energies obtained by molecular docking study of the four aptamer structures A, B, C and D. The magenta dashed line indicates the mean energy value.*

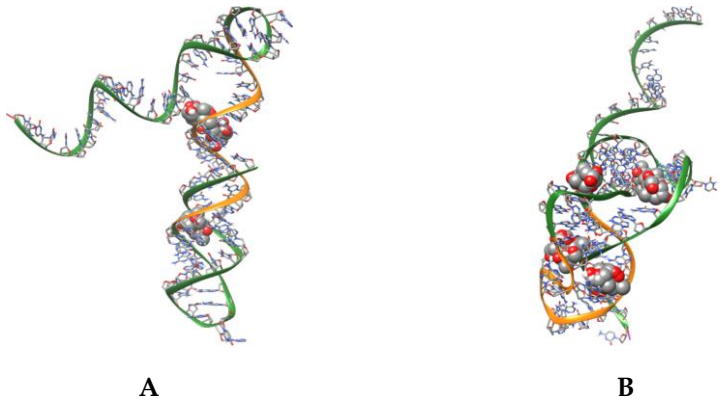

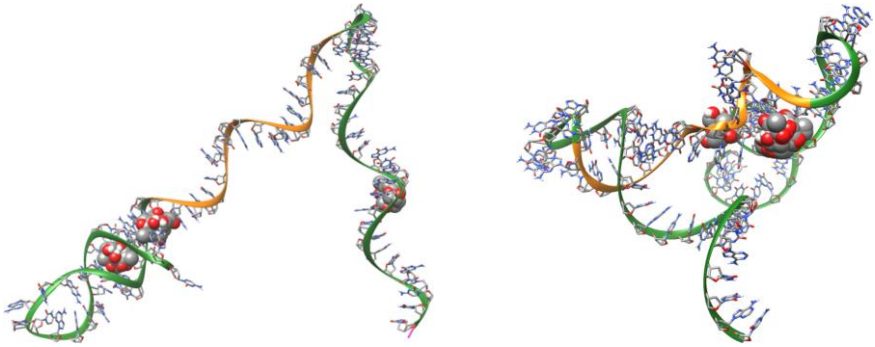

C D

Figure S - 8.3. *Representation of the DON conformations which show binding energy values below −4.8 kcal/mol. The orange region represents the sequence portion which binds the complementary oligonucleotide.*

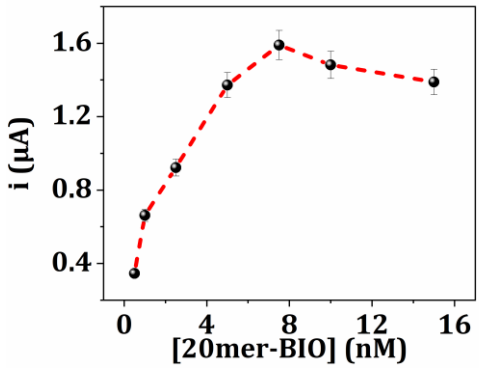

Figure S - 8.4. *Hybridization curve between the immobilized aptamer (2 μM) and the biotinylated oligonucleotide (0.5–15 nM) in immobilization buffer. Each measurement was repeated at least five times using different sensors.*

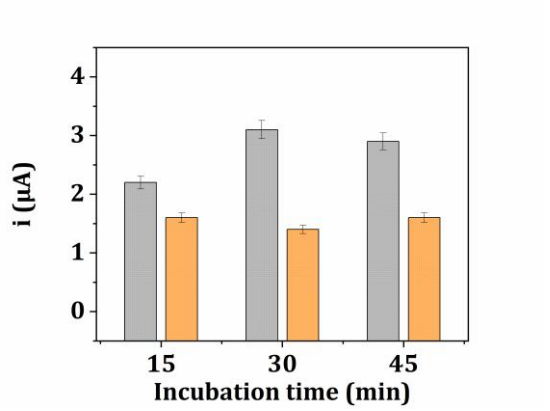

Figure S - 8.5. *Competition reaction time optimization. Current values obtained in buffer solution containing 1 nM 20mer-BIO and • 0 ng/mL or • 20 ng/mL deoxynivalenol. Each measurement was repeated at least five times using different sensors.*

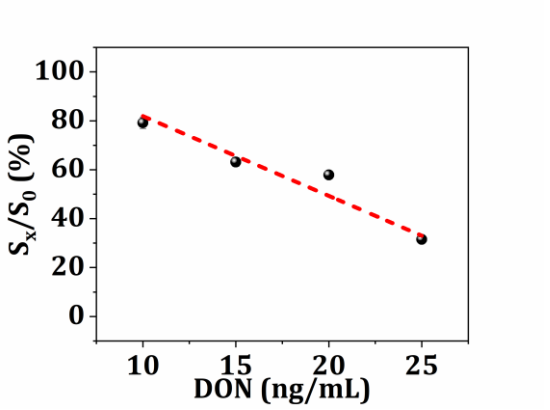

Figure S - 8.6. *Linear regression established in the range 10–25 ng/mL from the calibration curve obtained for DON standard solutions. Each measurement was repeated at least five times using different sensors.*

sensors

MDPI

9. Folding-based Electrochemical Aptasensor for the Determination of β-Lactoglobulin on Poly-L-Lysine Modified Graphite Electrodes

Sensors, **2020**, *20*(8), 2349 — **DOI**: 10.3390/s20082349

9.1 Abstract

Nowadays, food allergy is a very important health issue, causing adverse reactions of the immune system when exposed to different allergens present in food. Because of this, the development of point-of-use devices using miniaturized, user-friendly and low-cost instrumentation is becoming much of outstanding importance. According to this, electrochemical aptasensors have shown to be very useful tools to quantify a broad variety of targets. In this work, we developed a simple methodology for the determination of β-lactoglobulin (β-LG) in food samples using a folding-based electrochemical aptasensor built on poly-L-lysine-modified graphite screen-printed electrodes (PLL-GSPEs) and an anti-β-LG aptamer tagged with methylene blue (MB). This aptamer changes its conformation when the sample contains β-LG, and due to this, the spacing between MB and the electrode surface (and, therefore, the electron transfer efficiency) also changes. The response of this biosensor was linear for concentrations of β-LG within the range 0.1–10 ng/mL, with a LOD of 0.09 ng/mL. The biosensor was satisfactorily employed to the determination of spiked β-LG in real food samples.

Keywords: β-lactoglobulin; folding-based aptasensor; poly-L-lysine; conducting polymers; methylene blue.

9.2 Introduction

9.2.1 State of the Art

The developing of analytical approaches used to detect and quantify food allergens has become increasingly significant [260], because labeling in food is crucial for the consumers in order to avoid the major health problems. Analysis of allergens in food samples is usually carried out by immunoassay-based approaches [261], such as enzyme-linked immunosorbent assays (ELISAs) [117,123,262] or lateral-flow immunoassays (LFIAs) [263,264], and DNA-based methods, which detect the genes encoding for the proteins using amplifying strategies, for instance, the PCR [265,266]. Proteomic tests have been also used for the determination of allergens [267]. Although these methods are very sensitive, they are time-consuming, and the instrumentation needed is very expensive. Because of this, there is an increasing interest in developing new analytical tools which are faster, simpler and with a lower-cost, also keeping good analytical characteristics [71,116].
Hence, electrochemical biosensors satisfy all these requirements, and, in particular, aptamer-based sensors (also known as aptasensors) are listed as one of the most powerful type of biosensors [114]. In contrast to DNA biosensors, which cannot detect the allergen itself, aptasensors can directly indicate the presence of the analyte [18,268,269].

9.2.2 Target Analyte

β-LG is the major whey protein of ruminants in general (*e.g.* cow and sheep, 2–3 g/L) and is present also in other mammalian species but not in humans: for this reason, it may play the role of an important marker in detecting milk adulterations, especially when goat or sheep milk is replaced by cow's milk [270]. This protein belongs to the family of lipocalins, most of which bind small hydrophobic ligands and thus may

act as specific transporters [271]. The epitope of β-LG comprises six different short fragments of the polypeptide chain, which are especially located in the β strands and cover a flat area on the allergen surface [272]. Its quaternary structure, identified in 1997 using X-Ray diffraction [273], is dependent on the pH: for example, at pH values between 5.2 and 7.0 it is a dimer, and its molecular weight is around 37 kDa; at pH values over 8.0 it exists as a monomer and its molecular weight is approximately of 18 kDa [274]. This protein has a great potential as milk allergen because it is remarkably stable and it is not present in human milk [113]; moreover, it is also regularly added as an additive in lots of food products [275].

9.2.3 Assay Type

Among all electrochemical aptasensors, those based on structure-switching aptamers represent an encouraging methodology due to the fast, sensitive and cheap determination of different target analytes [276]. This approach benefits from the variations in the conformation of the recognition aptamer, immobilized on the electrode surface [277,278].
This aptamer is usually altered at the 5'-end by a molecule containing a group able to link to the surface of the electrode (for example, a thiol) and labeled at the opposite side (3'-end) with a redox probe, for instance MB [279], that has been widely used as label for DNA-based biosensors [280]. This type of aptasensors, also known as "folding-based aptasensors", requires an alteration on the aptamer's conformation when the analyte is present [281], allowing to detect the changes on the efficiency of the electron transfer, which relies on the spacing that exists between the surface of the electrode and the redox probe.

9.2.4 Strategy

In this work, we present a folding-based aptasensor able to quantify β-LG using GSPEs. On their surface, a film made of a conducting polymer, PLL, combined with electrogenerated AuNPs is used in order to improve the electrodic area. A thiolated aptamer that specifically recognizes β-LG is modified with MB on the 3'-end, a redox probe, and is linked to the AuNPs *via* a thiol modification on the 5'-end. The strategy presented here takes advantage of: i) the higher electroactive area of GSPEs when modified with PLL and AuNPs, ii) the strong binding between AuNPs and the thiolated aptamer, iii) the conformational changes the aptamer suffers when β-LG is present, and iv) the differences in the electron transfer, which is dependent on the space existent in between MB and the modified electrode. This approach represents a sensitive, simple and accurate methodology for the fast quantification of β-LG in real alimentary samples, using miniaturized and low-cost instrumentation.

9.3 Materials and Methods

9.3.1 Chemicals

L-lysine hydrochloride ($C_6H_{14}N_2O_2{\cdot}HCl$), tetrachloroauric acid ($HAuCl_4$), sulfuric acid (H_2SO_4), 6-mercapto-1-hexanol ($C_6H_{14}OS$), β-lactoglobulin B, casein, tris(hydroxymethyl) aminomethane ($C_4H_{11}NO_3$), di-sodium hydrogen phosphate (Na_2HPO_4), sodium di-hydrogen phosphate di-hydrate ($NaH_2PO_4{\cdot}2H_2O$), sodium chloride (NaCl), potassium chloride (KCl), magnesium chloride hexahydrate ($MgCl_2{\cdot}6H_2O$), Tween-20, potassium ferrocyanide ($K_4[Fe(CN)_6]$), potassium ferricyanide ($K_3[Fe(CN)_6]$) were purchased from Merck KGaA (Darmstadt, Germany). All reagents were of analytical grade and used as received, without further purifications. Biscuits and soya yoghourt were purchased in a local market. Milli-Q water was used for all preparations.

The MB-modified thiolated aptamer (Apt-MB) was purchased from Biomers.net GmbH (Ulm, Germany) and is reported as the following: 5'-(SH)-$(CH_2)_6$-CGA CGA TCG GAC CGC AGT ACC CAC CCA CCA GCC CCA ACA TCA TGC CCA TCC GTG TGT G-MB-3'.

The buffer solutions used in this work are the following:

1. immobilization buffer: 50 mM TRIS buffer, 150 mM NaCl, 2 mM $MgCl_2$, pH 7.4;
2. detection buffer: 0.1 M phosphate buffer, 150 mM NaCl, pH 7.4;
3. extraction buffer: 20 mM TRIS buffer, 2% Tween-20, pH 8.0.

9.3.2 Aptasensor Development

The described aptasensor works according to a folding-based mechanism (**Figure 9.1**), using a thiolated aptamer tagged with the redox probe MB. The aptamer immobilization takes advantage of the covalent linking between thiolated groups and AuNPs. In absence of *β*-LG target, the distance between the redox probe and the electrode surface is high, resulting in a reduced electron transfer and thus in a low signal.
However, when adding the analyte, the conformation of the aptamer changes, thus bringing the redox probe closer to the electrode surface, facilitating the electron transfer and increasing the signal.

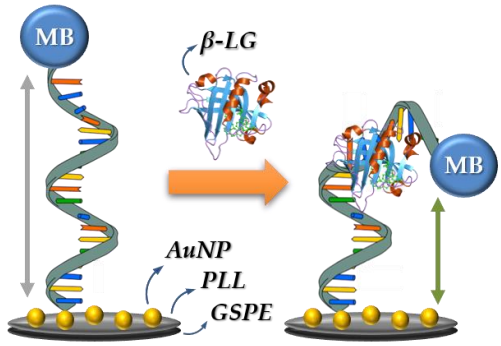

Figure 9.1. *Schematic representation of the sensing strategy of the proposed aptasensor.*

9.3.2.1 Aptamer Immobilization

The aptamer immobilization was carried out by depositing 1 μM of the thiolated aptamer in immobilization buffer and letting it to react overnight. The aptamer was immobilized by chemisorption between AuNPs and the thiol groups; then, a SAM was formed by incubating 1 mM MCH aqueous solution for 60 min, as previously described by our group [282]. Finally, the aptasensors were washed with detection buffer.

9.3.2.2 β-Lactoglobulin Detection

With the aim of obtaining a calibration curve for β-LG, various protein concentrations have been tested. Several β-LG solutions of increasing concentration (between 0.1 ng/mL and 10 ng/mL) in detection buffer were dropped onto the aptasensor surface and incubated for 45 min. DPV measurements were then carried out in detection buffer by scanning the potential from −0.6 V to +0.15 V at 10 mV/s (5 mV step potential, 100 mV pulse potential, 0.02 s pulse time, 0.5 s interval time). The height of the resulting peak at around −0.03 V, corresponding to the oxidation of MB attached to the aptamer, was taken as the analytical signal.

9.3.2.3 Real Samples Analysis

Spike-and-recovery experiments were done in order to see if a real sample matrix affects the quantification of β-LG, comparing it to the electrolyte solution used in the standard calibration curve (PBS).
Real samples were treated by following a procedure described elsewhere [283]. Briefly, 1 g of biscuit or soya yoghourt was dissolved in 20 mL of extraction buffer and stirred at room temperature for 5 h. The mixtures were centrifuged at 10000 rpm for 15 min; then, the supernatant was collected and enriched with 1 ng/mL and 5 ng/mL of β-LG and the resulting samples were analyzed by using the developed aptasensor. Finally, the recovery of the concentration in real samples was calculated.

9.4 Results and Discussion

9.4.1 Aptasensor Assay

For the purpose of obtaining the best analytical characteristics of this aptasensor, different parameters were optimized, as detailed in the following paragraphs.

9.4.1.1 Electrolyte Solution

Different buffer solutions were tested as electrolytes for MB signal acquisition with the objective of obtaining the highest signal-to-noise ratio: 50 mM TRIS buffer, 150 mM NaCl, pH 7.5 (with and without 2 mM $MgCl_2$) and 0.1 M phosphate buffer, 150 mM NaCl, pH 7.4 (with and without 2 mM $MgCl_2$). Solutions containing 0 ng/mL β-LG (background electrolyte) and 5 ng/mL β-LG were incubated for 45 min and the results of this optimization are depicted in **Figure 9.2**.

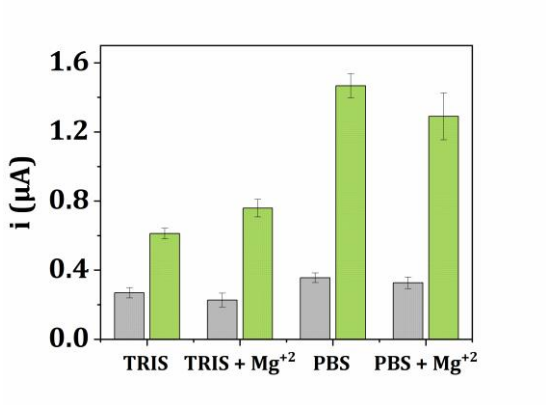

Figure 9.2. *Electrolyte solution optimization. Current values obtained in different buffer solutions containing • 0 ng/mL or • 5 ng/mL β-lactoglobulin in different media. [Apt-MB] = 1 μM, incubation time: 45 min. Each measurement was repeated at least three times using different sensors.*

The highest signal-to-background ratio was obtained when PBS-based buffers were used. In particular, the signal-to-noise ratio is bigger

without $MgCl_2$, so this buffer solution was selected for the following measurements. This suggests that magnesium ions can influence the conformation of the aptamer and, therefore, its interaction with the protein, taking into account the decrease in the mobility of the aptamer and the water molecules when Mg^{+2} is present [284].

9.4.1.2 Aptamer Concentration

A crucial stage in the development of the aptasensor is the concentration of the immobilized aptamer. Different concentrations of Apt-MB (0.5, 1 and 2 μM) were immobilized onto the AuNPs/PLL/GSPEs, and the aptasensor response in presence of 5 ng/mL β-LG was compared after 45 min with that of the blank solution (**Figure 9.3**).

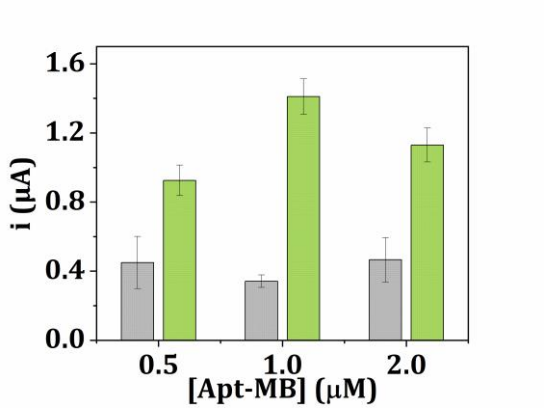

Figure 9.3. *Aptamer concentration optimization. Current values obtained in detection buffer containing • 0 ng/mL or • 5 ng/mL β-lactoglobulin. Incubation time: 45 min. Each measurement was repeated at least three times using different sensors.*

The best concentration was chosen to be 1 μM, because of the higher signal-to-background ratio obtained. The precision was also better in this case.

9.4.1.3 Incubation Time

Incubation time is a very important parameter that can affect the measurements, inasmuch as it can affect an appropriate conformational change in the aptamer structure when it binds the analyte. Solutions containing 5 ng/mL β-LG were incubated for different times (30, 45 and 60 min) and the response was compared with that of the blank. The results of this optimization are depicted in **Figure 9.4**. As it can be seen, a bigger signal-to-noise ratio is obtained for 45 min, being that time chosen as the optimum incubation time.

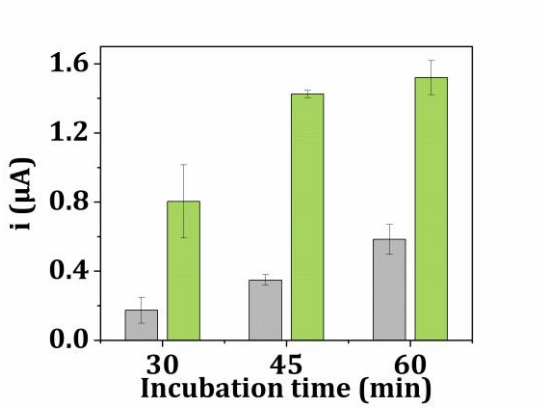

Figure 9.4. *β-lactoglobulin incubation time optimization. Current values obtained in detection buffer containing • 0 ng/mL or • 5 ng/mL β-lactoglobulin. [Apt-MB] = 1 μM. Each measurement was repeated at least three times using different sensors.*

9.4.2 β-Lactoglobulin Detection in Standard Solutions

Under the optimized experimental conditions, a dose-response curve for β-LG in buffered solutions was obtained in the range 0.1–10 ng/mL β-LG by DPV (**Figure 9.5**, a panel). The current peak intensity resulted to be directly proportional to β-LG concentration, so the experimental data were fitted with a linear relationship ($i_{ox} = 0.224\,[\beta\text{-LG}] + 0.411$), retrieving a good regression and a R^2 value of 0.997 (**Figure 9.5**, b panel).

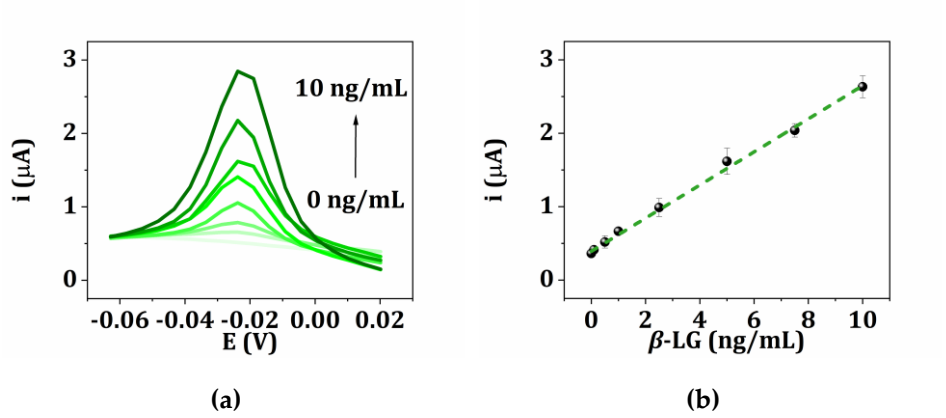

Figure 9.5. *β-lactoglobulin detection by Apt-MB at AuNPs/PLL/GSPEs.* ***(a)*** *Differential pulse voltammograms obtained with different β-LG concentrations;* ***(b)*** *calibration curve for β-LG. Each measurement was repeated at least three times using different sensors.*

The LOD, calculated as three times the standard deviation of the intercept divided by the slope, was found to be 0.09 ng/mL. This value is below the threshold established for proteins in cow's milk [285,286], resulting to be very suitable for the determination of trace concentrations in food in order to avoid undesired reactions in allergic patients.
In addition, the levels of β-LG assayed in this work are close (and even beneath) to those achieved using alternative approaches based on liquid chromatography combined with mass spectrometry [260], ELISA [283], capillary-electrophoresis and laser-induced fluorescence [287] or magneto-immunoassays [111]. Moreover, the reproducibility of the method was very good, with a %RSD below 13% (obtained with 3 repetitive measurements for all the tested concentrations).

The effect of interferents was assessed in presence of casein, one of the main components present in milk samples. Solutions containing 1 ng/mL of casein, 1 ng/mL of β-LG and a mixture of both were analyzed and the results are shown in **Figure 9.6**.

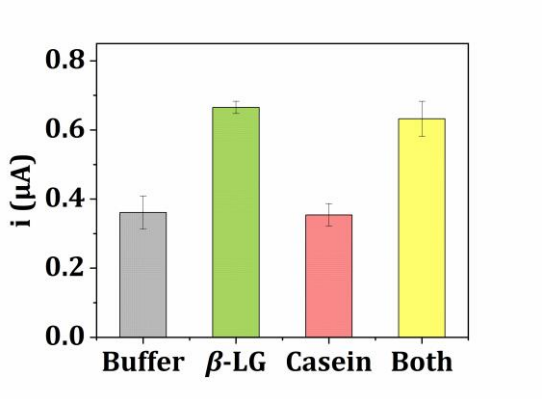

Figure 9.6. *Interference study. Current values in buffer solutions containing • 0 ng/mL proteins, • 1 ng/mL β-lactoglobulin, • 1 ng/mL casein, • 1 ng/mL of both. Each measurement was repeated at least three times using different sensors.*

It can be seen, casein, on its own, did not produce any interference, giving a signal very similar to the one obtained with buffer. In the case of the mixture, the presence of casein hardly affects the β-LG signal, demonstrating the high specificity of the employed aptamer.

9.4.3 β-Lactoglobulin Detection in Real Samples

The performance of the aptasensor towards the analysis of real food samples, and thus its applicability, was verified by testing its response in commercially available biscuits and soya yoghourt under the same conditions applied for β-LG calibration curve.

A spike-and-recovery experiment was performed on both matrices and the results are summarized in **Table 9.1**. The recovery rates of the concentration reveal that the matrix does not affect the methodology in great extent. This opens up the way to β-LG quantification in food samples with high accuracy for the detection of allergens.

Table 9.1. *Recovery values obtained from the analysis of β-lactoglobulin-spiked biscuits and soya yoghourt extracts. Each measurement was repeated at least three times using different sensors.*

	β-LG spiked (ng/mL)	**β-LG found (ng/mL)**	**Recovery (%)**	**%RSD**
Biscuit	1.0	1.17	117	8
	5.0	5.18	103	6
Soya yoghourt	1.0	1.16	116	9
	5.0	4.78	95	7

9.5 Conclusions

In this work, a simple and sensitive aptasensor for the detection of β-LG, one of the most important proteins found in milk, was designed. The aptasensor here developed is built on disposable GSPEs modified with a conducting polymer (PLL) and AuNPs. The modification of the biosensor surface was carried out by electropolymerization of L-lysine, in a first step, and electrogeneration of AuNPs using tetrachloroauric acid.

The thiolated aptamer used in this aptasensor is modified with the redox probe MB at the 3'-end. The strategy presented in this work benefits from the conformational changes of the aptamer when β-LG is present, and, as a result, from the changes on the electron transfer, hanging on the distance between MB and the electrodic surface. A good linear relationship between the peak current values and β-LG concentration in the range between 0.10 ng/mL and 10 ng/mL, with a LOD of 0.09 ng/mL, was obtained. The aptasensor was also applied in the determination of spiked β-LG in real food samples.

10. Concluding Remarks

In this work, nanostructured electrochemical biosensors for the detection of contaminants related to food and environmental analysis were presented. In order to overcome the limitations related to the use of antibodies, the employment of biomimetic receptors (such as aptamers) was investigated. In the last years, many different systems were developed, describing advances in aptamer sequences realization, as well as combination of probe sequences, with nanomaterials in order to improve the detection procedures. Nanostructures provide a useful and suitable platform for biomolecules immobilization (which retain their biological activity) and facilitate the electron transfer from the electrodic surface.

Starting from this point, conductive polymers and gold nanoparticles were used as signal amplification platforms in three different approaches. Nanostructured surfaces were obtained by means of cyclic voltammetry and used to enhance the electrochemical performances of graphite screen-printed working electrodes, as well as their active surface in order to immobilize probe molecules. Each modification step was characterized by cyclic voltammetry and electrochemical impedance spectroscopy measurements.

The developed platforms were applied for the electrochemical detection of profenofos pesticide, aflatoxin B_1 and deoxynivalenol mycotoxins in a competitive assay, and β-lactoglobulin allergen in a switch-on assay. Streptavidin-alkaline phosphatase was used as enzymatic label in the competitive approaches and the electrochemical behavior of 1-naphthol enzymatic product was analyzed by differential pulse voltammetry; conversely, the electroactive molecule methylene blue was used as redox moiety in the switch-on approach and its oxidation was monitored by differential pulse voltammetry. In each case, the

experimental parameters were optimized and the analytical performances of the aptasensor in terms of sensitivity, reproducibility and selectivity were studied. Calibration curves were constructed under optimized experimental conditions and the applicability of the sensors was assessed by the analysis of spiked real samples.

In summary, this thesis presents the employment of three different nanostructured platforms for the development of three different aptamer assays to detect compounds of interest for food and environmental analysis. The proposed works show that aptamer-based devices still represent one of the most promising strategies for biosensor development and their application in environmental analysis, and small molecules analysis in general, is still one of the most fascinating field in analytical chemistry.

Moreover, because the analysis of a single contaminant lacks in completeness, it will be interesting to build multianalyte arrays (*e.g.* exploiting different electrode modifications, in which each single working electrode bears the proper receptor), as the ability to optimally combine information on a panel of compounds becomes necessary for an useful on-field screening analysis.

References

1. D. R. THÉVENOT, K. TOTH, R. A. DURST, G. S. WILSON. "Electrochemical Biosensors: Recommended Definitions and Classification." *Biosens. Bioelectron.* **2001**, *16*, 121–131.
2. N. J. RONKAINEN, H. B. HALSALL, W. R. HEINEMAN. "Electrochemical Biosensors." *Chem. Soc. Rev.* **2010**, *39*, 1747–1763.
3. H. H. NGUYEN, S. H. LEE, U. J. LEE, C. D. FERMIN, M. KIM. "Immobilized Enzymes in Biosensor Applications." *Materials* **2019**, *12*, 121–154.
4. U. YOGESWARAN, S.-M. CHEN. "A Review on the Electrochemical Sensors and Biosensors Composed of Nanowires as Sensing Material." *Sensors* **2008**, *8*, 290–313.
5. S. M. BORISOV, O. S. WOLFBEIS. "Optical Biosensors." *Chem. Rev.* **2008**, *108*, 423–461.
6. F. LUCARELLI, S. TOMBELLI, M. MINUNNI, G. MARRAZZA, M. MASCINI. "Electrochemical and Piezoelectric DNA Biosensors for Hybridisation Detection." *Anal. Chim. Acta* **2008**, *609*, 139–159.
7. K. RAMANATHAN, B. DANIELSSON. "Principles and Applications of Thermal Biosensors." *Biosens. Bioelectron.* **2001**, *16*, 417–423.
8. J. LLANDRO, J. J. PALFREYMAN, A. IONESCU, C. H. W. BARNES. "Magnetic Biosensor Technologies for Medical Applications: A Review." *Med. Biol. Eng. Comput.* **2010**, *48*, 977–998.
9. J. WANG. "*Analytical Electrochemistry*," Wiley-VCH, **2006**.
10. B. R. EGGINS. "*Chemical Sensors and Biosensors*," John Wiley & Sons, **2002**.
11. J. MORAL-VICO, J. BARALLAT, L. ABAD, R. OLIVÉ-MONLLAU, F. X. MUÑOZ-PASCUAL, A. GALÁN ORTEGA, F. J. DEL CAMPO, E. BALDRICH. "Dual Chronoamperometric Detection of Enzymatic Biomarkers Using Magnetic Beads and a Low-Cost Flow Cell." *Biosens. Bioelectron.* **2015**, *69*, 328–336.

12. N. KARIMIAN, M. VAGIN, M. H. A. ZAVAR, M. CHAMSAZ, A. P. F. TURNER, A. TIWARI. "An Ultrasensitive Molecularly-Imprinted Human Cardiac Troponin Sensor." *Biosens. Bioelectron.* **2013**, *50*, 492–498.

13. A. C. GRAY, S. S. SIDHU, C. CHANDRASEKERA, C. F. M. HENDRIKSEN, C. A. K. BORREBAECK. "Animal-Friendly Affinity Reagents: Replacing the Needless in the Haystack." *Trends Biotechnol.* **2016**, *34*, 960–969.

14. A. SASSOLAS, B. PRIETO-SIMÓN, J.-L. MARTY. "Biosensors for Pesticide Detection: New Trends." *Am. J. Anal. Chem.* **2012**, *3*, 210–232.

15. F. JAHANGIRI DEHAGHANI, H. R. ZARE, Z. SHEKARI. "Measurement of Aflatoxin M1 in Powder and Pasteurized Milk Samples by Using a Label – Free Electrochemical Aptasensor Based on Platinum Nanoparticles Loaded on Fe – Based Metal – Organic Frameworks." *Food Chem.* **2019**, *310*, 125820.

16. P. BAYAT, R. NOSRATI, M. ALIBOLANDI, H. RAFATPANAH, K. ABNOUS, M. KHEDRI, M. RAMEZANI. "SELEX Methods on the Road to Protein Targeting with Nucleic Acid Aptamers." *Biochimie* **2018**, *154*, 132–155.

17. A. S. DAVYDOVA, M. A. VOROBJEVA, A. G. VENYAMINOVA. "Escort Aptamers: New Tools for the Targeted Delivery of Therapeutics into Cells." *Acta Naturae* **2011**, *3*, 12–29.

18. S. SONG, L. WANG, J. LI, C. FAN, J. ZHAO. "Aptamer-Based Biosensors." *TrAC - Trends Anal. Chem.* **2008**, *27*, 108–117.

19. J. H. LEE, M. V. YIGIT, D. MAZUMDAR, Y. LU. "Molecular Diagnostic and Drug Delivery Agents Based on Aptamer-Nanomaterial Conjugates." *Adv. Drug Deliv. Rev.* **2010**, *62*, 592–605.

20. J. TOULMÉ, J. DAGUER, E. DAUSSE. "Aptamers: Ligands For All Reasons" in *Aptamers in Bioanalysis*. Ed. M. Mascini. John Wiley & Sons, **2008**, 1–30.

21. L. RIVAS, C. C. MAYORGA-MARTINEZ, D. QUESADA-GONZÁLEZ, A.

ZAMORA-GÁLVEZ, A. DE LA ESCOSURA-MUÑIZ, A. MERKOÇI. "Label-Free Impedimetric Aptasensor for Ochratoxin-A Detection Using Iridium Oxide Nanoparticles." *Anal. Chem.* **2015**, *87*, 5167–5172.

22. G. SELVOLINI, M. LETTIERI, L. TASSONI, S. GASTALDELLO, M. GRILLO, C. MARAN, G. MARRAZZA. "Electrochemical Enzyme-Linked Oligonucleotide Array for Aflatoxin B1 Detection." *Talanta* **2019**, *203*, 49–57.

23. S. PANG, T. P. LABUZA, L. HE. "Development of a Single Aptamer-Based Surface Enhanced Raman Scattering Method for Rapid Detection of Multiple Pesticides." *Analyst* **2014**, *139*, 1895–1901.

24. D. L. ROBERTSON, G. F. JOYCE. "Selection in Vitro of an RNA Enzyme That Specifically Cleaves Single-Stranded DNA." *Nature* **1990**, *344*, 467–468.

25. H. K. BINZ, P. AMSTUTZ, A. PLÜCKTHUN. "Engineering Novel Binding Proteins from Nonimmunoglobulin Domains." *Nat. Biotechnol.* **2005**, *23*, 1257–1268.

26. M. GEBAUER, A. SKERRA. "Engineered Protein Scaffolds as Next-Generation Antibody Therapeutics." *Curr. Opin. Chem. Biol.* **2009**, *13*, 245–255.

27. A. SKERRA. "Alternative Non-Antibody Scaffolds for Molecular Recognition." *Curr. Opin. Biotechnol.* **2007**, *18*, 295–304.

28. S. B. LEE, M. HASSAN, R. FISHER, O. CHERTOV, V. CHERNOMORDIK, G. KRAMER-MAREK, A. GANDJBAKHCHE, J. CAPALA. "Affibody Molecules for In Vivo Characterization of HER2-Positive Tumors by Near-Infrared Imaging." *Clin. Cancer Res.* **2008**, *14*, 3840–3849.

29. A. ORLOVA, M. MAGNUSSON, T. L. J. ERIKSSON, M. NILSSON, B. LARSSON, I. HÖIDÉN-GUTHENBERG, C. WIDSTRÖM, J. CARLSSON, V. TOLMACHEV, S. STÅHL, F. Y. NILSSON. "Tumor Imaging Using a Picomolar Affinity HER2 Binding Affibody Molecule." *Cancer Res.* **2006**, *66*, 4339–4348.

30. V. TOLMACHEV, A. ORLOVA, F. Y. NILSSON, J. FELDWISCH, A. WENNBORG, L. ABRAHMSÉN. "Affibody Molecules: Potential for in

Vivo Imaging of Molecular Targets for Cancer Therapy." *Expert Opin. Biol. Ther.* **2007**, *7*, 555–568.

31. V. TOLMACHEV, A. ORLOVA, R. PEHRSON, J. GALLI, B. BAASTRUP, K. ANDERSSON, M. SANDSTRÖM, D. ROSIK, J. CARLSSON, H. LUNDQVIST, A. WENNBORG, F. Y. NILSSON. "Radionuclide Therapy of HER2-Positive Microxenografts Using a 177Lu-Labeled HER2-Specific Affibody Molecule." *Cancer Res.* **2007**, *67*, 2773–2782.

32. P.-A. NYGREN. "Alternative Binding Proteins: Affibody Binding Proteins Developed from a Small Three-Helix Bundle Scaffold." *FEBS J.* **2008**, *275*, 2668–2676.

33. M. HARRIS, S. TOMBELLI, G. MARRAZZA, A. P. F. TURNER. "Affibodies as an Alternative to Antibodies in Biosensors for Cancer Markers" in *Biosensors for Medical Applications*. Ed. S. Higson. Woodhead Publishing Limited, **2012**, 217–232.

34. G. WULFF. "Molecular Imprinting in Cross-Linked Materials with the Aid of Molecular Templates - A Way towards Artificial Antibodies." *Angew. Chemie Int. Ed. English* **1995**, *34*, 1812–1832.

35. A. G. MAYES, K. MOSBACH. "Molecularly Imprinted Polymers: Useful Materials for Analytical Chemistry?" *Trends Anal. Chem.* **1997**, *16*, 321–332.

36. K. HAUPT. "Biomaterials: Plastic Antibodies." *Nat. Mater.* **2010**, *9*, 612–614.

37. S. PILETSKY, A. TURNER. "A New Generation of Chemical Sensors Based on MIPs" in *Molecular Imprinting of Polymers*. Eds. S. A. Piletsky, A. P. F. Turner. Landes Bioscience, **2006**, 64–79.

38. S. A. PILETSKY, E. V. PILETSKAYA, T. L. PANASYUK, A. V. EL'SKAYA, R. LEVI, I. KARUBE, G. WULFF. "Imprinted Membranes for Sensor Technology: Opposite Behavior of Covalently and Noncovalently Imprinted Membranes." *Macromolecules* **1998**, *31*, 2137–2140.

39. E. MAZZOTTA, A. TURCO, I. CHIANELLA, A. GUERREIRO, S. A. PILETSKY, C. MALITESTA. "Solid-Phase Synthesis of Electroactive Nanoparticles of Molecularly Imprinted Polymers. A Novel

Platform for Indirect Electrochemical Sensing Applications." *Sensors Actuators B Chem.* **2016**, *229*, 174–180.

40. P. KARFA, E. ROY, S. PATRA, D. KUMAR, R. MADHURI, P. K. SHARMA. "A Fluorescent Molecularly-Imprinted Polymer Gate with Temperature and PH as Inputs for Detection of Alpha-Fetoprotein." *Biosens. Bioelectron.* **2016**, *78*, 454–463.

41. N. KARIMIAN, A. P. F. TURNER, A. TIWARI. "Electrochemical Evaluation of Troponin T Imprinted Polymer Receptor." *Biosens. Bioelectron.* **2014**, *59*, 160–165.

42. M. PEETERS. "Molecularly Imprinted Polymers (Mips) for Bioanalytical Sensors: Strategies for Incorporation of Mips into Sensing Platforms." *Austin J. Biosens. Bioelectron.* **2015**, *1*, 1–5.

43. C. MALITESTA, E. MAZZOTTA, R. A. PICCA, A. POMA, I. CHIANELLA, S. A. PILETSKY. "MIP Sensors - the Electrochemical Approach." *Anal. Bioanal. Chem.* **2012**, *402*, 1827–1846.

44. J. WACKERLIG, P. A. LIEBERZEIT. "Molecularly Imprinted Polymer Nanoparticles in Chemical Sensing - Synthesis, Characterisation and Application." *Sensors Actuators B Chem.* **2015**, *207*, 144–157.

45. A. RAVALLI, G. MARRAZZA. "Electrochemical-Based Biosensor Technologies in Disease Detection and Diagnostics" in *Biosensors and Nanotechnology*. John Wiley & Sons, Inc., **2017**, 95–123.

46. A. RAVALLI, D. VOCCIA, I. PALCHETTI, G. MARRAZZA. "Electrochemical, Electrochemiluminescence, and Photoelectrochemical Aptamer-Based Nanostructured Sensors for Biomarker Analysis." *Biosensors* **2016**, *6*, 39–58.

47. I. DIACONU, C. CRISTEA, V. HÂRCEAGĂ, G. MARRAZZA, I. BERINDAN-NEAGOE, R. SĂNDULESCU. "Electrochemical Immunosensors in Breast and Ovarian Cancer." *Clin. Chim. Acta* **2013**, *425*, 128–138.

48. N. PANIEL, J. BAUDART, A. HAYAT, L. BARTHELMEBS. "Aptasensor and Genosensor Methods for Detection of Microbes in Real World Samples." *Methods* **2013**, *64*, 229–240.

49. J.-G. WALTER, A. HEILKENBRINKER, J. AUSTERJOST, S. TIMUR, F.

STAHL, T. SCHEPE. "Aptasensors for Small Molecule Detection." *Zeitschrift für Naturforsch. B* **2012**, *67*, 976–986.

50. K. HAN, Z. LIANG, N. ZHOU. "Design Strategies for Aptamer-Based Biosensors." *Sensors* **2010**, *10*, 4541–4557.

51. A. J. BARD, L. R. FAULKNER. "*Electrochemical Methods: Fundamentals and Applications,*" John Wiley & Sons, **2001**.

52. F. LISDAT, D. SCHÄFER. "The Use of Electrochemical Impedance Spectroscopy for Biosensing." *Anal. Bioanal. Chem.* **2008**, *391*, 1555–1567.

53. J. S. DANIELS, N. POURMAND. "Label-Free Impedance Biosensors: Opportunities and Challenges." *Electroanalysis* **2007**, *19*, 1239–1257.

54. A. RAVALLI, C. GOMES DA ROCHA, H. YAMANAKA, G. MARRAZZA. "A Label-Free Electrochemical Affisensor for Cancer Marker Detection: The Case of HER2." *Bioelectrochemistry* **2015**, *106*, 268–275.

55. S. SANG, Y. WANG, Q. FENG, Y. WEI, J. JI, W. ZHANG. "Progress of New Label-Free Techniques for Biosensors: A Review." *Crit. Rev. Biotechnol.* **2016**, *36*, 465–481.

56. M. A. ALONSO-LOMILLO, O. DOMÍNGUEZ-RENEDO, M. J. ARCOS-MARTÍNEZ. Screen-printed biosensors in microbiology; A review. *Talanta* **2010**, *82*, 1629–1636

57. M. TUDORACHE, C. BALA. "Biosensors Based on Screen-Printing Technology, and Their Applications in Environmental and Food Analysis." *Anal. Bioanal. Chem.* **2007**, *388*, 565–578.

58. Z. TALEAT, A. KHOSHROO, M. MAZLOUM-ARDAKANI. "Screen-Printed Electrodes for Biosensing: A Review (2008–2013)." *Microchim. Acta* **2014**, *181*, 865–891.

59. F. LUCARELLI, L. AUTHIER, G. BAGNI, G. MARRAZZA, T. BAUSSANT, E. AAS, M. MASCINI. "DNA Biosensor Investigations in Fish Bile for Use as a Biomonitoring Tool." *Anal. Lett.* **2003**, *36*, 1887–1901.

60. S. KRÖGER, A. P. F. TURNER. "Solvent-Resistant Carbon Electrodes

Screen Printed onto Plastic for Use in Biosensors." *Anal. Chim. Acta* **1997**, *347*, 9–18.

61. P. FANJUL-BOLADO, D. HERNÁNDEZ-SANTOS, P. J. LAMAS-ARDISANA, A. MARTÍN-PERNÍA, A. COSTA-GARCÍA. "Electrochemical Characterization of Screen-Printed and Conventional Carbon Paste Electrodes." *Electrochim. Acta* **2008**, *53*, 3635–3642.

62. K. C. HONEYCHURCH, J. P. HART. "Screen-Printed Electrochemical Sensors for Monitoring Metal Pollutants." *TrAC - Trends Anal. Chem.* **2003**, *22*, 456–469.

63. F. ARDUINI, F. DI NARDO, A. AMINE, L. MICHELI, G. PALLESCHI, D. MOSCONE. "Carbon Black-Modified Screen-Printed Electrodes as Electroanalytical Tools." *Electroanalysis* **2012**, *24*, 743–751.

64. E. AKANELE, S. MGBO, O. CHUKWU, C. M. AHUDIE. "Microbiological Contamination Of Food: The Mechanisms, Impacts And Prevention." *Int. J. Sci. Technol. Res.* **2016**, *5*, 65–78.

65. WHO (WORLD HEALTH ORGANIZATION). Food Safety. Available online: https://www.who.int/news-room/fact-sheets/detail/food-safety

66. K. KAMALA, V. P. KUMAR. "Food Products and Food Contamination" in *Microbial Contamination and Food Degradation*. Elsevier Inc., **2018**, 1–19.

67. G. K. MISHRA, A. BARFIDOKHT, F. TEHRANI, R. K. MISHRA. "Food Safety Analysis Using Electrochemical Biosensors." *Foods* **2018**, *7*, 141–152.

68. A. WILCOCK, M. PUN, J. KHANONA, M. AUNG. "Consumer Attitudes, Knowledge and Behaviour: A Review of Food Safety Issues." *Trends Food Sci. Technol.* **2004**, *15*, 56–66.

69. J. ACEÑA, S. STAMPACHIACCHIERE, S. PÉREZ, D. BARCELÓ. "Advances in Liquid Chromatography–High-Resolution Mass Spectrometry for Quantitative and Qualitative Environmental Analysis." *Anal. Bioanal. Chem.* **2015**, *407*, 6289–6299.

70. H. C. LIANG, M. BILON, M. T. HAY. "Analytical Methods for Pesticide Residues in the Water Environment." *Water Environ. Res.* **2015**, *87*, 1923–1937.

71. L. ROTARIU, F. LAGARDE, N. JAFFREZIC-RENAULT, C. BALA. "Electrochemical Biosensors for Fast Detection of Food Contaminants - Trends and Perspective." *TrAC - Trends Anal. Chem.* **2016**, *79*, 80–87.

72. G. SELVOLINI, I. BĂJAN, O. HOSU, C. CRISTEA, R. SĂNDULESCU, G. MARRAZZA. "DNA-Based Sensor for the Detection of an Organophosphorus Pesticide: Profenofos." *Sensors* **2018**, *18*, 2035–2046.

73. FAO (FOOD AND AGRICULTURE ORGANIZATION), WHO (WORLD HEALTH ORGANIZATION). "Manual On Development And Use Of FAO And WHO Specifications For Pesticides" in *FAO Plant Production and Protection Paper*. **2016**,

74. GEORGE W. WARE. "Ecological History of DDT in Arizona." *J. Arizona Acad. Sci.* **1974**, *9*, 61–65.

75. I. A. RATHER, W. Y. KOH, W. K. PAEK, J. LIM. "The Sources of Chemical Contaminants in Food and Their Health Implications." *Front. Pharmacol.* **2017**, *8*, 1–8.

76. R. RAPINI, G. MARRAZZA. "Electrochemical Aptasensors for Contaminants Detection in Food and Environment: Recent Advances." *Bioelectrochemistry* **2017**, *118*, 47–61.

77. R. ZAMORA-SEQUEIRA, R. STARBIRD-PÉREZ, O. ROJAS-CARILLO, S. VARGAS-VILLALOBOS. "What Are the Main Sensor Methods for Quantifying Pesticides in Agricultural Activities? A Review." *Molecules* **2019**, *24*, 1–26.

78. M. LIU, A. KHAN, Z. WANG, Y. LIU, G. YANG, Y. DENG, N. HE. "Aptasensors for Pesticide Detection." *Biosens. Bioelectron.* **2019**, *130*, 174–184.

79. R. RAPINI, G. MARRAZZA. "Biosensor Potential in Pesticide Monitoring" in *Biosensors for Sustainable Food - New Opportunities*

and Technical Challenges. Eds. V. Scognamiglio, G. Rea, F. Arduini, G. Palleschi. Elsevier B.V., **2016**, 3–31.

80. H. F. VAN EMDEN, D. B. PEAKALL. "*Beyond Silent Spring: Integrated Pest Management and Chemical Safety*," Springer, **1996**.

81. N. VERMA, A. BHARDWAJ. "Biosensor Technology for Pesticides—A Review." *Appl. Biochem. Biotechnol.* **2015**, *175*, 3093–3119.

82. S. LIU, Z. ZHENG, X. LI. "Advances in Pesticide Biosensors: Current Status, Challenges, and Future Perspectives." *Anal. Bioanal. Chem.* **2013**, *405*, 63–90.

83. Toxin. Available online: https://web.archive.org/web/20090628224336/http://www.mercksource.com/pp/us/cns/cns_hl_dorlands_split.jsp?pg=/ppdocs/us/common/dorlands/dorland/eight/000109718.htm

84. J. L. RICHARD. "Some Major Mycotoxins and Their Mycotoxicoses-An Overview." *Int. J. Food Microbiol.* **2007**, *119*, 3–10.

85. E. M. FOX, B. J. HOWLETT. "Secondary Metabolism: Regulation and Role in Fungal Biology." *Curr. Opin. Microbiol.* **2008**, *11*, 481–487.

86. N. W. TURNER, S. SUBRAHMANYAM, S. A. PILETSKY. "Analytical Methods for Determination of Mycotoxins: A Review." *Anal. Chim. Acta* **2009**, *632*, 168–180.

87. C. WANG, J. QIAN, K. AN, X. HUANG, L. ZHAO, Q. LIU, N. HAO, K. WANG. "Magneto-Controlled Aptasensor for Simultaneous Electrochemical Detection of Dual Mycotoxins in Maize Using Metal Sulfide Quantum Dots Coated Silica as Labels." *Biosens. Bioelectron.* **2017**, *89*, 802–809.

88. V. L. PEREIRA, J. O. FERNANDES, S. C. CUNHA. "Mycotoxins in Cereals and Related Foodstuffs: A Review on Occurrence and Recent Methods of Analysis." *Trends Food Sci. Technol.* **2014**, *36*, 96–136.

89. C. JUAN, L. COVARELLI, G. BECCARI, V. COLASANTE, J. MAÑES. "Simultaneous Analysis of Twenty-Six Mycotoxins in Durum Wheat Grain from Italy." *Food Control* **2016**, *62*, 322–329.

90. M. PERAICA, B. RADIĆ, A. LUCIĆ, M. PAVLOVIĆ. "Toxic Effects of Mycotoxins in Humans." *Bull. World Heal. Organ.* **1999**, *77*, 754–766.

91. Y. WANG, N. LIU, B. NING, M. LIU, Z. LV, Z. SUN, Y. PENG, C. CHEN, J. LI, Z. GAO. "Simultaneous and Rapid Detection of Six Different Mycotoxins Using an Immunochip." *Biosens. Bioelectron.* **2012**, *34*, 44–50.

92. G. CASTILLO, K. SPINELLA, A. POTURNAYOVÁ, M. ŠNEJDÁRKOVÁ, L. MOSIELLO, T. HIANIK. "Detection of Aflatoxin B1 by Aptamer-Based Biosensor Using PAMAM Dendrimers as Immobilization Platform." *Food Control* **2015**, *52*, 9–18.

93. N. W. TURNER, H. BRAMHMBHATT, M. SZABO-VEZSE, A. POMA, R. COKER, S. A. PILETSKY. "Analytical Methods for Determination of Mycotoxins: An Update (2009-2014)." *Anal. Chim. Acta* **2015**, *901*, 12–33.

94. J. C. VIDAL, L. BONEL, A. EZQUERRA, S. HERNÁNDEZ, J. R. BERTOLÍN, C. CUBEL, J. R. CASTILLO. "Electrochemical Affinity Biosensors for Detection of Mycotoxins: A Review." *Biosens. Bioelectron.* **2013**, *49*, 146–158.

95. C. C. WANNOP. "The Histopathology of Turkey 'X' Disease in Great Britain." *Avian Dis.* **1961**, *5*, 371–381.

96. M. D. ASEMOLOYE, S. G. JONATHAN, R. SADDAF, Z. HABIBA, E. E. OKOAWO, T. S. BELLO. "Incidence and Chemical Implications of Aflatoxin in Street-Vended Foods" in *Aflatoxin - Control, Analysis, Detection and Health Risks*. Ed. L. Abdulra'Uf. InTech, **2017**, 153–176.

97. M. CARVAJAL-MORENO, M. VARGAS-ORTIZA, E. HERNÁNDEZ-CAMARILLO, S. RUIZ-VELASCO, F. ROJO-CALLEJAS. "Presence of Unreported Carcinogens, Aflatoxins and Their Hydroxylated Metabolites, in Industrialized Oaxaca Cheese from Mexico City." *Food Chem. Toxicol.* **2019**, *124*, 128–138.

98. X. DU, D. E. SCHRUNK, D. SHAO, P. M. IMERMAN, C. WANG, S. M. ENSLEY, W. K. RUMBEIHA. "Intra-Laboratory Development and Evaluation of a Quantitative Method for Measurement of Aflatoxins B1, M1 and Q1 in Animal Urine by High Performance

Liquid Chromatography with Fluorescence Detection." *J. Anal. Toxicol.* **2017**, *41*, 698–707.

99. J. W. BENNETT, M. KLICH. "Mycotoxins." *Clin. Microbiol. Rev.* **2003**, *16*, 497–516.

100. A. Z. JOFFE. "*Fusarium Species: Their Biology and Toxicology*," John Wiley & Sons, **1986**.

101. S. H. SICHERER. "Epidemiology of Food Allergy." *J. Allergy Clin. Immunol.* **2011**, *127*, 594–602.

102. X. X. DONG, J. Y. YANG, L. LUO, Y. F. ZHANG, C. MAO, Y. M. SUN, H. T. LEI, Y. D. SHEN, R. C. BEIER, Z. L. XU. "Portable Amperometric Immunosensor for Histamine Detection Using Prussian Blue-Chitosan-Gold Nanoparticle Nanocomposite Films." *Biosens. Bioelectron.* **2017**, *98*, 305–309.

103. M. YANG, J. ZHANG, X. CHEN. "Competitive Electrochemical Immunosensor for the Detection of Histamine Based on Horseradish Peroxidase Initiated Deposition of Insulating Film." *J. Electroanal. Chem.* **2015**, *736*, 88–92.

104. L. E. DELLE, C. HUCK, M. BÄCKER, F. MÜLLER, S. GRANDTHYLL, K. JACOBS, R. LILISCHKIS, X. T. VU, M. J. SCHÖNING, P. WAGNER, R. THOELEN, M. WEIL, S. INGEBRANDT. "Impedimetric Immunosensor for the Detection of Histamine Based on Reduced Graphene Oxide." *Phys. Status Solidi Appl. Mater. Sci.* **2015**, *212*, 1327–1334.

105. W. YE, Y. XU, L. ZHENG, Y. ZHANG, M. YANG, P. SUN. "A Nanoporous Alumina Membrane Based Electrochemical Biosensor for Histamine Determination with Biofunctionalized Magnetic Nanoparticles Concentration and Signal Amplification." *Sensors* **2016**, *16*, 1767–1779.

106. R. C. ALVES, F. B. PIMENTEL, H. P. A. NOUWS, T. H. B. SILVA, M. B. P. P. OLIVEIRA, C. DELERUE-MATOS. "Improving the Extraction of Ara h 6 (a Peanut Allergen) from a Chocolate-Based Matrix for Immunosensing Detection: Influence of Time, Temperature and Additives." *Food Chem.* **2017**, *218*, 242–248.

107. X. WENG, S. NEETHIRAJAN. "A Microfluidic Biosensor Using Graphene Oxide and Aptamer-Functionalized Quantum Dots for Peanut Allergen Detection." *Biosens. Bioelectron.* **2016**, *85*, 649–656.

108. K. SUGAWARA, T. KADOYA, H. KURAMITZ. "Magnetic Beads Modified with an Electron-Transfer Carbohydrate-Mimetic Peptide for Sensing of a Galactose-Dependent Protein." *Anal. Chim. Acta* **2018**, *1001*, 158–167.

109. K. SUGAWARA, H. KURAMITZ, H. SHINOHARA. "Fabrication of Micromagnetic Beads with Molecular Recognition/Electron-Transfer Peptides for the Sensing of Ovalbumin." *Anal. Chim. Acta* **2017**, *958*, 30–37.

110. V. RUIZ-VALDEPEÑAS MONTIEL, S. CAMPUZANO, R. M. TORRENTE-RODRÍGUEZ, A. J. REVIEJO, J. M. PINGARRÓN. "Electrochemical Magnetic Beads-Based Immunosensing Platform for the Determination of α-Lactalbumin in Milk." *Food Chem.* **2016**, *213*, 595–601.

111. V. RUIZ-VALDEPEÑAS MONTIEL, S. CAMPUZANO, F. CONZUELO, R. M. TORRENTE-RODRÍGUEZ, M. GAMELLA, A. J. REVIEJO, J. M. PINGARRÓN. "Electrochemical Magnetoimmunosensing Platform for Determination of the Milk Allergen β-Lactoglobulin." *Talanta* **2015**, *131*, 156–162.

112. S. EISSA, C. TLILI, L. L'HOCINE, M. ZOUROB. "Electrochemical Immunosensor for the Milk Allergen B-Lactoglobulin Based on Electrografting of Organic Film on Graphene Modified Screen-Printed Carbon Electrodes." *Biosens. Bioelectron.* **2012**, *38*, 308–313.

113. M. LETTIERI, O. HOSU, A. ADUMITRACHIOAIE, C. CRISTEA, G. MARRAZZA. "Beta-Lactoglobulin Electrochemical Detection Based with an Innovative Platform Based on Composite Polymer." *Electroanalysis* **2019**, *32*, 217–225.

114. S. CAMPUZANO, P. YÁÑEZ-SEDEÑO, J. PINGARRÓN. "Electrochemical Affinity Biosensors in Food Safety." *Chemosensors* **2017**, *5*, 8–46.

115. S. NEETHIRAJAN, X. WENG, A. TAH, J. O. CORDERO, K. V. RAGAVAN. "Nano-Biosensor Platforms for Detecting Food Allergens – New

Trends." *Sens. Bio-Sensing Res.* **2018**, *18*, 13–30.

116. O. HOSU, G. SELVOLINI, G. MARRAZZA. "Recent Advances of Immunosensors for Detecting Food Allergens." *Curr. Opin. Electrochem.* **2018**, *10*, 149–156.

117. P. SCHUBERT-ULLRICH, J. RUDOLF, P. ANSARI, B. GALLER, M. FÜHRER, A. MOLINELLI, S. BAUMGARTNER. "Commercialized Rapid Immunoanalytical Tests for Determination of Allergenic Food Proteins: An Overview." *Anal. Bioanal. Chem.* **2009**, *395*, 69–81.

118. E. NG, K. C. NADEAU, S. X. WANG. "Giant Magnetoresistive Sensor Array for Sensitive and Specific Multiplexed Food Allergen Detection." *Biosens. Bioelectron.* **2016**, *80*, 359–365.

119. Y. WANG, T. V. DUNCAN. "Nanoscale Sensors for Assuring the Safety of Food Products." *Curr. Opin. Biotechnol.* **2017**, *44*, 74–86.

120. B. SOCAS-RODRÍGUEZ, J. GONZÁLEZ-SÁLAMO, J. HERNÁNDEZ-BORGES, M. Á. RODRÍGUEZ-DELGADO. "Recent Applications of Nanomaterials in Food Safety." *Trends Anal. Chem.* **2017**, *96*, 172–200.

121. S. A. LIM, M. U. AHMED. "A Label Free Electrochemical Immunosensor for Sensitive Detection of Porcine Serum Albumin as a Marker for Pork Adulteration in Raw Meat." *Food Chem.* **2016**, *206*, 197–203.

122. B. I. NWARU, L. HICKSTEIN, S. S. PANESAR, G. ROBERTS, A. MURARO, A. SHEIKH. "Prevalence of Common Food Allergies in Europe: A Systematic Review and Meta-Analysis." *Allergy Eur. J. Allergy Clin. Immunol.* **2014**, *69*, 992–1007.

123. C. VILLA, J. COSTA, M. B. P. P. OLIVEIRA, I. MAFRA. "Cow's Milk Allergens: Screening Gene Markers for the Detection of Milk Ingredients in Complex Meat Products." *Food Control* **2020**, *108*, 106823.

124. E. D'AURIA, C. MAMELI, C. PIRAS, L. COCOCCIONI, A. URBANI, G. V. ZUCCOTTI, P. RONCADA. "Precision Medicine in Cow's Milk Allergy: Proteomics Perspectives from Allergens to Patients." *J.*

Proteomics **2018**, *188*, 173–180.

125. L. A. LEE, A. W. BURKS. "Food Allergies: Prevalence, Molecular Characterization, and Treatment/Prevention Strategies." *Annu. Rev. Nutr.* **2006**, *26*, 539–565.

126. C. VILLA, J. COSTA, M. B. P. P. OLIVEIRA, I. MAFRA. "Bovine Milk Allergens: A Comprehensive Review." *Compr. Rev. Food Sci. Food Saf.* **2018**, *17*, 137–164.

127. H. NEGAOUI, K. E. EL MECHERFI, S. A. TADJER, H. GRAR, O. KHEROUA, D. SAIDI. "Bovine Lactoferrin Allergenicity as Studied in Murine Model of Allergy." *Food Agric. Immunol.* **2016**, *27*, 711–723.

128. A. COSCIA, S. ORRÙ, P. DI NICOLA, F. GIULIANI, I. ROVELLI, C. PEILA, C. MARTANO, F. CHIALE, E. BERTINO. "Cow's Milk Proteins in Human Milk." *J. Biol. Regul. Homeost. Agents* **2012**, *26*, 39–42.

129. R. LI, Y. LIU, L. CHENG, C. YANG, J. ZHANG. "Photoelectrochemical Aptasensing of Kanamycin Using Visible Light-Activated Carbon Nitride and Graphene Oxide Nanocomposites." *Anal. Chem.* **2014**, *86*, 9372–9375.

130. Y. WENJUAN, A. LE GOFF, N. SPINELLI, M. LHOLZINGER, G.-W. DIAO, D. SHAN, E. DEFRANCQ, S. COSNIER. "Electrogenerated Trisbipyridyl Ru(II)-/Nitrilotriacetic-Polypyrene Copolymer for the Easy Fabrication of Label-Free Photoelectrochemical Immunosensor and Aptasensor: Application to the Determination of Thrombin and Anti-Cholera Toxin Antibody." *Biosens. Bioelectron.* **2013**, *42*, 556–562.

131. N. ELGRISHI, K. J. ROUNTREE, B. D. MCCARTHY, E. S. ROUNTREE, T. T. EISENHART, J. L. DEMPSEY. "A Practical Beginner's Guide to Cyclic Voltammetry." *J. Chem. Educ.* **2018**, *95*, 197–206.

132. G. A. MABBOTT. "An Introduction to Cyclic Voltammetry." *J. Chem. Educ.* **1983**, *60*, 697–702.

133. S. J. KONOPKA, B. MCDUFFIE. "Diffusion Coefficients of Ferri- and Ferrocyanide Ions in Aqueous Media, Using Twin-Electrode Thin-Layer Electrochemistry." *Anal. Chem.* **1970**, *42*, 1741–1746.

134. E. LABORDA, J. GONZÁLEZ, Á. MOLINA. "Recent Advances on the Theory of Pulse Techniques: A Mini Review." *Electrochem. Commun.* **2014**, *43*, 25–30.

135. E. KATZ, I. WILLNER. "Probing Biomolecular Interactions at Conductive and Semiconductive Surfaces by Impedance Spectroscopy: Routes to Impedimetric Immunosensors, DNA-Sensors, and Enzyme Biosensors." *Electroanalysis* **2003**, *15*, 913–947.

136. A. RAVALLI, G. PILON DOS SANTOS, M. FERRONI, G. FAGLIA, H. YAMANAKA, G. MARRAZZA. "New Label Free CA125 Detection Based on Gold Nanostructured Screen-Printed Electrode." *Sensors Actuators, B Chem.* **2013**, *179*, 194–200.

137. F. LUCARELLI, G. MARRAZZA, M. MASCINI. "Enzyme-Based Impedimetric Detection of PCR Products Using Oligonucleotide-Modified Screen-Printed Gold Electrodes." *Biosens. Bioelectron.* **2005**, *20*, 2001–2009.

138. X. ZENG, S. MA, J. BAO, W. TU, Z. DAI. "Using Graphene-Based Plasmonic Nanocomposites to Quench Energy from Quantum Dots for Signal-On Photoelectrochemical Aptasensing." *Anal. Chem.* **2013**, *85*, 11720–11724.

139. C. ALIX-PANABIÈRES, K. PANTEL. "Challenges in Circulating Tumour Cell Research." *Nat. Rev. Cancer* **2014**, *14*, 623–631.

140. A. RAVALLI, G. MARRAZZA. "Gold and Magnetic Nanoparticles-Based Electrochemical Biosensors for Cancer Biomarker Determination." *J. Nanosci. Nanotechnol.* **2015**, *15*, 3307–3319.

141. S. HIETALA, P. MONONEN, S. STRANDMAN, P. JÄRVI, M. TORKKELI, K. JANKOVA, S. HVILSTED, H. TENHU. "Synthesis and Rheological Properties of an Associative Star Polymer in Aqueous Solutions." *Polymer* **2007**, *48*, 4087–4096.

142. Y. JAVADZADEH, S. HAMEDEYAZ. "Floating Drug Delivery Systems for Eradication of Helicobacter Pylori in Treatment of Peptic Ulcer Disease" in *Trends in Helicobacter Pylori Infection*. Eds. C. Ravariu, D. Mihaiescu. InTech, **2014**, 303–319.

143. R.-S. SABERI, S. SHAHROKHIAN, G. MARRAZZA. "Amplified Electrochemical DNA Sensor Based on Polyaniline Film and Gold Nanoparticles." *Electroanalysis* **2013**, *25*, 1373–1380.

144. J. M. MARGOLIS. "*Conductive Polymers and Plastics*," Springer US, **1989**.

145. J. M. MOON, N. THAPLIYAL, K. K. HUSSAIN, R. N. GOYAL, Y. B. SHIM. "Conducting Polymer-Based Electrochemical Biosensors for Neurotransmitters: A Review." *Biosens. Bioelectron.* **2018**, *102*, 540–552.

146. I. M. TAYLOR, E. M. ROBBINS, K. A. CATT, P. A. CODY, C. L. HAPPE, X. T. CUI. "Enhanced Dopamine Detection Sensitivity by PEDOT/Graphene Oxide Coating on in Vivo Carbon Fiber Electrodes." *Biosens. Bioelectron.* **2017**, *89*, 400–410.

147. M. TERTIȘ, A. FLOREA, A. ADUMITRĂCHIOAIE, A. CERNAT, D. BOGDAN, L. BARBU-TUDORAN, N. JAFFREZIC RENAULT, R. SĂNDULESCU, C. CRISTEA. "Detection of Dopamine by a Biomimetic Electrochemical Sensor Based on Polythioaniline-Bridged Gold Nanoparticles." *Chempluschem* **2017**, *82*, 561–569.

148. M. TERTIȘ, A. CERNAT, D. LACATIȘ, A. FLOREA, D. BOGDAN, M. SUCIU, R. SĂNDULESCU, C. CRISTEA. "Highly Selective Electrochemical Detection of Serotonin on Polypyrrole and Gold Nanoparticles-Based 3D Architecture." *Electrochem. Commun.* **2017**, *75*, 43–47.

149. H. LETHEBY. "On the Production of a Blue Substance by the Electrolysis of Sulphate of Aniline." *J. Chem. Soc.* **1862**, *15*, 161–163.

150. F. YILMAZ. "Polyaniline: Synthesis, Characterization, Solution Properties and Composites." *Dep. Polym. Sci. Technol.* **2007**, 148.

151. M. ATES. "A Review Study of (Bio)Sensor Systems Based on Conducting Polymers." *Mater. Sci. Eng. C* **2013**, *33*, 1853–1859.

152. G. SELVOLINI, C. LAZZARINI, G. MARRAZZA. "Electrochemical Nanocomposite Single-Use Sensor for Dopamine Detection." *Sensors* **2019**, *19*, 3097–3106.

153. Q. ZENG, L. ZHANG, Z. LI, J. QIN, B. Z. TANG. "New Polyacetylene-Based Chemosensory Materials for the 'Turn-on' Sensing of α-Amino Acids." *Polymer* **2009**, *50*, 434–440.

154. J. WANG, M. JIANG, A. FORTES, B. MUKHERJEE. "New Label-Free DNA Recognition Based on Doping Nucleic-Acid Probes within Conducting Polymer Films." *Anal. Chim. Acta* **1999**, *402*, 7–12.

155. G. WANG, R. HAN, X. SU, Y. LI, G. XU, X. LUO. "Zwitterionic Peptide Anchored to Conducting Polymer PEDOT for the Development of Antifouling and Ultrasensitive Electrochemical DNA Sensor." *Biosens. Bioelectron.* **2017**, *92*, 396–401.

156. R. CHERRINGTON, J. LIANG. "Materials and Deposition Processes for Multifunctionality" in *Design and Manufacture of Plastic Components for Multifunctionality: Structural Composites, Injection Molding, and 3D Printing*. William Andrew Publishing, **2016**, 19–21.

157. A. G. MACDIARMID. "Synthetic metals": A novel role for organic polymers (Nobel lecture). *Angew. Chemie - Int. Ed.* **2001**, *40*, 2581–2590

158. W. J. FEAST, J. TSIBOUKLIS, K. L. POUWER, L. GROENENDAAL, E. W. MEIJER. "Synthesis, Processing and Material Properties of Conjugated Polymers." *Polymer* **1996**, *37*, 5017–5047.

159. F. YILMAZ, Z. KUKUKYAVUZ. "Solution Properties of Polyaniline." *Polym. Int.* **2010**, *59*, 552–556.

160. P. KUNZO, P. LOBOTKA, E. KOVACOVA, K. CHRISSOPOULOU, L. PAPOUTSAKIS, S. H. ANASTASIADIS, Z. KRIZANOVA, I. VAVRA. "Nanocomposites of Polyaniline and Titania Nanoparticles for Gas Sensors." *Phys. Status Solidi A* **2013**, *210*, 2341–2347.

161. H. BAI, Q. CHEN, C. LI, C. LU, G. SHI. "Electrosynthesis of Polypyrrole/Sulfonated Polyaniline Composite Films and Their Applications for Ammonia Gas Sensing." *Polymer* **2007**, *48*, 4015–4020.

162. K. CROWLEY, M. R. SMYTH, A. J. KILLARD, A. MORRIN. "Printing Polyaniline for Sensor Applications." *Chem. Pap.* **2013**, *67*, 771–780.

163. B. S. DAKSHAYINI, K. R. REDDY, A. MISHRA, N. P. SHETTI, S. J. MALODE, S. BASU, S. NAVEEN, A. V. RAGHU. "Role of Conducting Polymer and Metal Oxide-Based Hybrids for Applications in Ampereometric Sensors and Biosensors." *Microchem. J.* **2019**, *147*, 7–24.

164. R. RAPINI, A. CINCINELLI, G. MARRAZZA. "Acetamiprid Multidetection by Disposable Electrochemical DNA Aptasensor." *Talanta* **2016**, *161*, 15–21.

165. Z. TALEAT, A. RAVALLI, M. MAZLOUM-ARDAKANI, G. MARRAZZA. "CA125 Immunosensor Based on Poly-Anthranilic Acid Modified Screen-Printed Electrodes." *Electroanalysis* **2013**, *25*, 269–277.

166. B. DALKIRAN, P. E. ERDEN, C. KAÇAR, E. KILIÇ. "Disposable Amperometric Biosensor Based on Poly-L-Lysine and Fe3O4 NPs-Chitosan Composite for the Detection of Tyramine in Cheese." *Electroanalysis* **2019**, *31*, 1324–1333.

167. C. JIANG, T. YANG, K. JIAO, H. GAO. "A DNA Electrochemical Sensor with Poly-l-Lysine/Single-Walled Carbon Nanotubes Films and Its Application for the Highly Sensitive EIS Detection of PAT Gene Fragment and PCR Amplification of NOS Gene." *Electrochim. Acta* **2008**, *53*, 2917–2924.

168. L. LAURINAVIČIUS, A. RADZEVIČ, I. IGNATJEV, G. NIAURA, K. VITKUTĖ, T. ŠIRŠINAITIS, R. TRUSOVAS, R. PAULIUKAITE. "Investigation of Electrochemical Polymerisation of L-Lysine and Application for Immobilisation of Functionalised Graphene as Platform for Electrochemical Sensing." *Electrochim. Acta* **2019**, *299*, 936–945.

169. S. SHIMA, H. SAKAI. "Polylysine Produced by Streptomyces." *Agric. Biol. Chem.* **1977**, *41*, 1807–1809.

170. D. ZHANG, L. LI, W. MA, X. CHEN, Y. ZHANG. "Electrodeposited Reduced Graphene Oxide Incorporating Polymerization of L-Lysine on Electrode Surface and Its Application in Simultaneous Electrochemical Determination of Ascorbic Acid, Dopamine and Uric Acid." *Mater. Sci. Eng. C* **2017**, *70*, 241–249.

171. C. M. NIEMEYER. "Nanoparticles, Proteins, and Nucleic Acids: Biotechnology Meets Materials Science." *Angew. Chemie Int. Ed.* **2001**, *40*, 4128–4158.

172. S. K. GHOSH, T. PAL. "Interparticle Coupling Effect on the Surface Plasmon Resonance of Gold Nanoparticles: From Theory to Applications." *Chem. Rev.* **2007**, *107*, 4797–4862.

173. I. FREESTONE, N. MEEKS, M. SAX, C. HIGGITT. "The Lycurgus Cup - A Roman Nanotechnology." *Gold Bull.* **2008**, *40*, 270–277.

174. F. W. CAMPBELL, R. G. COMPTON. "The Use of Nanoparticles in Electroanalysis: An Updated Review." *Anal. Bioanal. Chem.* **2010**, *396*, 241–259.

175. Y. TAKAHASHI, T. TATSUMA. "Electrodeposition of Thermally Stable Gold and Silver Nanoparticle Ensembles through a Thin Alumina Nanomask." *Nanoscale* **2010**, *2*, 1494–1499.

176. F. KURALAY, N. DÜKAR, Y. BAYRAMLI. "Poly-L-Lysine Coated Surfaces for Ultrasensitive Nucleic Acid Detection." *Electroanalysis* **2018**, *30*, 1556–1565.

177. H. ZEMKOVÁ, S. S. STOJILKOVIC. "Neurotransmitter Receptors as Signaling Platforms in Anterior Pituitary Cells." *Mol. Cell. Endocrinol.* **2018**, *463*, 49–64.

178. A. BARANWAL, P. CHANDRA. "Clinical Implications and Electrochemical Biosensing of Monoamine Neurotransmitters in Body Fluids, in Vitro, in Vivo, and Ex Vivo Models." *Biosens. Bioelectron.* **2018**, *121*, 137–152.

179. E. S. BUCHER, R. M. WIGHTMAN. "Electrochemical Analysis of Neurotransmitters." *Annu. Rev. Anal. Chem.* **2015**, *8*, 239–261.

180. B. SI, E. SONG. "Recent Advances in the Detection of Neurotransmitters." *Chemosensors* **2018**, *6*, 1–24.

181. G. XIAO, S. XU, Y. SONG, Y. ZHANG, Z. LI, F. GAO, J. XIE, L. SHA, Q. XU, Y. SHEN, X. CAI. "In Situ Detection of Neurotransmitters and Epileptiform Electrophysiology Activity in Awake Mice Brains Using a Nanocomposites Modified Microelectrode Array." *Sensors*

Actuators, B Chem. **2019**, *288*, 601–610.

182. Z. TAVAKOLIAN-ARDAKANI, O. HOSU, C. CRISTEA, M. MAZLOUM-ARDAKANI, G. MARRAZZA. "Latest Trends in Electrochemical Sensors for Neurotransmitters: A Review." *Sensors* **2019**, *19*, 2037–2066.

183. M. Y. EMRAN, M. A. SHENASHEN, M. MEKAWY, A. M. AZZAM, N. AKHTAR, H. GOMAA, M. M. SELIM, A. FAHEEM, S. A. EL-SAFTY. "Ultrasensitive In-Vitro Monitoring of Monoamine Neurotransmitters from Dopaminergic Cells." *Sensors Actuators, B Chem.* **2018**, *259*, 114–124.

184. A. RAMACHANDRAN, S. PANDA, S. KARUNAKARAN YESODHA. "Physiological Level and Selective Electrochemical Sensing of Dopamine by a Solution Processable Graphene and Its Enhanced Sensing Property in General." *Sensors Actuators, B Chem.* **2018**, *256*, 488–497.

185. B. DINESH, R. SARASWATHI, A. SENTHIL KUMAR. "Water Based Homogenous Carbon Ink Modified Electrode as an Efficient Sensor System for Simultaneous Detection of Ascorbic Acid, Dopamine and Uric Acid." *Electrochim. Acta* **2017**, *233*, 92–104.

186. N. G. TSIERKEZOS, U. RITTER, Y. NUGRAHA THAHA, A. KNAUER, D. FERNANDES, A. KELARAKIS, E. K. MCCARTHY. "Boron-Doped Multi-Walled Carbon Nanotubes as Sensing Material for Analysis of Dopamine and Epinephrine in Presence of Uric Acid." *Chem. Phys. Lett.* **2018**, *710*, 157–167.

187. G. IBÁÑEZ-REDÍN, D. WILSON, D. GONÇALVES, O. N. OLIVEIRA. "Low-Cost Screen-Printed Electrodes Based on Electrochemically Reduced Graphene Oxide-Carbon Black Nanocomposites for Dopamine, Epinephrine and Paracetamol Detection." *J. Colloid Interface Sci.* **2018**, *515*, 101–108.

188. D. DIAZ-DIESTRA, B. THAPA, J. BELTRAN-HUARAC, B. R. WEINER, G. MORELL. "L-Cysteine Capped ZnS:Mn Quantum Dots for Room-Temperature Detection of Dopamine with High Sensitivity and Selectivity." *Biosens. Bioelectron.* **2017**, *87*, 693–700.

189. X. YAN, Y. GU, C. LI, B. ZHENG, Y. LI, T. ZHANG, Z. ZHANG, M. YANG. "Morphology-Controlled Synthesis of Bi2S3 Nanorods-Reduced Graphene Oxide Composites with High-Performance for Electrochemical Detection of Dopamine." *Sensors Actuators, B Chem.* **2018**, *257*, 936–943.

190. G. MADURAIVEERAN, M. SASIDHARAN, V. GANESAN. "Electrochemical Sensor and Biosensor Platforms Based on Advanced Nanomaterials for Biological and Biomedical Applications." *Biosens. Bioelectron.* **2018**, *103*, 113–129.

191. S. J. ZHANG, K. KANG, L. M. NIU, W. J. KANG. "Electroanalysis of Neurotransmitters via 3D Gold Nanoparticles and a Graphene Composite Coupled with a Microdialysis Device." *J. Electroanal. Chem.* **2019**, *834*, 249–257.

192. I. ZABLOCKA, M. WYSOCKA-ZOLOPA, K. WINKLER. "Electrochemical Detection of Dopamine at a Gold Electrode Modified with a Polypyrrole–Mesoporous Silica Molecular Sieves (MCM-48) Film." *Int. J. Mol. Sci.* **2019**, *20*, 111–127.

193. S. R. ALI, Y. MA, R. R. PARAJULI, Y. BALOGUN, W. Y. C. LAI, H. HE. "A Nonoxidative Sensor Based on a Self-Doped Polyaniline/Carbon Nanotube Composite for Sensitive and Selective Detection of the Neurotransmitter Dopamine." *Anal. Chem.* **2007**, *79*, 2583–2587.

194. X. CHEN, D. LI, W. MA, T. YANG, Y. ZHANG, D. ZHANG. "Preparation of a Glassy Carbon Electrode Modified with Reduced Graphene Oxide and Overoxidized Electropolymerized Polypyrrole, and Its Application to the Determination of Dopamine in the Presence of Ascorbic Acid and Uric Acid." *Microchim. Acta* **2019**, *186 (407)*, 1–10.

195. O. E. FAYEMI, A. S. ADEKUNLE, B. E. KUMARA SWAMY, E. E. EBENSO. "Electrochemical Sensor for the Detection of Dopamine in Real Samples Using Polyaniline/NiO, ZnO, and Fe3O4 Nanocomposites on Glassy Carbon Electrode." *J. Electroanal. Chem.* **2018**, *818*, 236–249.

196. H. FILIK, A. A. AVAN, S. AYDAR. "Simultaneous Detection of Ascorbic Acid, Dopamine, Uric Acid and Tryptophan with Azure

A-Interlinked Multi-Walled Carbon Nanotube/Gold Nanoparticles Composite Modified Electrode." *Arab. J. Chem.* **2016**, *9*, 471–480.

197. I. S. MURATOVA, K. N. MIKHELSON. "Voltammetric Sensing of Dopamine in Urine Samples with Electrochemically Activated Commercially Available Screen-Printed Carbon Electrodes." *Int. J. Biosens. Bioelectron.* **2018**, *4*, 169–173.

198. J. B. RAOOF, A. KIANI, R. OJANI, R. VALIOLLAHI. "Electrochemical Determination of Dopamine Using Banana-MWCNTs Modified Carbon Paste Electrodes." *Anal. Chim. Actaytical Bioanal. Electrochem.* **2011**, *3*, 59–66.

199. P. DAMIER, E. C. HIRSCH, Y. AGID, A. M. GRAYBIEL. "The Substantia Nigra of the Human Brain: II. Patterns of Loss of Dopamine-Containing Neurons in Parkinson's Disease." *Brain* **1999**, *122*, 1437–1448.

200. R. SANGUBOTLA, J. KIM. "Recent Trends in Analytical Approaches for Detecting Neurotransmitters in Alzheimer's Disease." *Trends Anal. Chem.* **2018**, *105*, 240–250.

201. P. KALIMUTHU, S. A. JOHN. "Electropolymerized Film of Functionalized Thiadiazole on Glassy Carbon Electrode for the Simultaneous Determination of Ascorbic Acid, Dopamine and Uric Acid." *Bioelectrochemistry* **2009**, *77*, 13–18.

202. W. DOBRAT, A. MARTIJN. "Analysis of Technical and Formulated Pesticides" in *CIPAC Handbook, Volume H*. **1998**, 223.

203. R. MAHAJAN, S. CHATTERJEE. "A Simple HPLC–DAD Method for Simultaneous Detection of Two Organophosphates, Profenofos and Fenthion, and Validation by Soil Microcosm Experiment." *Environ. Monit. Assess.* **2018**, *190*, 1–8.

204. P. WANG, Y. WAN, A. ALI, S. DENG, Y. SU, C. FAN, S. YANG. "Aptamer-Wrapped Gold Nanoparticles for the Colorimetric Detection of Omethoate." *Sci. China Chem.* **2016**, *59*, 237–242.

205. R. BALA, S. DHINGRA, M. KUMAR, K. BANSAL, S. MITTAL, R. K. SHARMA, N. WANGOO. "Detection of Organophosphorus Pesticide

– Malathion in Environmental Samples Using Peptide and Aptamer Based Nanoprobes." *Chem. Eng. J.* **2017**, *311*, 111–116.

206. G. XU, D. HUO, C. HOU, Y. ZHAO, J. BAO, M. YANG, H. FA. "A Regenerative and Selective Electrochemical Aptasensor Based on Copper Oxide Nanoflowers-Single Walled Carbon Nanotubes Nanocomposite for Chlorpyrifos Detection." *Talanta* **2018**, *178*, 1046–1052.

207. J. DONG, N. GAO, Y. PENG, C. GUO, Z. LV, Y. WANG, C. ZHOU, B. NING, M. LIU, Z. GAO. "Surface Plasmon Resonance Sensor for Profenofos Detection Using Molecularly Imprinted Thin Film as Recognition Element." *Food Control* **2012**, *25*, 543–549.

208. A. M. SHRIVASTAV, S. P. USHA, B. D. GUPTA. "Fiber Optic Profenofos Sensor Based on Surface Plasmon Resonance Technique and Molecular Imprinting." *Biosens. Bioelectron.* **2016**, *79*, 150–157.

209. H. SHI, G. ZHAO, T. CAO, M. LIU, C. GUAN, X. HUANG, Z. ZHU, N. YANG, O. A. WILLIAMS. "Selective and Visible-Light-Driven Profenofos Sensing with Calixarene Receptors on TiO2 Nanotube Film Electrodes." *Electrochem. Commun.* **2012**, *19*, 111–114.

210. M. G. NILLOS, G. RODRIGUEZ-FUENTES, J. GAN, D. SCHLENK. "Enantioselective Acetylcholinesterase Inhibition of the Organophosphorous Insecticides Profenofos, Fonofos, and Crotoxyphos." *Environ. Toxicol. Chem.* **2007**, *26*, 1949–1954.

211. EUROPEAN COMMISSION. Profenofos. Available online: https://ec.europa.eu/food/plant/pesticides/eu-pesticides-database/public/?event=activesubstance.detail&language=EN&selectedID=1755

212. L. WANG, X. LIU, Q. ZHANG, C. ZHANG, Y. LIU, K. TU, J. TU. "Selection of DNA Aptamers That Bind to Four Organophosphorus Pesticides." *Biotechnol. Lett.* **2012**, *34*, 869–874.

213. The Mfold Web Server. Available online: http://unafold.rna.albany.edu/?q=mfold/DNA-Folding-Form (accessed on 2 May 2018)

214. A. RAVALLI, C. ROSSI, G. MARRAZZA. "Bio-Inspired Fish Robot Based on Chemical Sensors." *Sensors Actuators, B Chem.* **2017**, *239*, 325–329.

215. F. LUCARELLI, G. MARRAZZA, M. MASCINI. "Dendritic-like Streptavidin/Alkaline Phosphatase Nanoarchitectures for Amplified Electrochemical Sensing of DNA Sequences." *Langmuir* **2006**, *22*, 4305–4309.

216. S. CENTI, E. SILVA, S. LASCHI, I. PALCHETTI, M. MASCINI. "Polychlorinated Biphenyls (PCBs) Detection in Milk Samples by an Electrochemical Magneto-Immunosensor (EMI) Coupled to Solid-Phase Extraction (SPE) and Disposable Low-Density Arrays." *Anal. Chim. Acta* **2007**, *594*, 9–16.

217. J. TAYLOR, G. PICELLI, D. J. HARRISON. "An Evaluation of the Detection Limits Possible for Competitive Capillary Electrophoretic Immunoassays." *Electrophoresis* **2001**, *22*, 3699–3708.

218. L. S. DESHPANDE, D. S. CARTER, K. F. PHILLIPS, R. E. BLAIR, R. J. DELORENZO. "Development of Status Epilepticus, Sustained Calcium Elevations and Neuronal Injury in a Rat Survival Model of Lethal Paraoxon Intoxication." *Neurotoxicology* **2014**, *44*, 17–26.

219. R. MIRANDA-CASTRO, N. DE-LOS-SANTOS-ÁLVAREZ, M. J. LOBO-CASTAÑÓN. "Aptamers as Synthetic Receptors for Food Quality and Safety Control" in *Comprehensive Analytical Chemistry*. **2016**, Vol. 74, 155–191.

220. N. M. DANESH, H. B. BOSTAN, K. ABNOUS, M. RAMEZANI, K. YOUSSEFI, S. M. TAGHDISI, G. KARIMI. "Ultrasensitive Detection of Aflatoxin B1 and Its Major Metabolite Aflatoxin M1 Using Aptasensors: A Review." *TrAC - Trends Anal. Chem.* **2018**, *99*, 117–128.

221. A. SHARMA, R. KHAN, G. CATANANTE, T. A. SHERAZI, S. BHAND, A. HAYAT, J. L. MARTY. "Designed Strategies for Fluorescence-Based Biosensors for the Detection of Mycotoxins." *Toxins* **2018**, *10*, 197–215.

222. F. S. SABET, M. HOSSEINI, H. KHABBAZ, M. DADMEHR, M. R. GANJALI.

"FRET-Based Aptamer Biosensor for Selective and Sensitive Detection of Aflatoxin B1 in Peanut and Rice." *Food Chem.* **2017**, *220*, 527–532.

223. L. CHEN, F. WEN, M. LI, X. GUO, S. LI, N. ZHENG, J. WANG. "A Simple Aptamer-Based Fluorescent Assay for the Detection of Aflatoxin B1 in Infant Rice Cereal." *Food Chem.* **2017**, *215*, 377–382.

224. L. SUN, L. WU, Q. ZHAO. "Aptamer Based Surface Plasmon Resonance Sensor for Aflatoxin B1." *Microchim. Acta* **2017**, *184*, 2605–2610.

225. C. ZHU, G. ZHANG, Y. HUANG, S. YANG, S. REN, Z. GAO, A. CHEN. "Dual-Competitive Lateral Flow Aptasensor for Detection of Aflatoxin B1in Food and Feedstuffs." *J. Hazard. Mater.* **2018**, *344*, 249–257.

226. K. YUGENDER GOUD, S. K. KALISA, V. KUMAR, Y. F. TSANG, S. E. . LEE, K. V. GOBI, K.-H. KIM. "Progress on Nanostructured Electrochemical Sensors and Their Recognition Elements for Detection of Mycotoxins: A Review." *Biosens. Bioelectron.* **2018**, *121*, 205–222.

227. K. ABNOUS, N. M. DANESH, M. ALIBOLANDI, M. RAMEZANI, A. SARRESHTEHDAR EMRANI, R. ZOLFAGHARI, S. M. TAGHDISI. "A New Amplified π-Shape Electrochemical Aptasensor for Ultrasensitive Detection of Aflatoxin B1." *Biosens. Bioelectron.* **2017**, *94*, 374–379.

228. S. PIERMARINI, G. VOLPE, L. MICHELI, D. MOSCONE, G. PALLESCHI. "An ELIME-Array for Detection of Aflatoxin B1 in Corn Samples." *Food Control* **2009**, *20*, 371–375.

229. W. B. SHIM, H. MUN, H.-A. JOUNG, J. A. OFORI, D.-H. CHUNG, M.-G. KIM. "Chemiluminescence Competitive Aptamer Assay for the Detection of Aflatoxin B1 in Corn Samples." *Food Control* **2014**, *36*, 30–35.

230. L. SUN, Q. ZHAO. "Competitive Horseradish Peroxidase-Linked Aptamer Assay for Sensitive Detection of Aflatoxin B1." *Talanta* **2018**, *179*, 344–349.

231. T. CHEN, R. H. HEFLICH, M. M. MOORE, N. MEI. "Differential Mutagenicity of Aflatoxin B1 in the Liver of Neonatal and Adult Mice." *Environ. Mol. Mutagen.* **2010**, *51*, 156–163.

232. G. M. MEISSONNIER, P. PINTON, J. LAFFITTE, A.-M. COSSALTER, Y. Y. GONG, C. P. WILD, G. BERTIN, P. GALTIER, I. P. OSWALD. "Immunotoxicity of Aflatoxin B1: Impairment of the Cell-Mediated Response to Vaccine Antigen and Modulation of Cytokine Expression." *Toxicol. Appl. Pharmacol.* **2008**, *231*, 142–149.

233. F. GEISSLER, E. M. FAUSTMAN. "Developmental Toxicity of Aflatoxin B1 in the Rodent Embryo in Vitro: Contribution of Exogenous Biotransformation Systems to Toxicity." *Teratology* **1988**, *37*, 101–111.

234. J. BOONEN, S. V. MALYSHEVA, L. TAEVERNIER, J. D. DI MAVUNGU, B. DE SPIEGELEER, S. DE SAEGER. "Human Skin Penetration of Selected Model Mycotoxins." *Toxicology* **2012**, *301*, 21–32.

235. L. CHRYSEIS LE, J. A. CRUZ-AGUADO, G. A. PENNER. DNA Ligands for Aflatoxin and Zearalenone **2011**

236. X. HUANG, T. HUANG, X. LI, Z. HUANG. "Flower-like Gold Nanoparticles-Based Immunochromatographic Test Strip for Rapid Simultaneous Detection of Fumonisin B1 and Deoxynivalenol in Chinese Traditional Medicine." *J. Pharm. Biomed. Anal.* **2020**, *177*, 112895–112903.

237. J. C. VIDAL, J. R. BERTOLÍN, A. EZQUERRA, S. HERNÁNDEZ, J. R. CASTILLO. "Rapid Simultaneous Extraction and Magnetic Particle-Based Enzyme Immunoassay for the Parallel Determination of Ochratoxin A, Fumonisin B1 and Deoxynivalenol Mycotoxins in Cereal Samples." *Anal. Methods* **2017**, *9*, 3602–3611.

238. J. LIU, S. ZANARDI, S. POWERS, M. SUMAN. "Development and Practical Application in the Cereal Food Industry of a Rapid and Quantitative Lateral Flow Immunoassay for Deoxynivalenol." *Food Control* **2012**, *26*, 88–91.

239. T. WEI, P. REN, L. HUANG, Z. OUYANG, Z. WANG, X. KONG, T. LI, Y. YIN, Y. WU, Q. HE. "Simultaneous Detection of Aflatoxin B1,

Ochratoxin A, Zearalenone and Deoxynivalenol in Corn and Wheat Using Surface Plasmon Resonance." *Food Chem.* **2019**, *300*, 125176–125182.

240. T. KADOTA, Y. TAKEZAWA, S. HIRANO, O. TAJIMA, C. M. MARAGOS, T. NAKAJIMA, T. TANAKA, Y. KAMATA, Y. SUGITA-KONISHI. "Rapid Detection of Nivalenol and Deoxynivalenol in Wheat Using Surface Plasmon Resonance Immunoassay." *Anal. Chim. Acta* **2010**, *673*, 173–178.

241. J. YAN, Q. SHI, K. YOU, Y. LI, Q. HE. "Phage Displayed Mimotope Peptide-Based Immunosensor for Green and Ultrasensitive Detection of Mycotoxin Deoxynivalenol." *J. Pharm. Biomed. Anal.* **2019**, *168*, 94–101.

242. C. E. SUNDAY, M. MASIKINI, L. WILSON, C. RASSIE, T. WARYO, P. G. L. BAKER, E. I. IWUOHA. "Application on Gold Nanoparticles-Dotted 4-Nitrophenylazo Graphene in a Label-Free Impedimetric Deoxynivalenol Immunosensor." *Sensors* **2015**, *15*, 3854–3871.

243. D. ROMANAZZO, F. RICCI, G. VOLPE, C. T. ELLIOTT, S. VESCO, K. KROEGER, D. MOSCONE, J. STROKA, H. VAN EGMOND, M. VEHNIÄINEN, G. PALLESCHI. "Development of a Recombinant Fab-Fragment Based Electrochemical Immunosensor for Deoxynivalenol Detection in Food Samples." *Biosens. Bioelectron.* **2010**, *25*, 2615–2621.

244. E. VALERA, R. GARCÍA-FEBRERO, C. T. ELLIOTT, F. SÁNCHEZ-BAEZA, M. P. MARCO. "Electrochemical Nanoprobe-Based Immunosensor for Deoxynivalenol Mycotoxin Residues Analysis in Wheat Samples." *Anal. Bioanal. Chem.* **2019**, *411*, 1915–1926.

245. L. WANG, X. PENG, H. FU, C. HUANG, Y. LI, Z. LIU. "Recent Advances in the Development of Electrochemical Aptasensors for Detection of Heavy Metals in Food." *Biosens. Bioelectron.* **2020**, *147*, 111777–111787.

246. G. EVTUGYN, A. PORFIREVA, V. STEPANOVA, R. SITDIKOV, I. STOIKOV, D. NIKOLELIS, T. HIANIK. "Electrochemical Aptasensor Based on Polycarboxylic Macrocycle Modified with Neutral Red for

Aflatoxin B1 Detection." *Electroanalysis* **2014**, *26*, 2100–2109.

247. Y. ZHOU, C. MAHAPATRA, H. CHEN, X. PENG, S. RAMAKRISHNA, H. S. NANDA. "Recent Developments in Fluorescent Aptasensors for Detection of Antibiotics." *Curr. Opin. Biomed. Eng.* **2020**, *13*, 16–24.

248. H. B. BOSTAN, N. M. DANESH, G. KARIMI, M. RAMEZANI, S. A. M. SHAEGH, K. YOUSSEF, F. CHARBGOO, K. ABNOUSAG, S. M. TAGHDISI. "Ultrasensitive Detection of Ochratoxin A Using Aptasensors." *Biosens. Bioelectron.* **2017**, *98*, 168–179.

249. C. C. ONG, S. SIVA SANGU, N. M. ILLIAS, S. CHANDRA BOSE GOPINATH, M. S. M. SAHEED. "Iron Nanoflorets on 3D-Graphene-Nickel: A 'Dandelion' Nanostructure for Selective Deoxynivalenol Detection." *Biosens. Bioelectron.* **2020**, *154*, 112088–112093.

250. L. XU, Z. ZHANG, Q. ZHANG, P. LI. "Mycotoxin Determination in Foods Using Advanced Sensors Based on Antibodies or Aptamers." *Toxins* **2016**, *8*, 239–254.

251. G. EVTUGYN, T. HIANIK. "Electrochemical Immuno- and Aptasensors for Mycotoxin Determination." *Chemosensors* **2019**, *7*, 10–38.

252. B. WARTH, M. SULYOK, F. BERTHILLER, R. SCHUHMACHER, R. KRSKA. "New Insights into the Human Metabolism of the Fusarium Mycotoxins Deoxynivalenol and Zearalenone." *Toxicol. Lett.* **2013**, *220*, 88–94.

253. J. J. PESTKA. "Deoxynivalenol: Mechanisms of Action, Human Exposure, and Toxicological Relevance." *Arch. Toxicol.* **2010**, *84*, 663–679.

254. C. J. MIROCHA, E. KOLACZKOWSKI, W. XIE, H. YU, H. JELEN. "Analysis of Deoxynivalenol and Its Derivatives (Batch and Single Kernel) Using Gas Chromatography/Mass Spectrometry." *J. Agric. Food Chem.* **1998**, *46*, 1414–1418.

255. S. WU, H. LIU, Y. LIU. Deoxynivalenol nucleic acid aptamer and application thereof **2011**

256. M. ZUKER. "Mfold Web Server for Nucleic Acid Folding and

Hybridization Prediction." *Nucleic Acids Res.* **2003**, *31*, 3406–3415.

257. N. R. MARKHAM, M. ZUKER. "DINAMelt Web Server for Nucleic Acid Melting Prediction." *Nucleic Acids Res.* **2005**, *33*, W577–W581.

258. D. LIPMAN, W. PEARSON. "Rapid and Sensitive Protein Similarity Searches." *Science* **1985**, *227*, 1435–1441.

259. G. M. MORRIS, R. HUEY, W. LINDSTROM, M. F. SANNER, R. K. BELEW, D. S. GOODSELL, A. J. OLSON. "AutoDock4 and AutoDockTools4: Automated Docking with Selective Receptor Flexibility." *J. Comput. Chem.* **2009**, *30*, 2785–2791.

260. J. JI, P. ZHU, F. PI, C. SUN, J. SUN, M. JIA, C. YING, Y. ZHANG, X. SUN. "Development of a Liquid Chromatography-Tandem Mass Spectrometry Method for Simultaneous Detection of the Main Milk Allergens." *Food Control* **2017**, *74*, 79–88.

261. L. MONACI, A. VISCONTI. "Immunochemical and DNA-Based Methods in Food Allergen Analysis and Quality Assurance Perspectives." *Trends Food Sci. Technol.* **2010**, *21*, 272–283.

262. S. L. TAYLOR, J. A. NORDLEE, L. M. NIEMANN, D. M. LAMBRECHT. "Allergen Immunoassays-Considerations for Use of Naturally Incurred Standards." *Anal. Bioanal. Chem.* **2009**, *395*, 83–92.

263. G. M. S. ROSS, G. I. SALENTIJN, M. W. F. NIELEN. "A Critical Comparison between Flow-through and Lateral Flow Immunoassay Formats for Visual and Smartphone-Based Multiplex Allergen Detection." *Biosensors* **2019**, *9*, 143–163.

264. J. MASIRI, B. BARRIOS-LOPEZ, L. BENOIT, J. TAMAYO, J. DAY, C. NADALA, S. L. SUNG, M. SAMADPOUR. "Development and Validation of a Lateral Flow Immunoassay Test Kit for Dual Detection of Casein and B-Lactoglobulin Residues." *J. Food Prot.* **2016**, *79*, 477–483.

265. C. VILLA, J. COSTA, I. MAFRA. "Detection and Quantification of Milk Ingredients as Hidden Allergens in Meat Products by a Novel Specific Real-Time PCR Method." *Biomolecules* **2019**, *9*, 804–818.

266. J. COSTA, T. J. R. FERNANDES, C. VILLA, M. B. P. P. OLIVEIRA, I.

MAFRA. "Advances in Food Allergen Analysis." *Food Saf. Innov. Anal. Tools Saf. Assess.* **2016**, 305–360.

267. A. I. SANCHO, E. N. C. MILLS. "Proteomic Approaches for Qualitative and Quantitative Characterisation of Food Allergens." *Regul. Toxicol. Pharmacol.* **2010**, *58*, S42–S46.

268. T. CUCU, L. JACXSENS, B. DE MEULENAER. "Analysis to Support Allergen Risk Management: Which Way to Go?" *J. Agric. Food Chem.* **2013**, *61*, 5624–5633.

269. R. MANSOURI, A. AZADBAKHT. "Aptamer-Based Approach as Potential Tools for Construction the Electrochemical Aptasensor." *J. Inorg. Organomet. Polym. Mater.* **2019**, *29*, 517–527.

270. L. RUPRICHOVÁ, M. KRÁLOVÁ, I. BORKOVCOVÁ, L. VORLOVÁ, I. BEDÁŇOVÁ. "Determination of Whey Proteins in Different Types of Milk." *Acta Vet. Brno* **2014**, *83*, 67–72.

271. G. KONTOPIDIS, C. HOLT, L. SAWYER. "Invited Review: β-Lactoglobulin: Binding Properties, Structure, and Function." *J. Dairy Sci.* **2004**, *87*, 785–796.

272. M. NIEMI, S. JYLHÄ, M. L. LAUKKANEN, H. SÖDERLUND, S. MÄKINEN-KILJUNEN, J. M. KALLIO, N. HAKULINEN, T. HAAHTELA, K. TAKKINEN, J. ROUVINEN. "Molecular Interactions between a Recombinant IgE Antibody and the β-Lactoglobulin Allergen." *Structure* **2007**, *15*, 1413–1421.

273. S. BROWNLOW, J. H. MORAIS CABRAL, R. COOPER, D. R. FLOWER, S. J. YEWDALL, I. POLIKARPOV, A. C. T. NORTH, L. SAWYER. "Bovine β-Lactoglobulin at 1.8 Å Resolution - Still an Enigmatic Lipocalin." *Structure* **1997**, *5*, 481–495.

274. P. KELLY, B. W. WOONTON, G. W. SMITHERS. "*Improving the Sensory Quality, Shelf-Life and Functionality of Milk*," Woodhead Publishing Limited, **2009**.

275. M. STOJADINOVIC, R. PIETERS, J. SMIT, T. C. VELICKOVIC. "Cross-Linking of β-Lactoglobulin Enhances Allergic Sensitization through Changes in Cellular Uptake and Processing." *Toxicol. Sci.* **2014**, *140*,

224–235.

276. G. CATANANTE, R. K. MISHRA, A. HAYAT, J. L. MARTY. "Sensitive Analytical Performance of Folding Based Biosensor Using Methylene Blue Tagged Aptamers." *Talanta* **2016**, *153*, 138–144.

277. Y. XIAO, A. A. LUBIN, A. J. HEEGER, K. W. PLAXCO. "Label-Free Electronic Detection of Thrombin in Blood Serum by Using an Aptamer-Based Sensor." *Angew. Chemie* **2005**, *117*, 5592–5595.

278. L. R. SCHOUKROUN-BARNES, S. WAGAN, R. J. WHITE. "Enhancing the Analytical Performance of Electrochemical RNA Aptamer-Based Sensors for Sensitive Detection of Aminoglycoside Antibiotics." *Anal. Chem.* **2014**, *86*, 1131–1137.

279. L. WU, X. ZHANG, W. LIU, E. XIONG, J. CHEN. "Sensitive Electrochemical Aptasensor by Coupling "Signal-on'' and "Signal-off'' Strategies." *Anal. Chem.* **2013**, *85*, 8397–8402.

280. R. GARCÍA-GONZÁLEZ, A. COSTA-GARCÍA, M. T. FERNÁNDEZ-ABEDUL. "Methylene Blue Covalently Attached to Single Stranded DNA as Electroactive Label for Potential Bioassays." *Sensors Actuators, B Chem.* **2014**, *191*, 784–790.

281. E. E. FERAPONTOVA, E. M. OLSEN, K. V. GOTHELF. "An RNA Aptamer-Based Electrochemical Biosensor for Detection of Theophylline in Serum." *J. Am. Chem. Soc.* **2008**, *130*, 4256–4258.

282. G. CARPINI, F. LUCARELLI, G. MARRAZZA, M. MASCINI. "Oligonucleotide-Modified Screen-Printed Gold Electrodes for Enzyme-Amplified Sensing of Nucleic Acids." *Biosens. Bioelectron.* **2004**, *20*, 167–175.

283. S. HE, X. LI, Y. WU, S. WU, Z. WU, A. YANG, P. TONG, J. YUAN, J. GAO, H. CHEN. "Highly Sensitive Detection of Bovine β-Lactoglobulin with Wide Linear Dynamic Range Based on Platinum Nanoparticles Probe." *J. Agric. Food Chem.* **2018**, *66*, 11830–11838.

284. A. D. MACKERELL. "Influence of Magnesium Ions on Duplex DNA Structural, Dynamic, and Solvation Properties." *J. Phys. Chem. B* **1997**, *101*, 646–650.

285. S. L. TAYLOR, S. M. GENDEL, G. F. HOUBEN, E. JULIEN. "The Key Events Dose-Response Framework: A Foundation for Examining Variability in Elicitation Thresholds for Food Allergens." *Crit. Rev. Food Sci. Nutr.* **2009**, *49*, 729–739.

286. K. J. ALLEN, B. C. REMINGTON, J. L. BAUMERT, R. W. R. CREVEL, G. F. HOUBEN, S. BROOKE-TAYLOR, A. G. KRUIZINGA, S. L. TAYLOR. "Allergen Reference Doses for Precautionary Labeling (VITAL 2.0): Clinical Implications." *J. Allergy Clin. Immunol.* **2014**, *133*, 156–164.

287. C. PELAEZ-LORENZO, J. C. DIEZ-MASA, I. VASALLO, M. DE FRUTOS. "A New Sample Preparation Method Compatible with Capillary Electrophoresis and Laser-Induced Fluorescence for Improving Detection of Low Levels of β-Lactoglobulin in Infant Foods." *Anal. Chim. Acta* **2009**, *649*, 202–210.